Universidade Nova de Lisboa

Instituto de Higiene e Medicina Tropical

Evaluation of the antifungal potential of natural marine compounds

Diana Mendes Grilo

DISSERTATION PRESENTED TO FULFILL THE REQUIREMENTS TO OBTAIN A DEGREE OF MASTER'S IN MEDICAL MICROBIOLOGY

OCTOBER, 2022

Universidade Nova de Lisboa

Instituto de Higiene e Medicina Tropical

Evaluation of the antifungal potential of natural marine compounds

Autor: Diana Mendes Grilo

Supervisor: Dr. Catarina Pimentel

Co-supervisor: Dr. Oscar Rojas

Dissertation presented to fulfill the requirements to obtain a degree of master's in Medical Microbiology

The work was supported by MOSTMICRO-ITQB R&D Unit (UIDB/04612/2020, UIDP/04612/2020) and LS4FUTURE Associated Laboratory (LA/P/0087/2020).

Acknowledgments

First and foremost, I would like to thank my supervisor, Dr. Catarina Pimentel, for trusting me to work on this project and for always being available to support and advise me throughout this process. Sharing her scientific approach to research and inspiration was a great privilege for me.

I would also like to thank my co-supervisor, Dr. Oscar Rojas, for his support, availability, and valuable suggestions.

I thank current and former Yeast Molecular Biology Lab members for being wonderful colleagues who have been always available to help me whenever I needed it.

I thank ITQB NOVA for the excellent working conditions, particularly the CERMAX NMR facility, the Mass Spectrometry Unit (UniMS), and Cristina Leitão for assisting with the HPLC. I am also grateful to the ITQB NOVA maintenance staff for being available to try to solve and find solutions for the issues that appeared during this project.

This work was supported by MOSTMICRO-ITQB R&D Unit (UIDB/04612/2020, UIDP/04612/2020) and LS4FUTURE Associated Laboratory (LA/P/0087/2020).

List of publications

Submitted articles in peer-reviewed international scientific journals directly related to the research work presented in this thesis:

Antifungal potential of marine organisms of the Yucatan Peninsula (Mexico) against medically important *Candida* spp., Pech-Puch, D., Grilo, D., Calva-Pérez, S., Pedras, A., Villegas-Hernández, H., Guillén-Hernández, S., Díaz-Gamboa, R., Forero Tunjano, M., Rodríguez, J., Rojas, O., Jiménez C., Pimentel, C.

Communications in scientific meetings directly related to the research work presented in this thesis:

Grilo, D., Calva Pérez, E., S., Afonso, G., Silva, S., Pech-Puch, D., González Salas, C., Rojas, O., Pimentel, C., (2022) Evaluation of the antifungal activity of marine extracts against *Candida* spp., IUBMB-FEBS-PABMB 2022 Congress, 9 – 14 July 2022, Lisbon, Portugal.

Calva Pérez, E., Pech Puch, D., González Salas, C., Villegas Hernández, H., Guillén Hernández, S., Rojas, O., Grilo, D., Rodríguez, J., Jiménez, C., (2022), Potencial antifúngico de las esponjas marinas de la península de Yucatan, Simposio Recorecos, 20 – 24 June 2022, Yucatan, Mexico.

Grilo, D., Calva-Pérez, S. E.; Afonso, G.; González-Salas, C., Pimentel, C.; Pech-Puch, D., Rojas, O., (2022) Evaluation of the antifungal potential of marine organisms from the Yucatan Peninsula (Mexico), 1st International Symposium on Products of Natural Origin "For a Healthy Life" (CNIC ProNat), 27 September - 1 October , 2022, Varadero, Cuba.

Abstract

Invasive fungal infections represent a global health threat. They are associated with high mortality and morbidity rates, in part due to the ineffectiveness of available antifungal agents. The rampant increase in infections recalcitrant to current antifungals has worsened this scenario and made the development of new and more effective antifungals a priority. The still unexplored marine biodiversity provides an unlimited source of new metabolites with potential clinical applications and may accelerate drug discovery. The weak investment in new antifungal drugs over last years, together with the emergence species resistant to current antifungal drugs, are widely acknowledged to contribute to the burden that these diseases cause in patients and healthcare systems.

In this work, two libraries of 65 and 44 extracts from marine organisms of the Yucatan Peninsula, Mexico, were tested for antifungal activity against *Candida* species, opportunistic yeasts known to cause nosocomial invasive fungal infections. We have identified four marine extracts with high antifungal potential. All of them are fungicidal and, at least two, are minimally toxic to mammalian cells. The fractionation of promising extracts through bioguided assays coupled with biochemical and biophysical methodologies allowed partial purification of the active compounds while preserving their fungicidal activity. Through a dereplication approach, it was possible to identify two compounds - mirabilin B and penaresidin B - in one of the subfractions, which have already been reported to have antifungal activity. This finding underscores this type of approach as a valuable strategy for prioritizing the analysis of subsequent fractions.

Overall, this study highlights marine organisms as promising resources for the discovery of new and more effective antifungal drugs.

Keywords: Invasive fungal infections, antifungals, marine biodiversity, natural products, *Candida* spp..

Resumo

As infeções fúngicas invasivas representam uma ameaça à saúde global. Estas infeções estão associadas a altas taxas de mortalidade e morbidade, em parte devido à ineficácia dos fármacos antifúngicos disponíveis. Nos últimos anos, o aumento de infeções deste tipo, resistentes aos atuais antifúngicos tem vindo a agravar este cenário e tornou prioritário o desenvolvimento de novos fármacos mais eficazes. A biodiversidade marinha, ainda pouco explorada, constitui uma fonte ilimitada de novos metabolitos com potencial aplicação clínica que pode acelerar a descoberta de novos fármacos. O fraco investimento no desenvolvimento de novos medicamentos, juntamente com a emergência de espécies resistentes aos antifúngicos atuais, tem aumentado o impacto negativo destas doenças nos pacientes e sistemas de saúde.

Neste trabalho, o potencial antifúngico de duas bibliotecas de 65 e 44 extratos marinhos recolhidos na Península de Yucatan, México, foi testado utilizando espécies de *Candida*, leveduras oportunistas que podem causar infeções fúngicas invasivas nosocomiais. Foram identificados quatro extratos marinhos com atividade antifúngica promissora. Todos eles tinham atividade fungicida e, pelo menos dois, eram minimamente tóxicos *in vitro*. O fracionamento destes extratos com recurso a ensaios bioguiados aliados a metodologias bioquímicas e biofísicas permitiu a purificação parcial dos compostos ativos, preservando a sua atividade fungicida. Através de uma abordagem de desreplicação, foi possível, numa subfração, identificar dois compostos – mirabilin B e penaresidin B –, cuja atividade antifúngica já tinha sido documentada.

Este resultado reforça este tipo de abordagem como uma estratégia valiosa para priorizar a análise das frações com atividade. No geral, este estudo destaca os organismos marinhos como recursos promissores para a descoberta de novos e mais eficazes fármacos antifúngicos.

Palavras-chave: Infeções fúngicas invasivas, antifúngicos, biodiversidade marinha, produtos naturais, *Candida* spp..

Table of contents

List of Figures

Chapter 1 – Introduction

Chapter 2 – Materials and Methods

Chapter 3 – Results and Discussion

Chapter 6 - Supplementary Material

List of tables

Chapter 1 – Introduction

Chapter 3 – Results and Discussion

Chapter 6 - Supplementary Material

List of abbreviations and acronyms

ºC	Celsius degree
AIDS	Acquired immunodeficiency syndrome
AMR	Antimicrobial resistance
ABC	ATP-binding cassette
ATCC	American Type Culture Collection
BSI	Bloodstream infection
BF	*n*- butanol fraction
C.	*Candida*
COVID-19	Coronavirus Disease 2019
CDC	Centers for Disease Control and Prevention, United States
CLSI	Clinical Laboratory and Standards Institute
CFU	Colony forming unit
DMSO	Dimethyl sulfoxide
DMEM	Dulbecco's Modified Eagle Medium
DF	Dichloromethane fraction
e.g.	*exempli gratia*
EPS	Extracellular polysaccharide substance
EPA	Epithelial adhesin
ESI	Electrospray Ionization Process
ECTA	9α,11α-epoxycholest-7-ene-3β,5α,6α,19-tetrol 6-acetate
FDA	Food and Drug Administration, United States
FBS	Fetal Bovine serum
GI	Gastrointestinal
GPI	Glycosylphosphatidylinositol
g	g force
HIV	Human immunodeficiency virus
HAART	Highly active antiretroviral therapy

HTS	High-throughput screening
HF	Hexane fraction
HPLC	High-performance liquid chromatography
HRMS	High-resolution mass spectrometry
ICU	Intensive care unit
IFI	Invasive fungal infection
IC	Invasive candidiasis
LC-MS	Liquid chromatography-mass spectrometry
MNP	Marine Natural Product
MoA	Mechanism of action
MTT	3-(4,5-dimethylthiazol-2-yl)-2,5-diphenyltetrazolium bromide
MOPS	Morpholinepropanesulfonic acid
MIC	Minimum inhibitory concentration
MFC	Minimum fungicidal concentration
MFS	Major facilitator superfamily
NP	Natural products
NMR	Nuclear magnetic resonance
OD	Optical density
PBS	Phosphate-buffered saline
PFA	Plakortide F acid
RPMI	Roswell Park Memorial Institute
ppm	Parts *per* million
sp.	species (singular)
spp.	species (plural)
SCUBA	Self-Contained Underwater Breathing Apparatus
SPE	Solid phase extraction
UV	Ultraviolet
UG	Urogenital
UHPLC	Ultra-High Performance Liquid Chromatography

v/v	Volume *per* volume
WHO	World Health Organization
WF	Water fraction
WMF	Water-Methanol fraction
YP	Yucatan Peninsula
YPD	Yeast extract peptone dextrose media
Zd1	(Z)-5-(4-hydroxybenzylidene) imidazolidine-2,4-dione

Chapter 1 – Introduction

Humankind has faced many infectious diseases throughout history. Infectious diseases caused by bacteria, fungi, and viruses are a threat to public health despite all medical progress and remain a major cause of morbidity and mortality [1]. The new coronavirus, SARS-CoV-2, responsible for the global pandemic, Coronavirus Disease 2019 (COVID-19) is a chilling reminder that such a risk persists in modern society. COVID-19 also put the spotlight on invasive fungal diseases, reinforcing the need for more effective antifungal drugs to address those infections. Indeed, while superinfections were uncommon at the beginning of the pandemic, they are now becoming more common [2], and it is well documented that patients with severe COVID-19 pneumonia are at higher risk of acquiring life-threatening secondary infections, such as invasive fungal infections (IFIs) [3].

1.1. Fungal infections

There are 1.5 to 5 million species of fungi on Earth, but only a few hundred can cause disease in humans and even fewer are capable of affecting healthy individuals [4]. Every day we are confronted with thousands of fungal spores and colonized by fungi without developing disease. Mammalians coevolved with fungi, and the human immune system has developed strategies to coexist with these microorganisms [4]. However, in some situations, fungal infections can result in severe disease and even death [5].

Fungi cause infections in two distinct ways: as primary pathogens or as opportunistic pathogens. Primary pathogens have the ability to infect healthy people. Opportunistic pathogens, including commensal fungi found in the healthy population, can establish infection under particular conditions, such as immunosuppression [6].

The prevalence of fungal infections has increased in the last decades, but they are still neglected. These infections affect more than 1 billion people, resulting in about 11.5 million life-threatening infections and more than 1.5 million deaths per year [7]. As a striking comparison, tuberculosis and malaria which have received much more attention are estimated to be responsible for 1.5 million and 627,000 deaths each year, respectively, a number similar to or well below that reported for fungal infections [8, 9].

Clinical presentations in fungal infections range from superficial infections, affecting skin, hair, and nails, to systemic infections with dissemination and invasion of internal organs [10]. Superficial fungal infections, although common, are rarely fatal, but can spread to other regions of the body [11].

Among fungal infections, invasive fungal infections are the most concerning, since they are associated with a high number of case fatalities if not diagnosed and treated promptly [12]. They represent a significant burden for healthcare systems and patients, often associated with high morbidity and mortality rates and increased hospital stays that lead to high healthcare costs [13]. *Candida*, *Aspergillus*, *Cryptococcus*, and *Pneumocystis* species are the most frequently isolated fungi causing invasive fungal infections [7, 11, 14].

Predisposing factors for IFIs can be intrinsic when associated with host characteristics (necrotizing pancreatitis, immunosuppression), or extrinsic. The latter include long-term ICU (Intensive Care Unit) stays, invasive medical devices (*e.g.* catheters, prostheses, implants), exposure to broad-spectrum antimicrobials, recent major surgery, dialysis, total parenteral nutrition, immunosuppressive treatments, organ transplantation, chemotherapy, among others [10, 15, 16].

Fortunately, modern medicine can effectively treat life-threatening health conditions. However, life-saving treatments put many patients at risk for IFIs, which together with the emergence of fungi resistant to available antifungals, certainly explains the rapid increase in IFIs in the last decades and led the CDC (Centers for Disease Control and Prevention, United States) and WHO (World Health Organization) to issue an urgent alert to the need to develop or discover new and more effective antifungal agents [17].

1.2. Fungal infections caused by *Candida* spp.

There are approximately 200 different species of *Candida*, but only a few are human colonizers and opportunistic pathogens. More than 90% of all invasive *Candida* infections are due to *Candida albicans, Candida glabrata, Candida parapsilosis, Candida tropicalis,* and *Candida krusei* [5, 18]. They are an integral part of the human microbiota, and under normal conditions can asymptomatically colonize several niches such as the oral cavity, skin, gastrointestinal, urogenital tracts, and lungs (**Figure 1.1**)

[19]. *C. albicans* is the most prevalent species, but the other species mentioned above have been increasing in recent years [4, 20, 21].

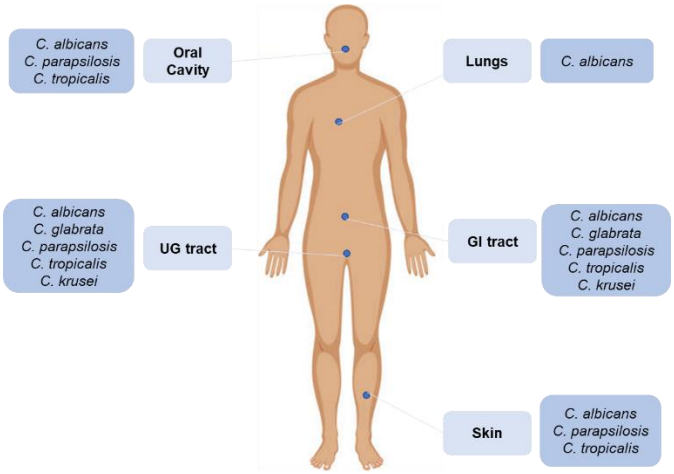

Figure 1.1. ***Biogeography of Candida species in human colonization.*** *The most frequently isolated Candida species are listed according to their niche in the human body. In the oral cavity, the most frequent species are C. albicans, C. parapsilosis, and C. tropicalis. In urogenital (UG) and gastrointestinal (GI) tract the most common species are C. albicans, C. glabrata, C. parapsilosis, C. tropicalis, and C. krusei. C. albicans remains the most frequent in the lungs and C. albicans, C. parapsilosis, and C. tropicalis prevail in the skin. Adapted from* [19].

Northern and Central Europe and the United States have the largest proportion of *C. albicans* clinical isolates, whereas non-*albicans* species are more frequent in South America, Southern Europe, and Asia [18]. *C. glabrata* is the second most abundant clinical isolate, both in Europe and in the United States [22], and infections caused by this yeast are a major concern due to its intrinsic reduced susceptibility to antifungals [20].

For infection by *Candida* spp., pre-colonization is required. Abnormal or increased colonization triggered by many factors leads to infection [21].

Candida infections, like other fungal infections, can cause a diverse spectrum of diseases, from superficial and mucosal infections to invasive disease with internal organ involvement [10]. Invasive infections caused by these organisms are often referred to as invasive candidiasis (IC) and are responsible for most cases of IFIs [10, 15]. IC is a growing concern in healthcare facilities being the most common fungal disease among hospitalized patients, with mortality rates that can reach 40% even when patients are receiving antifungal therapy [21]. The infection consists of the presence of *Candida* spp. in sterile sites such as internal organs (deep-seated), *e.g.*, peritonitis, intra-abdominal, abscess, and/or bloodstream. The latter is often referred to as candidemia. Deep-seated candidiasis may be due to direct inoculation or hematogenous dissemination [15, 21]. It

may occur with or without candidemia, in some cases, fungi are detected in blood cultures, but no primary source of infection is recognized [15, 21]. *C. albicans* has been reported as one of the top five infection agents involved in sepsis [24].

Fungal infections are not mandatory reportable diseases, therefore there is no accurate data on their global prevalence [13]. Candidemia accounts for more than 90% of all fungal bloodstream infections (BSIs). It is the third to fourth most common cause of healthcare-associated BSIs in the United States and sixth to tenth in Europe [18, 25, 26].

Candida spp. can establish infection thanks to several virulence factors. These factors include the ability of adherence to epithelial cells, secretion of hydrolytic enzymes that induce host cell damage, ability to produce biofilms, metabolic and stress adaptation, and, with the exception of *C. glabrata*, the ability to shift between yeast and filamentous forms [4, 5].

Almost all *Candida* spp. are polymorphic organisms that can switch between two distinct states, yeast, and hyphal morphologies. Morphogenetic flexibility contributes to the species virulence, as mutants that are unable to undergo the transition are often attenuated in virulence and have reduced pathogenicity [5].

Filamentous forms are associated with tissue invasion and dissemination [5, 27, 28]. Hyphal cells are implicated in pathogenicity, as they express virulence factors, such as adhesins and proteases [28]. Hyphal initiation and maintenance depend on the host environment and different signaling cascades are pivotal in this process [5, 28].

Morphogenesis is also linked to the ability of *C. albicans* to defeat the host immune system, facilitating the escape from neutrophils and macrophages. In fact, part of the pathogenicity of *C. albicans* is due to the ability to evade the immune system and deceive the host immune cells [5, 13].

C. glabrata virulence factors are not as well understood as those of *C. albicans*, but there seem to be significant differences. *C. glabrata* pathogenicity appears to be independent of the yeast morphology [29]. The intrinsic high resistance of *C. glabrata* to fluconazole, the first-line treatment for IC, is a significant factor underlying this pathogen's success and emergence, moreover, this species appears to develop drug resistance at a higher rate compared to other *Candida* spp. [29, 30].

C. glabrata has unique cell wall organization features, including a group of GPI-linked aspartyl proteases, also known as yapsins, which are important virulence factors as they

modulate the host immune response [29]. The main adhesins in *C. glabrata* belong to the epithelial adhesin (EPA) family and assist *C. glabrata* to bind to the host epithelial cells and enter macrophages [29, 31]. These proteins are also important in the ability of the pathogen to adhere to medical devices and initiate biofilm formation [29]. Another important pathogenic attribute is the capacity of *C. glabrata* to evade and surpass the host immune system, survive cellular engulfment and resist antifungal treatment [29]. *C. glabrata* does not cause significant damage to macrophages, but once engulfed, it can inhibit phagosome maturation, presumably by preventing its acidification [32]. The yeast also induces a low level of cytokine response and appears to be adapted to long-term confinement within macrophage phagosomes [33]. It is acknowledged that *C. glabrata* may use the 'trojan horse mechanism' of macrophage phagocytosis to cross epithelial barriers and disseminate [33].

Biofilm formation is also important in yeast virulence (**Figure 1.2**) [28]. Most diseases caused by *Candida* spp. are associated with the formation of biofilms on abiotic (*e.g.* medical devices) or host surfaces and are significant risk factors for IC [28]. Biofilms are complex organized structures composed of microbial cells (single or mixed species), embedded in an extracellular polysaccharide substance (EPS) that provides protection. Biofilms are intrinsically resistant to the host immune system and antifungal drugs [34].

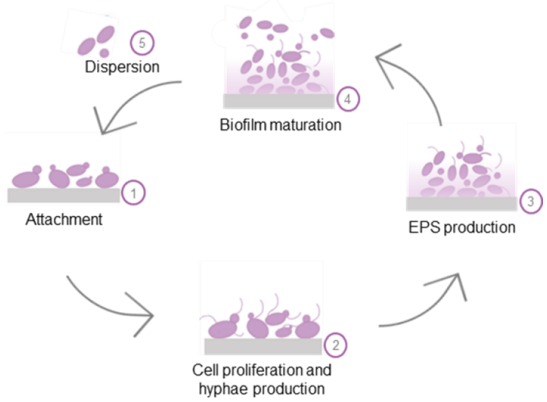

Figure 1.2. ***Candida spp. biofilm formation****. The first step is the attachment of yeast cells to a biotic or abiotic surface (**1**). In the early phase of biofilm formation, cell proliferation and hyphae formation occur (**2**) and the extracellular matrix is produced afterward (**3**). In the maturation phase, there is an accumulation of extracellular matrix (**4**). Finally, cells can disperse to a new location and form a new biofilm (**5**). Adapted from [35].*

1.3. Antifungals available to treat invasive fungal infections

The main challenges for the management of IFIs are prevention, early diagnosis with identification of the causative species, and timely adequate antifungal therapy [21].

A very limited number of antifungal drugs have shown to be effective in the treatment of IFIs. The current treatment of systemic mycoses is mainly based on polyenes, azoles, and echinocandins antifungals, but these drugs are far from meeting all clinical needs [36].

The conventional drugs used in IFIs treatment have limitations such as restricted formulations (some are exclusively intravenous), toxicity, side effects, interactions with other substances, and emergence of drug resistance, among others [12].

Fungi are metabolically similar to mammalian cells and offer few pathogen-specific druggable targets, which makes the development of new antifungals a demanding task. Many antifungal drugs have been designed to target specific representative components of the fungal cell structure (membrane and cell wall) in order to minimize host toxicity [5]. The current arsenal of antifungal drugs targets either ergosterol (polyenes and azoles) or 1,3-β-D-glucans (echinocandins), major components of the fungal membrane and cell wall, respectively (**Table 1.1**) [5, 37]. According to pharmacodynamic properties, these antifungals are categorized as fungistatic (azoles and echinocandins on *Aspergillus* spp.) or fungicidal (amphotericin B and echinocandins on *Candida* spp.) [38].

Table 1.1. ***Systemic antifungal agents.***

Site of action	Mode of action	Drug Class	Drugs
Cell membrane	Inhibition of ergosterol biosynthesis	Azoles	Triazoles: Fluconazole, Itraconazole, Voriconazole, Posaconazole
	Interaction with ergosterol and oxidative stress	Polyenes	Amphotericin B
Cell Wall	Inhibition of 1,3-β-D-glucan synthesis	Echinocandins	Anidulafungin, Caspofungin, Micafungin

1.3.1. Polyenes

Polyenes were the first class of antifungal drugs developed. They are natural compounds produced by *Streptomyces nodosus*, and amphotericin B was the first drug to be licensed (**Figure 1.3**) [37, 38]. For more than 30 years, amphotericin B was the only drug available to treat IFIs [37, 38]. Polyenes form membrane aggregates that bind irreversibly to ergosterol, resulting in destabilization and disruption of membrane integrity, which ultimately leads to cell death (**Table 1.1**). Additionally, they are thought to generate oxidative stress, which increases membrane permeability and boosts the drugs antifungal action [12, 37]. Polyene drugs also interact with cholesterol and therefore can be toxic to mammalian cells, which to some extent limits their widespread use [37, 38].

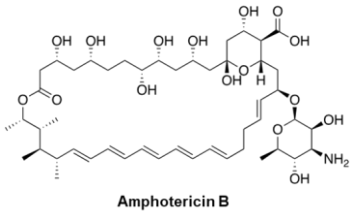

Figure 1.3. ***Chemical structure of Amphotericin B.***

1.3.2. Azoles

The approval of azoles at the turn of the 20th century was a major advance in the effective treatment of local and systemic fungal infections [17].

Azoles are synthetic organic molecules that include triazoles (*e.g.*, fluconazole, itraconazole, voriconazole, and posaconazole) (**Figure 1.4**) and imidazoles (*e.g.*, ketoconazole, miconazole, and clotrimazole). Current azole treatment of IFIs is primarily based on triazoles due to their safety profile [12, 39].

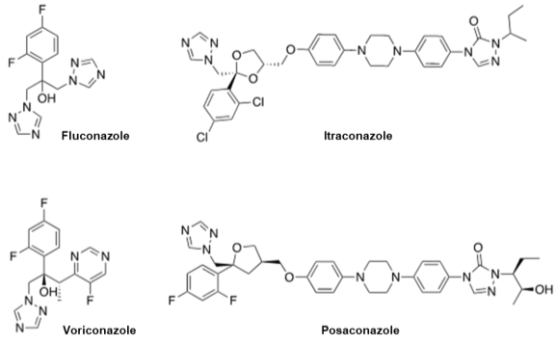

Figure 1.4. ***Chemical structure of some triazole antifungals in clinical use.***

Azole antifungals have been the treatment of choice for most IC for decades, since they have good bioavailability, a robust safety profile, and are available in intravenous and oral formulations [40]. These characteristics have made this drug class widely used in the prophylaxis of IC and cryptococcal infections that often afflicted HIV (human immunodeficiency virus) patients, especially in the pre-HAART (highly active antiretroviral therapy) era [40, 41].

Azoles function by inhibiting the C14α-demethylase, a fungal cytochrome P450 dependent enzyme, encoded by the *ERG11* gene, which converts lanosterol to C14-dimethyl-lanosterol (**Figure 1.5**). As a consequence, there is a reduction in the synthesis of ergosterol and cells accumulate toxic sterols that together lead to severe membrane stress and growth arrest [37, 42, 43]. However, the current available azoles are not completely selective for fungi, and the inhibition of human cytochrome enzymes is frequently responsible for pharmacokinetic interactions and adverse effects [12, 37, 42].

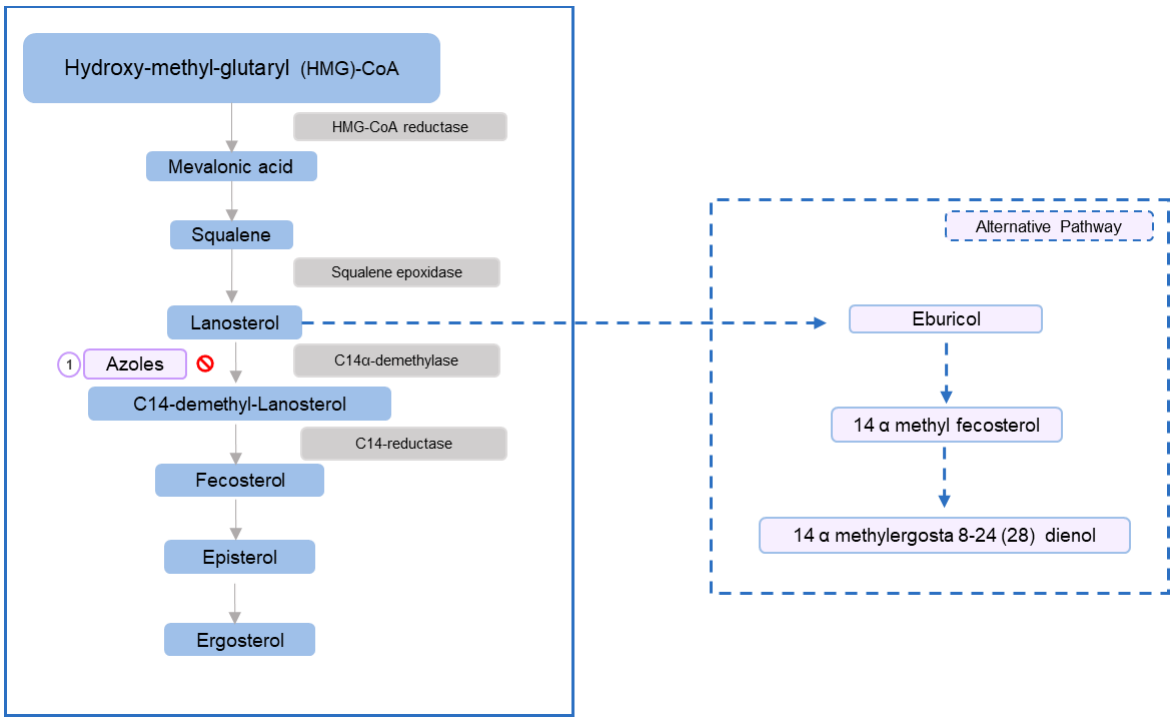

Figure 1.5. ***Mechanism of action of azole antifungals.*** *Azoles inhibit the enzyme C14α-demethylase of the ergosterol biosynthesis pathway (**1**). This inhibition reduces ergosterol and drives the accumulation of sterol precursors, including 14-methylated sterols, which results in a change in membrane fluidity and function. Adapted from [44].*

1.3.3. Echinocandins

Echinocandins are the newest class of antifungal agents, they are semisynthetic lipopeptides acting as inhibitors of 1,3-β-D-glucan synthase (an enzyme required for the synthesis of the cell wall 1,3-β-glucan) and promoting cell wall stress and loss of cell wall integrity (**Table 1.1**) [37].

The absence of cell wall in mammalian cells makes these agents selective for fungi and less toxic for other eukaryotes [5]. The safety and effective profile, together with low drug-drug interactions make this class of antifungals the preferred first-line therapy for most IC [21, 42]. In addition, echinocandins also have fungicidal activity against most *Candida* spp., which is particularly relevant in medical scenarios of immunosuppression [21].

The class of echinocandin antifungals includes the drugs caspofungin, anidulafungin, and micafungin, all of which require intravenous administration (**Figure 1.6**) [26].

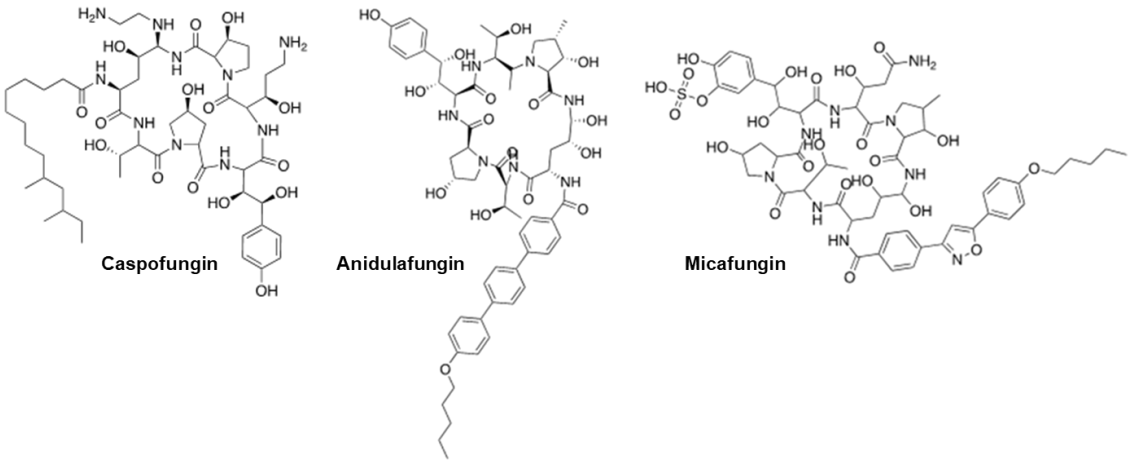

Figure 1.6. ***Chemical structures of available echinocandin antifungals.***

The antifungal classes currently available for the treatment of IFIs have some limitations, such as the narrow spectrum of action, issues related to both pharmacokinetics and pharmacodynamics, limited formulations, and of particular concern, the emergence of mechanisms of resistance [11].

1.4. Resistance to current antifungal agents

The prevalence of antimicrobial resistance has increased significantly in recent decades, and antifungal agents are no exception [17]. Misuse and overuse of antimicrobials are the main drivers of antimicrobial resistance (AMR) [45]. AMR is a frightening threat to people worldwide and is considered by WHO one of the top 10 global public health threats [45].

The prevalence of drug-resistant fungal infections is increasing, making the development of different treatment options an urgent matter [46]. In recent years we have witnessed a worrying increase in antifungal resistance to all classes of antifungal drugs [43]. This is especially concerning in the context of IFIs because only three classes are available for effective treatment [47].

Resistance to antifungal drugs can arise through several mechanisms, including altered drug-target interactions, overexpression of drug target or drug efflux transporters, and biofilm formation [48].

A variety of mechanisms for azole resistance have been identified, including target site modification, target site overexpression, decreased drug accumulation due to increased drug efflux, decreased permeability of the fungal membrane to the drug, and biofilm formation [49, 50]. Increased drug efflux is the most common mechanism of azole resistance and it is primarily caused by mutations in transcription factors that control ATP-binding cassette (ABC) transporters and major facilitator superfamily (MFS) pumps, leading to an increase of efflux drug pumps in the cell [47]. ABC and MFS transporters reduce drug activity by transporting it out of the cell, thereby decreasing its intracellular concentration [49].

Azole drug resistance can also be caused by changes in drug target expression or mutations within the target protein sequence [47]. Some mutations in *C. albicans ERG11* gene lead to overexpression of Erg11, which reduces azole susceptibility. This phenomenon has also been observed in resistant non-*albicans* species, but the underlying mechanism is unknown [47].

It appears that azole resistance develops gradually as a result of drug-induced sequential modifications, which are more likely to occur when the drug is taken for extended periods [49].

Polyene drugs act directly on the fungal membrane. Potential mechanisms involved in polyene resistance include a decrease in ergosterol content, replacement of ergosterol by sterols that do not bind to polyenes, and reorientation or masking of existing ergosterol [50].

Resistance to echinocandins is gradually increasing due to the intensified use of this drug class in hospitals. Resistance is associated with mutations in the *FKS* gene, which encodes the catalytic subunit of 1,3-β-D-glucan synthase, the enzyme involved in the synthesis of 1,3-β-D-glucan, major cell wall component [43, 48].

Resistance to echinocandins in *C. glabrata* clinical isolates is particularly concerning, considering that echinocandins are the first-line treatment for *C. glabrata* infections, which are inherently less susceptible to fluconazole [51]. *C. glabrata* and *C. tropicalis* have the highest rates of azole and echinocandin resistance [47].

Corroborating the severity of this scenario, the CDC has classified drug-resistant *Candida* species as a serious threat to human health [52].

In this context, it is clear that there is an urgent need to reinforce investment in the discovery of new antifungals to efficiently tackle fungal infections resistant to current drugs.

1.5. The marine environment: a reservoir of antifungal compounds

Nature has been a source of medicines, and in modern drug discovery, natural products (NPs) continue to play an important role. NPs are products of the secondary metabolism of organisms, some of which are interesting candidates for drug development [53]. The NPs used as medicines were mostly obtained from tropical and subtropical regions, certainly due to their great biodiversity [54]. *In vivo*, NPs are generally used as competitive tools to ensure survival [55]. They are not biosynthesized by typical metabolic pathways and have no primary functions in the growth, development, or reproduction of the organisms [54].

Water covers over 71% of the Earth's surface and 50-80% of all life on Earth resides in the oceans [56]. In the marine ecosystem, there are more than 250,000 studied species and a much larger number of unknown or undescribed species, which translates into a great diversity of unexplored NPs [57, 58]. Therefore, the marine environment, still poorly explored, provides one of the most abundant platforms for the discovery of new

high-value NPs [54] and, in this context, diving expeditions in the late 1970s drove drug discovery programs to the oceans [56].

Marine organisms can tolerate extreme conditions of pressure, luminosity, salinity, and temperature. To survive in this unique environment, they produce secondary metabolites that act as chemical defenses against predation, promote interspecies communication, or confer an advantage in the competition for space and food [56, 59, 60]. These secondary metabolites also known as marine natural products (MNPs) are unique and may have pharmacological activities of interest to human health [58, 61]. The MNPs identified so far comprise a wide variety of chemical compounds such as alkaloids, anthraquinones, peptides, polysaccharides, polyketides, and terpenes [62]. They are known to have diverse biological activities including antimicrobial, antidiabetic, antifungal, anticoagulant, anti-inflammatory, anti-cancer, and antioxidant activities, among others [54, 61, 63-65]. MNPs of interest may be used directly as pharmaceutical drugs or inspire researchers to develop or synthesize other drug-like molecules [66, 67].

Among the marine organisms producing MNPs of pharmaceutical interest are algae, sponges, corals, and other invertebrates, as well as their microbiota. Sponges, together with their microbial communities, synthesize MNPs with the broadest spectrum of bioactivity, including those with antifungal activity (**Figure 1.7**) [56, 68].

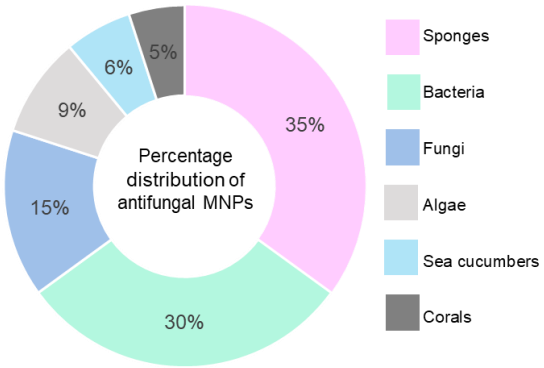

Figure 1.7. ***Distribution of isolated natural products with antifungal activity among different marine organism sources.*** *According to MarinLit* database [69], *until mid-2015 sponges were the predominant sources of MNPs. Adapted from* [63].

1.6. Approved marine natural products of pharmaceutical interest

Several MNP-derived drugs have already been approved and many others are in pre-clinical and clinical trials [58, 60]. It is difficult to accurately determine the current number of MNP drug candidates in clinical development, since this information is fragmented in the literature or not publicly available. Despite the high number of structurally unique bioactive MNPs identified so far, many of which with significant biological activity, the vast majority failed to pass pharmaceutical pre-clinical testing. In fact, just a few have been commercialized and the global marine drug discovery pipeline includes only 14 drugs approved and 33 in clinical trials (phase I-IV) (**Figure 1.8**) [54].

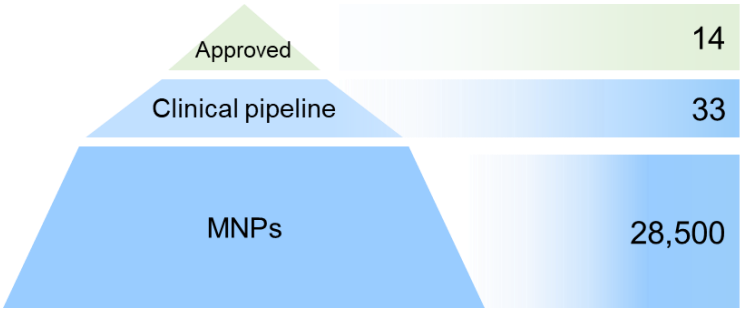

Figure 1.8. ***Approved drugs derived from MNPs.*** *Adapted* from [54].

The first MNPs discovered of pharmaceutical interest for humans were the arabinose-nucleosides spongouridine and spongothymidine, isolated from the Caribbean sponge *Tectitethya crypta* [56, 60]. The presence of arabinose instead of ribose in spongouridine and spongothyminide has inspired the development of the commercial drugs cytarabine and vidarabine [60]. Cytarabine or *ara*-C is an anti-leukemia drug approved by the FDA (Food and Drug Administration, United States) in 1969. Cytarabine is still used nowadays as the therapy of choice for myeloid leukemia, non-Hodgkin's lymphoma, and meningeal leukemia [54].

Vidarabine or *ara*-A was approved in 1976 by FDA as an antiviral drug, however, it is more toxic and less metabolically stable than other current antivirals and for these reasons, it is no longer in use [54, 60].

Halichondrin B is a macrocyclic polyether that was first isolated from the sponge *Halichondria okadai* in 1986 and found to be highly cytotoxic to murine leukemia cells. The difficulty in gathering enough material for further studies has affected the evaluation of its clinical application, but chemical synthesis was achieved in 1991 [54]. Later a

simpler macrocyclic ketone analog (eribulin mesylate) with similar activity was developed [54].

In 2004, the pain drug ziconotide was approved. Ziconotide was obtained by chemical synthesis but it is structurally identical to ω-conotoxin MVIIA isolated from the venom of the marine cone snail *Conus magus* [60, 66]. Ziconotide has been approved for the treatment of severe chronic pain associated with cancer, AIDS (acquired immunodeficiency syndrome), and neuropathies [54].

Trabectedin is a marine anticancer alkaloid with a mechanism of action that is still unknown. The active compound is a MNP derived from *Ecteinascidia turbinate*, a Caribbean sea squirt [54]. Trabectedin was licensed in 2007 as an anticancer drug for the treatment of advanced soft tissue sarcoma and relapsed platinum-sensitive ovarian cancer [54, 66].

Brentuximab vedotin was the latest marine drug to be approved and is used to treat Hodgkin and systemic anaplastic large cell lymphoma. Brentuximab vedotin is based on a synthetic dolastatin 10 analog linked to an antibody. Dolastatin 10 was discovered in the sea hare *Dolabella auricularia*, in 1972. Dolastatin 10 is one of the most powerful anticancer agents used against a variety of cancer types [54].

Carrageenans are sulfated polysaccharides derived from red edible seaweeds, typically of the *Rhodophyceae* class. A novel antiviral nasal spray containing iota-carrageenan has been demonstrated to be clinically effective against early symptoms of the common cold by forming a physical antiviral barrier in the nasal cavity [54].

The most significant marine drugs on the market are listed in **Table 1.2**, according to their marine source and clinical application.

Table 1.2. ***Approved drugs derived from MNPs.*** *Most important marine drugs and their structures [68]. High-resolution images of cytarabine, vidarabine, ziconotide, eribulin mesylate, omega-3-acid ethyl esters, trabectedin, brentuximab vedotin and, iota-carrageenan are available in Figure S.1.*

Name	Marine Source	Clinical application	Structure
Cytarabine (*ara*-C)	Sponge	Cancer	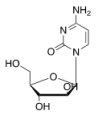
Vidarabine (*ara*-A)	Sponge	Antiviral	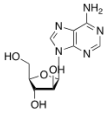
Ziconotide	Cone snail	Pain	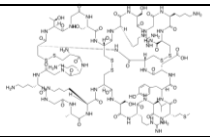
Eribulin mesylate	Sponge	Cancer	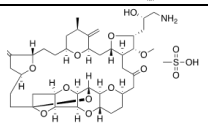
Omega-3-acid ethyl esters	Fish	Hypertriglyceridemia	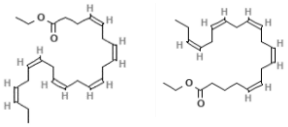
Trabectedin	Tunicate	Cancer	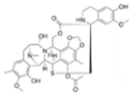
Brentuximab vedotin	Mollusk	Cancer	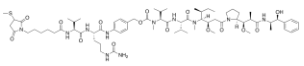
Iota-carrageenan	Seaweed	Common cold	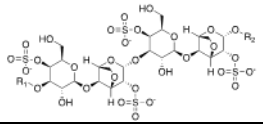

1.7. Antifungal activity of MNPs

Several antifungal compounds have been isolated from marine organisms, but so far, no antifungal MNP-based drugs have been approved. Most MNPs with antifungal activity have been isolated from marine invertebrates such as sponges, corals, algae, and sea cucumbers.

1.7.1. Antifungal compounds isolated from marine sponges

The marine sponge *Dysidea arenaria* produces the metabolite 9α,11α-epoxycholest-7-ene-3β,5α,6α,19-tetrol 6-acetate (ECTA) that when combined with fluconazole leads to an increase in the antifungal activity of the latter [49].

The compound 8,8′-dienecyclostellettamine isolated from the marine sponge *Amphimedon compressa* has antifungal activity against *Candida* spp., as does zamamidine D isolated from a species of the same genus [56].

The NPs 10-formamido-kalihinene and 15-formamido-kalihinene, found in the marine sponge *Acanthella cavernosa* have antifungal properties, including activity against *Candida* spp. [61].

Aaptamines are molecules extracted from the genus *Aaptos* with antifungal properties [61].

Crude extracts from the marine sponge *Agelas citrina* have antifungal activity against *Candida* spp. due to the presence of agelasidines C and F [70]. Agelasine B, C, J, and nemoechime G, are found in *Agelas nakamurai* and also have antifungal activity [56]. Ageloxime B and D from *Agelas mauritiana* also present antifungal potential [56]. *Agelas sceprum* is the source of sceptrin with antifungal activity against *Candida* spp. [71]. Nagelamide X to Z from the *Agelas* genus have antifungal activity against *Candida* spp. [56].

Four aurantosides, G to J, have been identified in the sponge *Theonella swinhoei*. Aurantosides G and I exhibit antifungal activity against *Candida* spp. Aurantoside K, found in sponges of the genus *Melophlus*, has antifungal activity, against some resistant strains of *C. albicans* [61].

Batzelladine L, identified in *Monanchora arbuscula,* also has antifungal activity [63, 72].

Callipeltins F to J are antifungal peptides isolated from the marine sponge *Latrunculia* sp. and are active on *C. albicans* [63].

Eurysterols A and B extracted from the marine sponge of the genus *Euryspongia* displayed antifungal activity against *Candida* spp. [49].

Epi-ilimaquinone isolated from the marine sponge *Hippospongia* sp. is active against *Candida* spp. [49].

Haliscosamine found in *Haliclona viscosa* shows antifungal activity [49, 61].

Hemimycalin A, hemimycalin B, and (Z)-5-(4-hydroxybenzylidene) imidazolidine-2,4-dione (Zd1) obtained from *Hemimycale arabica* also have antifungal activity [56].

Hyrtioerectine D to F from the marine sponge of the genus *Hyrtios* have antifungal activity against *Candida* spp. [56].

Plakortide F acid (PFA), derived from the marine sponge *Plakortis halichondrioides,* is active against *Candida* spp. [63].

Poecillastrosides C to E, found in the sponge *Poecillastra compressa,* have antifungal activity [61].

Theonella swinhoei contains theopapuamide A and theonellamide G, which have antifungal activity against *Candida* spp., theonellamide G appears to have antifungal activity against drug resistant *Candida* spp. [61].

Spongistatin 1 found in the marine sponge *Hyrtios erecta,* has antifungal activity against *Candida* spp. [49].

Theopapuamide B and C are molecules found in *Siliquariaspongia mirabilis* with potent antifungal activity [49].

Three polyketides, woodylides A to C were discovered in the sponge *Plakortis simplex*. Woodylides A and C have antifungal activity against *Candida* spp. [61].

Finally, in the sponge *Xestospongia exigua*, xestospongine A, C, and D, are active against antifungal resistant strains of *C. albicans* [49].

The chemical structures of the mentioned compounds are detailed in **Figure 1.9**.

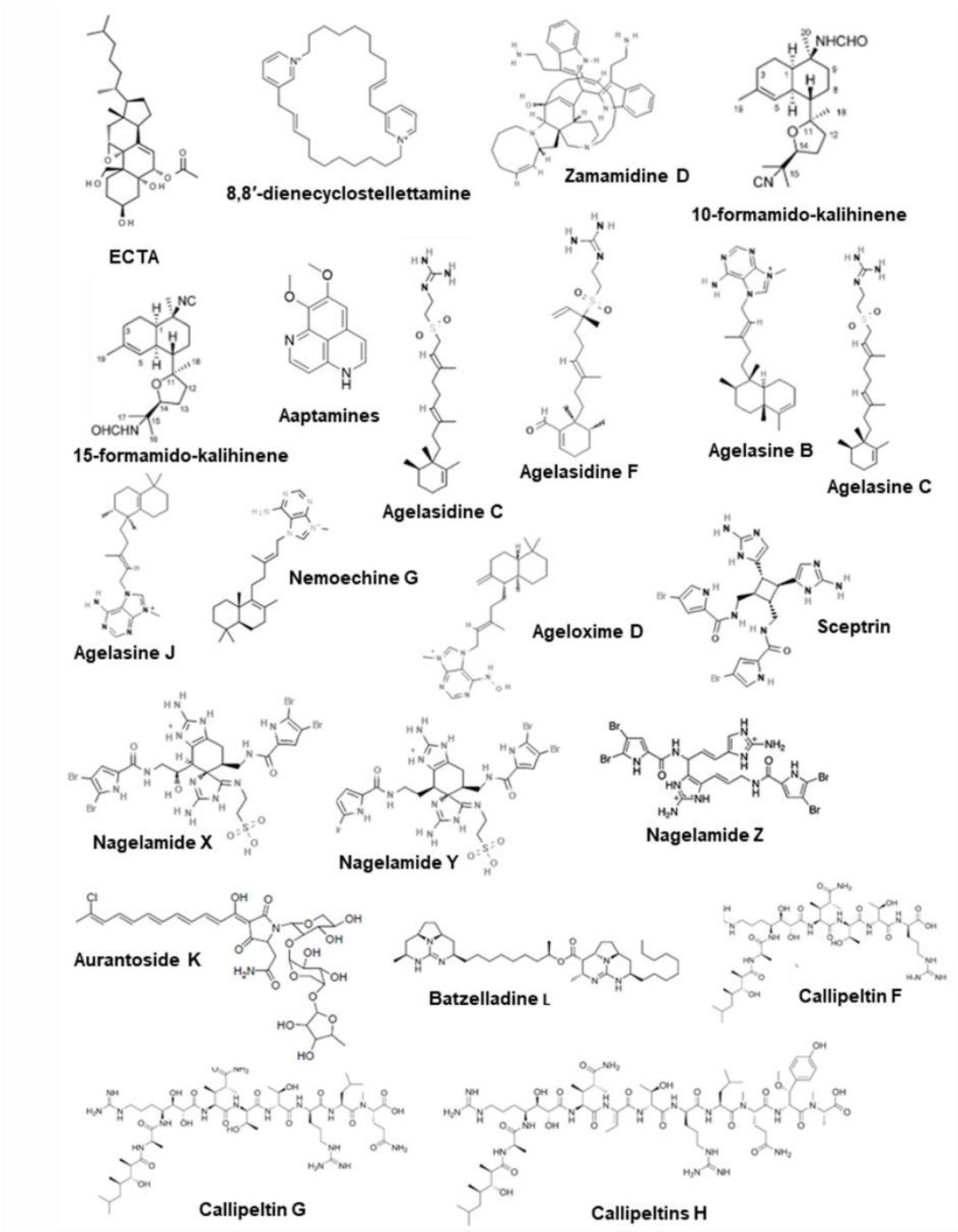
ECTA
8,8′-dienecyclostellettamine
Zamamidine D
10-formamido-kalihinene
15-formamido-kalihinene
Aaptamines
Agelasidine C
Agelasidine F
Agelasine B
Agelasine C
Agelasine J
Nemoechine G
Ageloxime D
Sceptrin
Nagelamide X
Nagelamide Y
Nagelamide Z
Aurantoside K
Batzelladine L
Callipeltin F
Callipeltin G
Callipeltins H

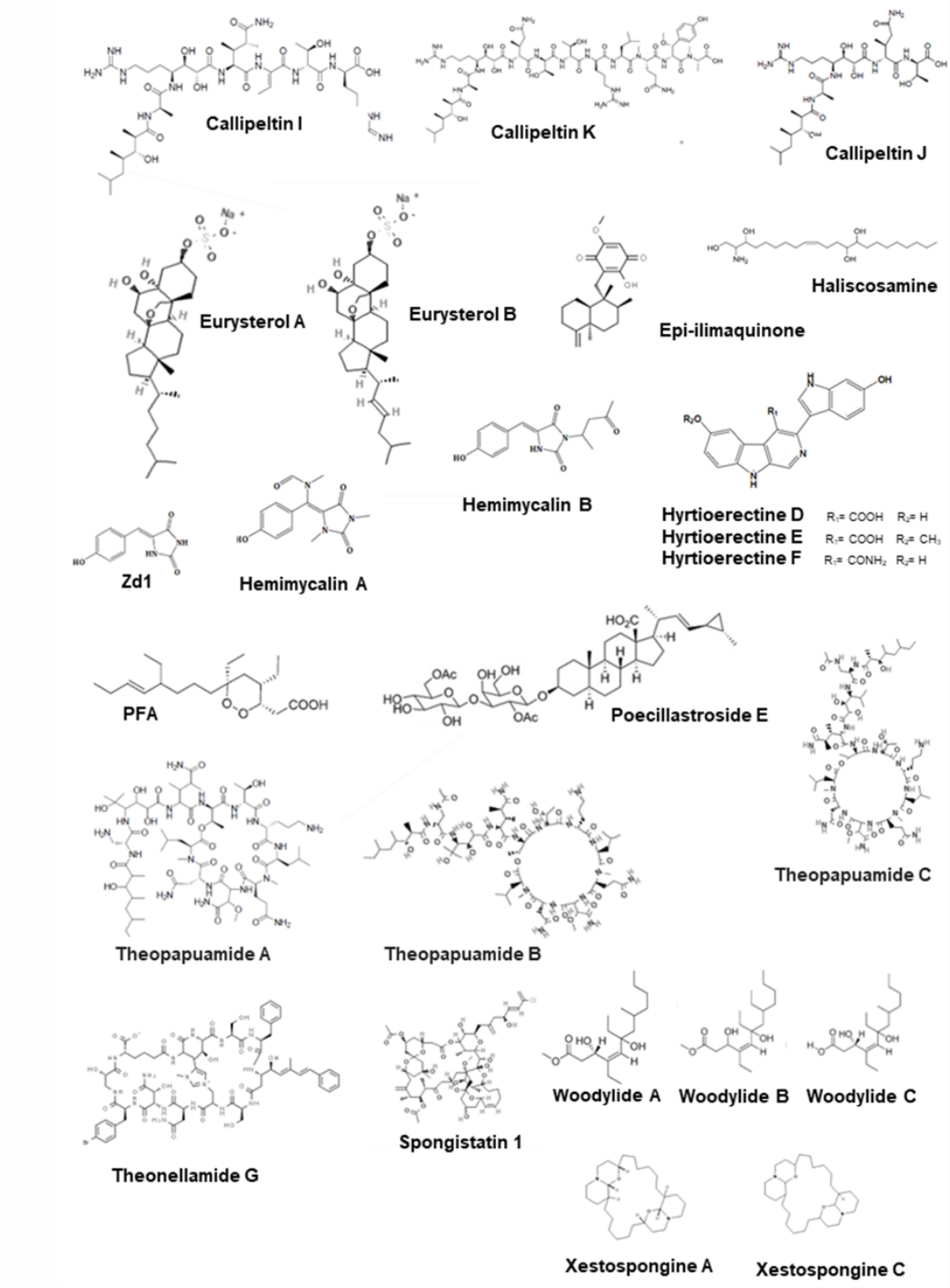

Figure 1.9. ***Selected structures of compounds from marine sponges with reported antifungal activity.***

1.7.2. Antifungal compounds isolated from corals

Cembrene C, isolated from the coral *Sarcophyton trocheliophorum* was shown to be active against *Candida* spp. [49]. The compound (2S,3R)-2-aminododecan-3-ol, isolated from the ascidian *Clavelina oblonga*, is active against *Candida* spp. [63]. The structures of these compounds are depicted in **Figure 1.10.**

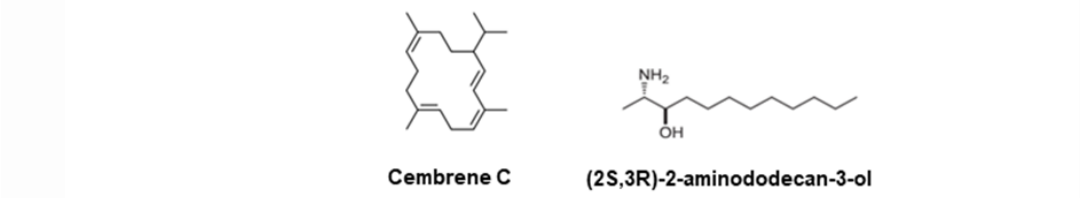

Figure 1.10. ***Selected structures of compounds from corals with reported antifungal activity.***

1.7.3. Antifungal compounds isolated from marine algae

Capisterones A and B from the marine green algae *Penicillus capitatus* have antifungal properties and can circumvent fluconazole resistance [73]. Caulerprenylol B, derived from the green alga *Caulerpa racemose*, has antifungal activity [63]. Lobophorolide, derived from the marine brown algae *Lobophora variegate*, is effective against *Candida* spp. [49]. **Figure 1.11** highlights the chemical structures of the mentioned compounds.

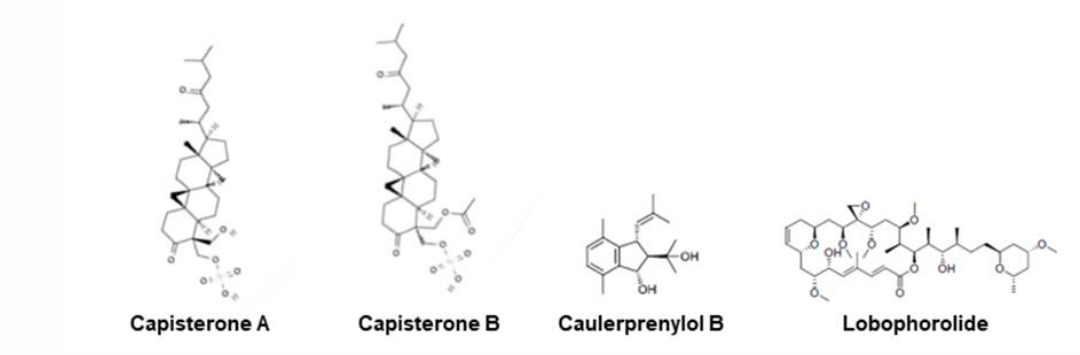

Figure 1.11. ***Selected structures of compounds from marine algae with reported antifungal activity.***

1.7.4. Antifungal compounds isolated from sea cucumbers

The sea cucumber *Stichopus variegates* produce variegatuside D and E, which have antifungal activity against *Candida* spp. [61]. Holothurin A and echinoside A, both isolated from the sea cucumber *Pearsontrhuria graeffei* were also effective against *Candida* spp. [61]. Marmoratoside A, 17-alpha-hydroxy impatienside A, 25-acetoxy bivittoside D, impatienside A and, bivittoside D isolated from *Bohadschia marmorata*

Jaeger have antifungal activity against *Candida* spp. [63]. Patagonicoside A isolated from *Psolus patagonicus* also has antifungal activity [63]. Holotoxin D1 and stichloroside C1 from the sea cucumber *Apostichopus japonicus*, have antifungal activity against *Candida* spp. [63]. Scabraside A was isolated from *Holothuria scabra* and showed antifungal activity against *Candida* spp. [63]. The structure of these compounds is represented in **Figure 1.12.**

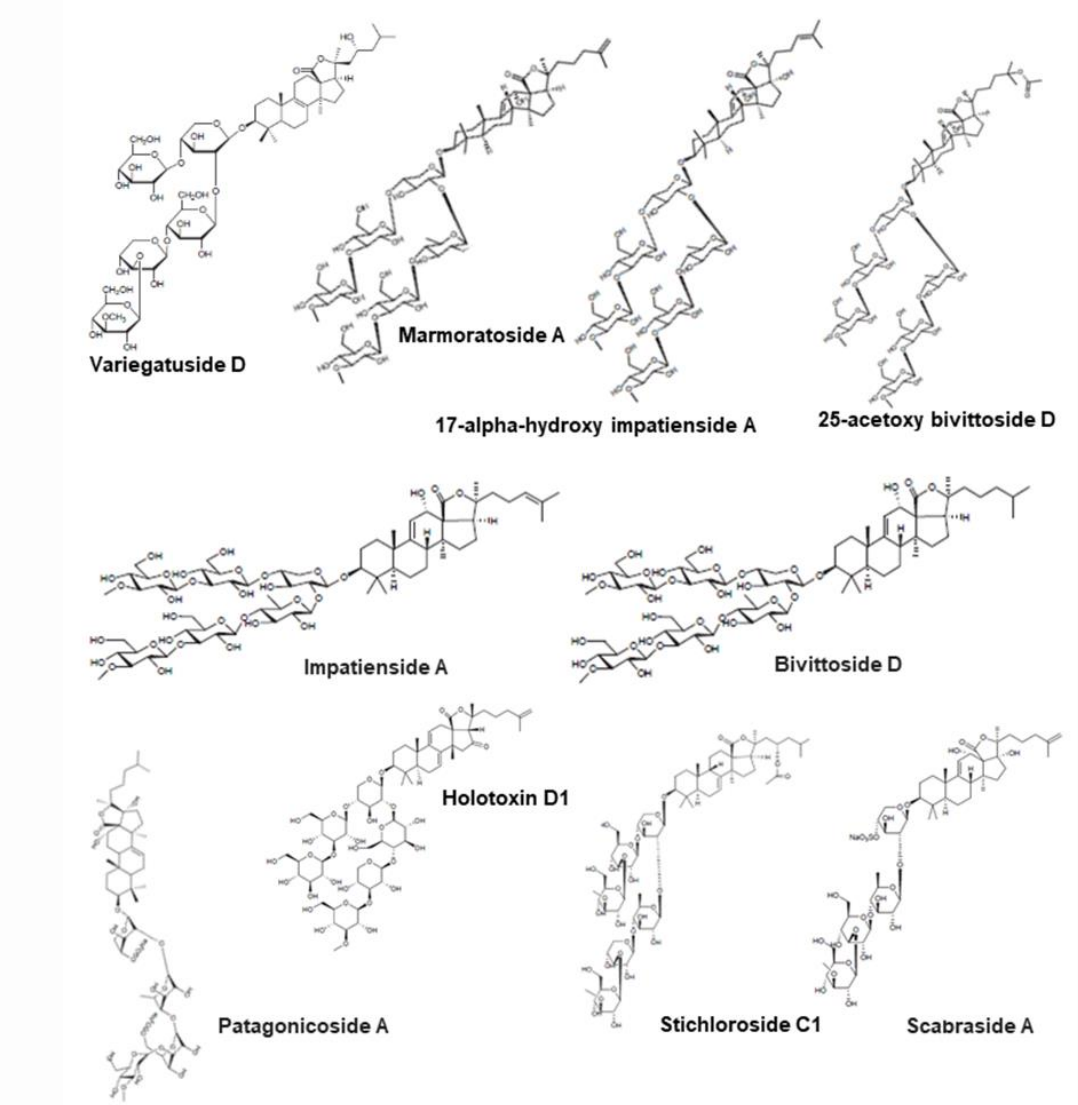

Figure 1.12. ***Selected structures of compounds from sea cucumbers with reported antifungal activity.***

1.8. Marine natural products: challenges in lab-to-market transfer

In order to reach the market, a MNP must go through several steps, as depicted in **Figure 1.13** [54, 74]. Crude marine extracts with promising pharmacological activities are fractionated until pure bioactive compounds are obtained. The extraction method chosen determines which compound classes are present in the extract and the compounds can be extracted with several solvents of different polarities to maximize the diversity of the extracted MNPs. Once the bioactive compound is isolated and characterized, the molecular targets must be identified, and the mechanism of action (MoA) determined. Pre-clinical studies and clinical trials are carried out with the pure compound before it can reach the market [54, 74].

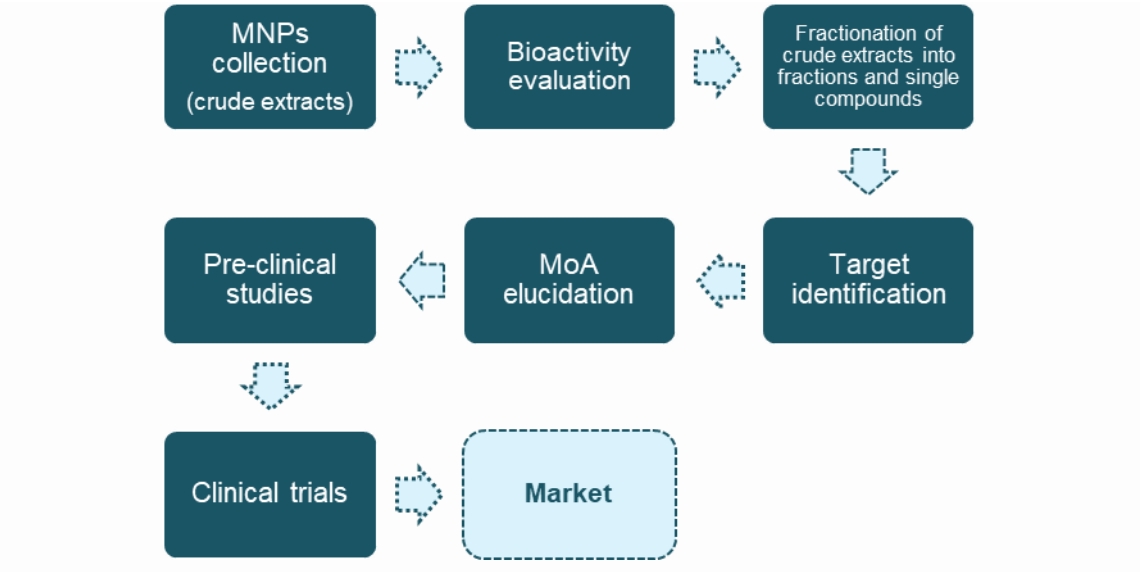

Figure 1.13. ***Flow chart summarizing the entry process of a marine natural product on the market.*** *Crude extracts are collected from marine species. After identifying a crude extract with promising pharmacological activity, fractionation is carried out to identify the bioactive chemical. The molecular targets must next be identified, and the mechanism of action defined. Before these drugs reach the market, preclinical studies and then clinical trials are conducted using pure MNP. Adapted from* [54, 74].

To identify hit compounds, a variety of screening options exist, with HTS (High-throughput screening) being the most extensively employed in the case of NPs. The HTS approach requires the creation of high-quality libraries. In NP discovery, the library should ideally be made of crude extracts, simplified extract fractions, or pure compounds. When compared to pure compound libraries, crude extract libraries are easier and cheaper to develop but they have significant drawbacks. Crude extracts are complex combinations of numerous chemicals that can synergistically interact, explaining why bioactivity disappears sometimes in purified fractions or in the final pure compounds. False-negative

results can also occur, either because an active metabolite is present in trace amounts in the crude extract or because other chemicals interfere antagonistically with its activity. Pre-fractionated library screening is an excellent method for avoiding these problems, as it can remove numerous unwanted molecules [54]. The resulting fractions can range in complexity from a combination of several compounds to a single major component, depending on the pre-fractionation procedure employed and on the number of compounds in the original crude extract.

MNP discovery may also face reproducibility issues. As an example, the high frequency of bioactive metabolites in sponges, functioning as defense compounds against predation and fouling organism overgrowth, is highest in ecosystems such as coral reefs, which are characterized by intense competition and food pressure [54]. However, environmental factors do not remain constant, and, as a consequence, the same organism does not always produce the same metabolite. Another factor to consider in the case of marine organisms is that bioactive metabolites are occasionally produced by their associated microbiota [54].

Another problem that researchers face in the development of MNP-based drugs is the amount of biological material needed. While initial *in vitro* experiments may only require small amounts (in the order of micrograms to milligrams), these numbers rapidly increase once *in vivo* testing for safety, toxicity, bioavailability, or formulation development is required [11, 75].

Together all these challenges make the development of MNPs difficult and delay their introduction on the market [56].

1.9. The potential of the marine Yucatan Peninsula

Marine organisms collected from tropical ecosystems are the major source of MNPs [56]. Mexico has 2,946,825 km^2 of maritime extension with coastlines that stretch along 11,122 km from the Pacific Ocean to the Caribbean Sea and the Gulf of Mexico [71, 76]. The Yucatan Peninsula (YP) in Mexico comprises 1,500 km of the coastline of the states of Campeche, Quintana Roo, and Yucatan. YP has great potential as a source of MNPs due to its unique biodiversity. It remains largely unexplored and is therefore a promising starting point for the development of new drugs [71, 72, 77].

The secondary metabolites already identified from marine organism that inhabit the YP showed a great diversity of chemical structures and biological activities [72]. So far, 66 MNPs were identified from 18 species belonging to the phyla Proteobacteria (*Acinetobacter* sp.), Chordata (ascidian: *Stomozoa roseola*), Cnidaria (coral: *Pterogorgia anceps),* Echinodermata (sea cucumbers: *Astichopus multifidus* and *Halodeima floridana*), Mollusca (mollusks: *Conasprella delessertii, Conus spurius, Octopus maya,* and *Polystira albida*), Porifera (sponges: *Halichondria magniconulosa, Haliclona Reniera tubifera, Spongia tubulifera,* and *Axinella corrugata*), Rhodophyta (red algae: *Solieria filiformis*), and Phaeophyta (brown algae: *Dictyota ciliolata, Lobophora variegata, Padina sanctae-crucis,* and *Turbinaria tricostata*) [72].

1.10. Objectives

New antifungals are urgently required to effectively fight invasive fungal infections recalcitrant to available treatments. MNPs have shown to be promising leads in drug development, and several studies suggest that these compounds might be the way forward to fulfill that medical need. In this context, the main objectives of this study are:

- To screen two libraries of marine extracts from Yucatan Peninsula, Mexico, for antifungal activity against *Candida* species;
- To fractionate the most promising marine extracts and characterize their antifungal activity;
- To assess their *in vitro* toxicity;
- To start identifying the active MNP.

Chapter 2 – Materials and Methods

2.1. Collection of marine species

Samples were collected by snorkelling and SCUBA (Self-Contained Underwater Breathing Apparatus) diving in different periods and coastal areas of the Yucatan Peninsula, Mexico (**Figure 2.1**). The selected species originated two different libraries: Library I with 65 crude marine extracts and Library II with 44 crude marine extracts. Species collection was conducted by the Autonomous University of Yucatan (Mexico).

Figure 2.1. ***The Yucatan Peninsula, Mexico***.

2.2. Species identification

The taxonomic information of the species that originated the 65 crude extracts composing Library I is shown in **Table S.1.** As for Library II, the taxonomic identification is still in progress (collaboration with the Autonomous University of Yucatan).

2.3. Preparation of the organic extracts

Tissue slices of each species were extracted several times with dichloromethane-methanol (1:1), at 25 ºC for 24 hours. The extracts were filtered and, the obtained filtrates were dried by evaporation under reduced pressure in a rotatory evaporator at 40 ºC. The dried crude extracts were stored at -20 ºC and sent to ITQB NOVA. The extracts were codified as A1 to A65 (Library I) and O1 to O44 (Library II).

2.4. Antifungal susceptibility testing

2.4.1. Stock solutions of crude extracts and fractions

Crude extracts of Library I were dissolved in dimethyl sulfoxide (DMSO) to the final concentration shown in **Table S.2**. Fractions of hexane (HF), dichloromethane (DF), *n*-butanol (BF), water-methanol (WMF), and water (WF), obtained after liquid-liquid and solid phase extraction (SPE) of Library I were dissolved in DMSO to the final concentration shown in **Tables S.3** and **S.4.** Crude extracts/fractions of Library II were dissolved in DMSO to a concentration of 10 mg/mL and a concentration of 250 µg/mL was tested for antifungal activity.

2.4.2. Strains and culture conditions

The fungal strains used in this work were purchased from the American Type Culture Collection (ATCC) and are listed in **Table 2.1**.

Candida spp. were maintained in YPD agar plates (Yeast extract peptone dextrose media: yeast extract 10 g/L; peptone 20 g/L; glucose 20 g/L; agar 1.5%, sterilized by autoclave) and grown at 37 ºC (*C. glabrata*) or 30 ºC (other *Candida* spp.).

Strains (glycerol stocks) were streaked on YPD agar plates every week.

Table 2.1. ***Yeast species used in the study.***

Species	Source
Candida glabrata ATCC 2001	ATCC
Candida albicans ATCC SC 5314	ATCC
Candida krusei ATCC 6258	ATCC
Candida tropicalis ATCC 7501	ATCC
Candida parapsilosis ATCC 22019	ATCC

2.4.3. Screening of the marine crude extracts and fractions

A volume of 5 µL of each crude extract dissolved in DMSO was added to individual wells of a 96-well plate, containing 95 µL of RPMI (Roswell Park Memorial Institute 1640 medium (Sigma-Aldrich) with 0.2% glucose and glutamine and buffered with

morpholinepropanesulfonic acid (MOPS) (Sigma-Aldrich) (0.165 M) adjusted to pH 7.0 ± 0.1) and sterilized by filtration using a polyester (PET) 0.2 μm filter) and 100 μL of yeast cell suspension. Preliminary experiments indicate that DMSO may affect yeast growth when added to the cultures at a concentration above 2.5% (*v/v*), and for this reason, 5 μL of crude extracts dissolved in DMSO was defined as the maximum volume added to the cultures (**Figures S.2** and **S.3)**. Cellular suspensions of *Candida* spp. ($3x10^3$ colony forming unit (CFU)/mL) were prepared from fresh cultures streaked on YPD agar plates, and 100 μL were added to each well of a 96-well plate. Growth in the RPMI-1640 medium was recorded after 24 and 48 hours at 30 °C (*C. albicans*) or 37 ºC (*C. glabrata*) by measuring optical density at 600 nm (OD_{600}) using the Epoch Microplate Spectrophotometer and BioTek Gen5 Data Analysis Software. The growth condition without extract but with DMSO (control condition, 2.5% DMSO) was used as the normalization condition, after background (RPMI-1640 medium) subtraction. Growth ratios below 0.5 were considered for further analyses.

2.4.4. Minimum inhibitory concentration

Minimum inhibitory concentrations of *Candida* spp. were determined by conducting broth microdilution assays based on the CLSI standard method M27 for yeasts with slight modifications [78]. Serial dilutions of the stock solutions (section 2.4.1) of the most promising crude extracts, fractions, or sub-fractions were prepared using DMSO. Growth in RPMI-1640 medium was recorded after 24 and 48 hours at 30 °C (*C. albicans, C. krusei, C. tropicalis,* and *C. parapsilosis*) or 37 ºC (*C. glabrata*) by measuring OD_{600} using the Epoch Microplate Spectrophotometer and BioTek Gen5 Data Analysis Software. The growth condition without extract, but with DMSO (final concentration 2.5%) was used as the normalization condition, after background (RPMI-1640 medium) subtraction. The MIC was defined as the extract/fraction concentration range where the relative OD_{600} fall below 50% of the mock control. At least, three independent assays were performed.

2.4.5. Minimum fungicidal concentration

To address whether crude extracts and fractions had a fungicidal or fungistatic activity 5 μL of the above cultures (section 2.4.4) were spotted on YPD agar plates after 24 and 48

hours. Plates were digitalized after 24 hours at 30 °C (*C. albicans, C. krusei, C. tropicalis,* and *C. parapsilosis*) or 37 °C (*C. glabrata*) with EPSON Perfection 4870 Photo scanner using EPSON software. Spotting cells on a YPD plate before adding extract/(sub-)fraction (0 hours) and digitalizing after 24 and 48 hours served as an inoculum control. The MFC (Minimum fungicidal concentration) corresponds to the crude extracts/fractions concentration that prevents yeast growth.

2.5. Liquid-liquid fractionation of the crude extracts

Promising extracts (A22, O23, O30, and O32; dry weight, 1.65 g, 4.1284 g, 5.2000 g, 3.57663 g, respectively) were partitioned between water and dichloromethane (1:1 *v/v*) and the aqueous phase was extracted with *n*-butanol originating, after removing the solvent under reduced pressure, the water fraction (WF) and the *n*-butanol fraction (BF). The organic phase was concentrated under reduced pressure and partitioned between water-methanol (1:10) and hexane to give, after removing the solvent under reduced pressure, the hexane fraction (HF). The water content (% *v/v*) of the methanolic fraction was adjusted to 50% with water-methanol, and the mixture was extracted with dichloromethane, originating, after solvent removal under reduced pressure, the dichloromethane fraction (DF) and the aqueous methanolic fraction (WMF). Fractions were redissolved in methanol and transferred to glass vials, and methanol was slowly evaporated using a nitrogen line until no solvent residues were observed. The fractions obtained were stored at 4 ºC until further analysis. Organic solvents of HPLC (High-performance liquid chromatography) grade and distilled and deionized water were used. The antifungal activity of HF, DF, BF, WMF, and WF fractions was assessed as described in section 2.4.3 and active fractions were selected for further fractionation.

2.6. Solid Phase Extraction

SPE was carried out using an RP-18 column (Merck KGaA) and a modified glass vacuum manifold (Waters). A stepped gradient of water (H_2O), methanol (CH_3OH), and dichloromethane (CH_2Cl_2) was used to yield seven sub-fractions: R1 to R7. The fractions were redissolved in methanol and transferred to glass vials, and methanol was slowly evaporated using a nitrogen line until no solvent residues were observed. The antifungal activity of the fractions was next assessed as described in section 2.4.3 and active

fractions were selected for further analysis. The fractions obtained were stored at 4 ºC. Organic solvents of HPLC grade and distilled and deionized water were used.

2.7. Dereplication

Promising sub-fractions were subjected to Ultra-Performance Liquid Chromatography–High-Resolution Mass Spectrometry (UHPLC/HRMS). UHPLC/HRMS was performed on Q Exactive Focus (Thermo Scientific) coupled to UltiMate 3000 UHPLC (Thermo Scientific), using Xcalibur software v.4.0.27.19 (Thermo Scientific). Separation was achieved using a Waters XBridge column C18, 2.1 x 150 mm, 3.5 µm particle size, P/N 186003023 (Optima LC/MS Grade, Fisher Scientific). The column temperature was maintained at 30 ºC. The eluents consisted of mobile phase A: water (H_2O) with 0.1 % formic acid (*v/v*); mobile phase B: acetonitrile (CH_3CN) with 0.1 % formic acid (*v/v*) at a flow rate of 400 µL/min. A combination of gradient and isocratic elution was used. The mass spectrometer was operated in positive ESI (Electrospray Ionization Process) mode. The exact mass of the components was compared against the AntiMarin database [79]. For the components with no matches in the database, the predicted molecular formula and exact mass were searched in the CAS SciFinder database platform [80].

^{13}C NMR spectra were recorded on a Bruker Avance 500 spectrometer at 500 and 125 MHz, respectively, using deuterated chloroform ($CDCl_3$) as the sample solvent.

A Pearson's chi-squared goodness of fit test (χ^2) was applied to determine whether our data (experimental chemical shift values of ^{13}C NMR) were significantly different from those expected (reported chemical shift values of ^{13}C NMR). Chi-squared tests were applied with the Yates continuity correction to reduce the error in approximation and prevent overestimation of statistical significance for small data. Herein, the chi-squared statistic was as follows:

$$\chi_Y^2 = \sum_{i=1}^{n} \frac{(|O_i - E_i| - 0.5)^2}{E_i}$$

where O_i would represent the observed values, and E_i would be the expected values.

2.8. *In vitro* toxicity assays

2.8.1. Cell culture and maintenance

Cultures were maintained following the ATCC Animal Cell Culture guidelines [81]. In a laminar flow chamber, 1 mL aliquot of 2 x 10^6 HeLa cells (ATCC) was thawed and transferred to a falcon with 5 mL of Dulbecco's Modified Eagle Medium (DMEM), (Biowest) with 10% Fetal Bovine serum (FBS), (Sigma-Aldrich). After gentle centrifugation (5 minutes at 200*g*) to remove the cryopreservation agent, DMSO, the supernatant was discarded and 5 mL of DMEM with 10% FBS was added to the falcon to resuspend the cells. Finally, the volume was transferred to a 25 cm^2 flask and incubated at 37 ºC in a humidified atmosphere with 5% CO_2. After 2 to 3 days of incubation, using an inverted microscope, the medium was checked for evidence of contamination, morphology, and distribution of the cells. When most of the cells had adhered to the bottom of the flask, the culture medium was aspirated to remove cellular debris and replaced with fresh medium. The flask was kept in the incubator until the cell monolayer reached about 80% confluence. For routine subculturing, DMEM in the flasks was aspirated and the cell monolayer was gently washed with 10 mL of phosphate-buffered saline (PBS), (Sigma-Aldrich) to remove dead cells and debris. To detach the cells, 2 mL of trypsin was added to the cell monolayer and incubated for 5 minutes at 37 ºC in a humidified atmosphere with 5% CO_2. After incubation, 4 mL of DMEM with 10% FBS was added to inactivate the trypsin. Viable cells were counted using trypan blue (0.4%) and a hemacytometer. Cells were then seeded on a new flask with approximately 0.8 x 10^4 to 1.6 x 10^4 cells/cm^2 density and incubated as described above for 2-3 days and seeded again.

2.8.2. Cytotoxicity assays

HeLa cells were cultured as described in section 2.8.1. We first defined the solvent (DMSO) concentrations that do not affect cellular viability and found that a maximum of 0.5% DMSO (*v/v*) could be used (**Figure S.5)**. HeLa cells (5 x 10^3 cells/well) were seeded in 96-well plates. After 24 hours of growth, different concentrations of extracts were added, and plates were incubated for 24 hours. Solutions of the extracts or fractions were prepared with culture medium (DMEM) and contained 0.5% DMSO (*v/v*). Cell viability

was determined using the 3-(4,5-dimethylthiazol-2-yl)-2,5-diphenyltetrazolium bromide (MTT) method [82]. MTT assay uses cellular metabolism as an indicator of viability. It is based on the ability of metabolically active cells to reduce yellow water-soluble tetrazolium salt to a purple insoluble formazan product by enzymes in active mitochondria. After 24 hours the culture medium was removed, and MTT (0.5 mg/mL final concentration in DMEM) was added to each well and incubated for 2 hours at 37 ºC. Formazan crystals were solubilized with DMSO (15 minutes, at room temperature) and quantified spectrophotometrically at optical density 570 nm (OD_{570}) using the Epoch Microplate Spectrophotometer and BioTek Gen5 Data Analysis Software. The results of HeLa cell viability were expressed as the percentage of MTT reduction of treated cells relative to control (untreated cells: DMEM supplemented with 0.5% DMSO) [82].

2.9. High-performance liquid chromatography (HPLC)

The most active fractions were further separated using HPLC with Waters 2695 Alliance HPLC system (Waters Chromatography, Milford, MA) equipped with a Photodiode Array (PDA) Detector 2996. Samples were prepared by dissolving dry fractions in methanol and 30 μL were injected into a reverse phase Symmetry C18 column (4.6x250 mm, 5 μm particle size, Waters Chromatography, Milford, MA) using an eluent mixture of acetonitrile/water with a constant flow rate of 0.3 mL/min. The column temperature was held at 30 ºC, and samples were kept at 10 ºC. The Empower 2 software (Waters Chromatography, Milford, MA) was used for data acquisition. Organic solvents of HPLC grade and distilled and deionized water were used.

Chapter 3 – Results and Discussion

3.1. Screening of the marine crude extracts for antifungal activity

Two libraries (I and II) were screened for antifungal activity against *Candida albicans* and *Candida glabrata*, two of the most prevalent fungi causing IFIs [20]. Library I was composed of 65 crude extracts (A1 to A65) and Library II gathered 44 crude extracts (O1 to O44) from organisms collected in the YP.

As a first approach to evaluate the antifungal activity of these extracts, yeast cultures were treated with 5 µL of each extract. Growth was assessed by measuring the OD_{600} of the cultures after incubation for 24 hours and 48 hours at 37 ºC (*C. glabrata*) or 30 ºC (*C. albicans*) and compared to extract-free cultures. The results are depicted in **Figures 3.1** to **3.4**.

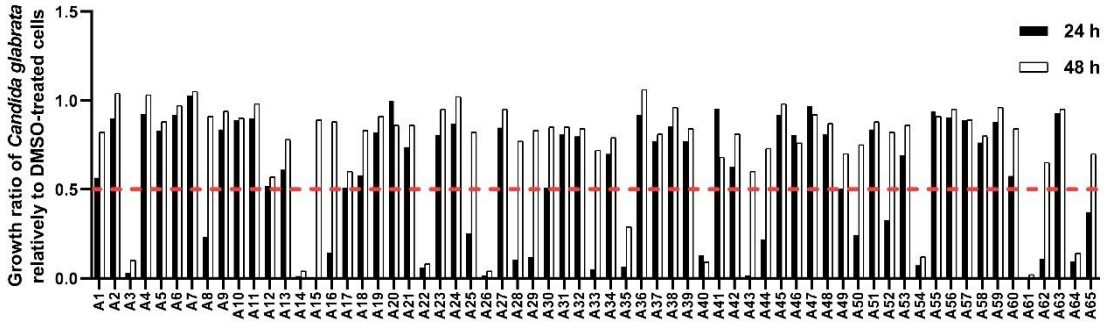

Figure 3.1. ***Susceptibility of C. glabrata to marine crude extracts (Library I).*** *Growth was monitored after 24 and 48 h of incubation at 37 ºC. Growth ratios were determined relative to control (DMSO-treated cells).* Ratios *below 0.5 (red line) indicate active extracts. The concentrations tested are listed in Table S.2.*

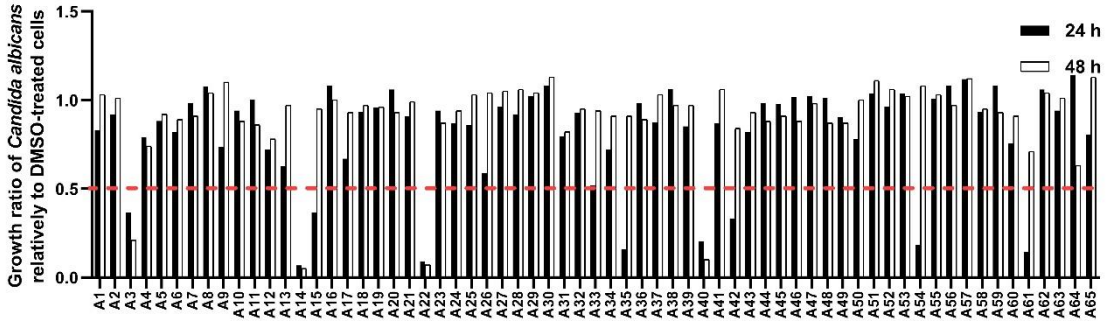

Figure 3.2. ***Susceptibility of C. albicans to marine crude extracts (Library I).*** *Growth was monitored after 24 and 48 h of incubation at 30 ºC. Growth ratios were determined relative to control (DMSO-treated cells). Ratios below 0.5 (red line) indicate active extracts. The concentrations tested are listed in Table S.2.*

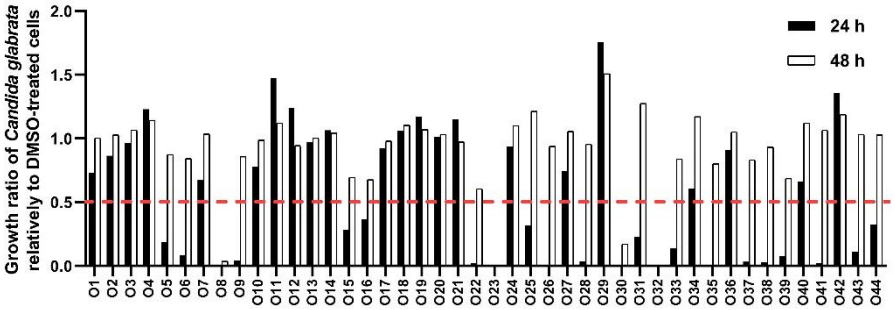

Figure 3.3. ***Susceptibility of C. glabrata to marine crude extracts (Library II).*** *Growth was monitored after 24 and 48 h of incubation at 37 ºC. Growth ratios were determined relative to control (DMSO-treated cells). Ratios below 0.5 (red line) indicate active extracts. Cells were incubated with 250 µg/mL of each crude extract.*

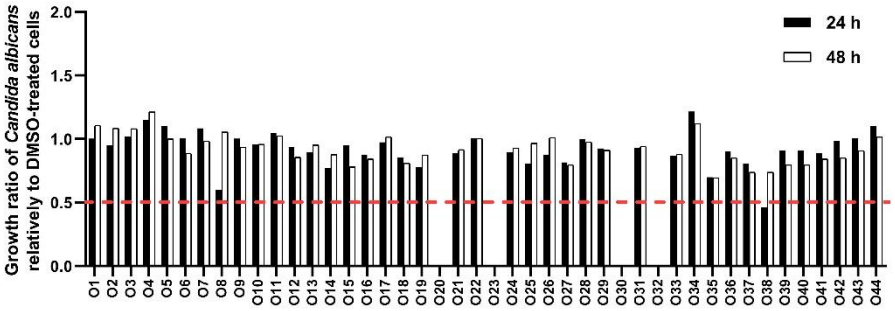

Figure 3.4. ***Susceptibility of C. albicans to marine crude extracts (Library II).*** *Growth was monitored after 24 and 48 h of incubation at 30 ºC. Growth ratios were determined relative to control (DMSO-treated cells). Ratios below 0.5 (red line) indicate active extracts. Cells were incubated with 250 µg/mL of each crude extract.*

In Library I extracts A3, A14, A22, and A40 appeared to be effective against both *C. glabrata* and *C. albicans* after 24 and 48 hours of incubation (**Figures 3.1** and **3.2**). Extracts A26, A35, A54, A61, and A64 showed antifungal activity only against *C. glabrata* (**Figure 3.1**).

As for Library II, extracts O23, O30 and O32 appeared to be effective against both *Candida* spp. (**Figures 3.3** and **3.4**). Extracts O8 and O20 showed selective antifungal activity against *C. glabrata* and *C. albicans*, respectively (**Figures 3.3** and **3.4**).

Crude marine extracts that showed antifungal activity after 24 and 48 hours against both species were chosen for further studies.

3.2. Evaluation of the fungicidal activity of crude marine extracts

We also carried out a preliminary phenotypic assay to determine whether crude extracts had fungistatic or fungicidal activity. To this end, 5 µL of the cultures used in the preliminary screening (**Section 3.1**) were spotted onto YPD agar plates, and growth was

recorded after 24 hours of incubation at 37 ºC (*C. glabrata*) or 30 ºC (*C. albicans*). The results are depicted in **Figures 3.5.** to **3.8**.

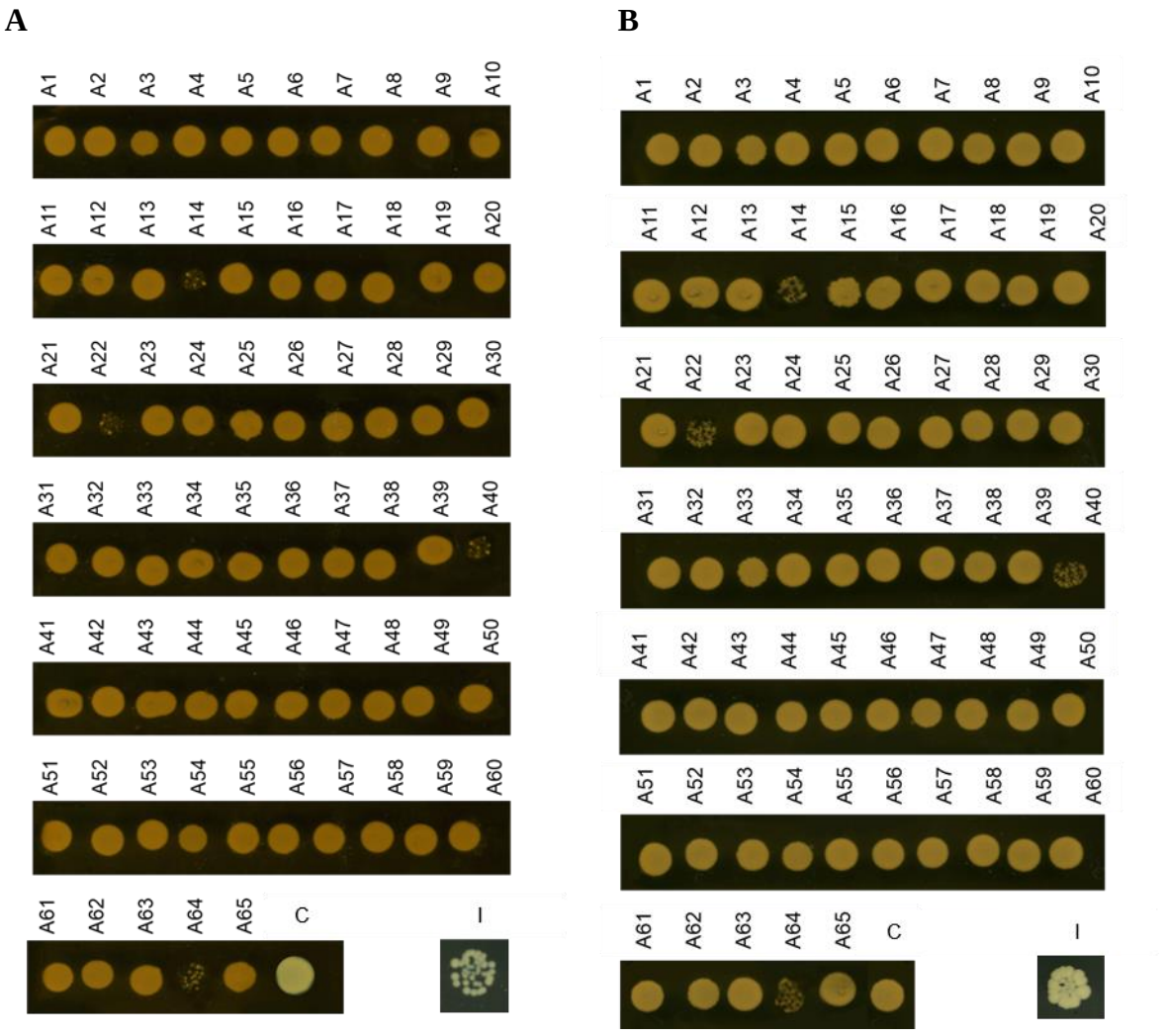

Figure 3.5. ***Growth of C. glabrata on YPD plates after incubation with crude marine extracts from Library I.*** *Yeast cells were incubated with the indicated extracts for 24 h* ***(A)*** *or 48 h* ***(B)*** *and a volume of 5 μL was spotted onto YPD agar plates. Images were digitalized after 24 h of incubation at 37 ºC. I Inoculum: growth prior extract addition. C: DMSO-treated cells control. The concentrations tested are listed in Table S.2.*

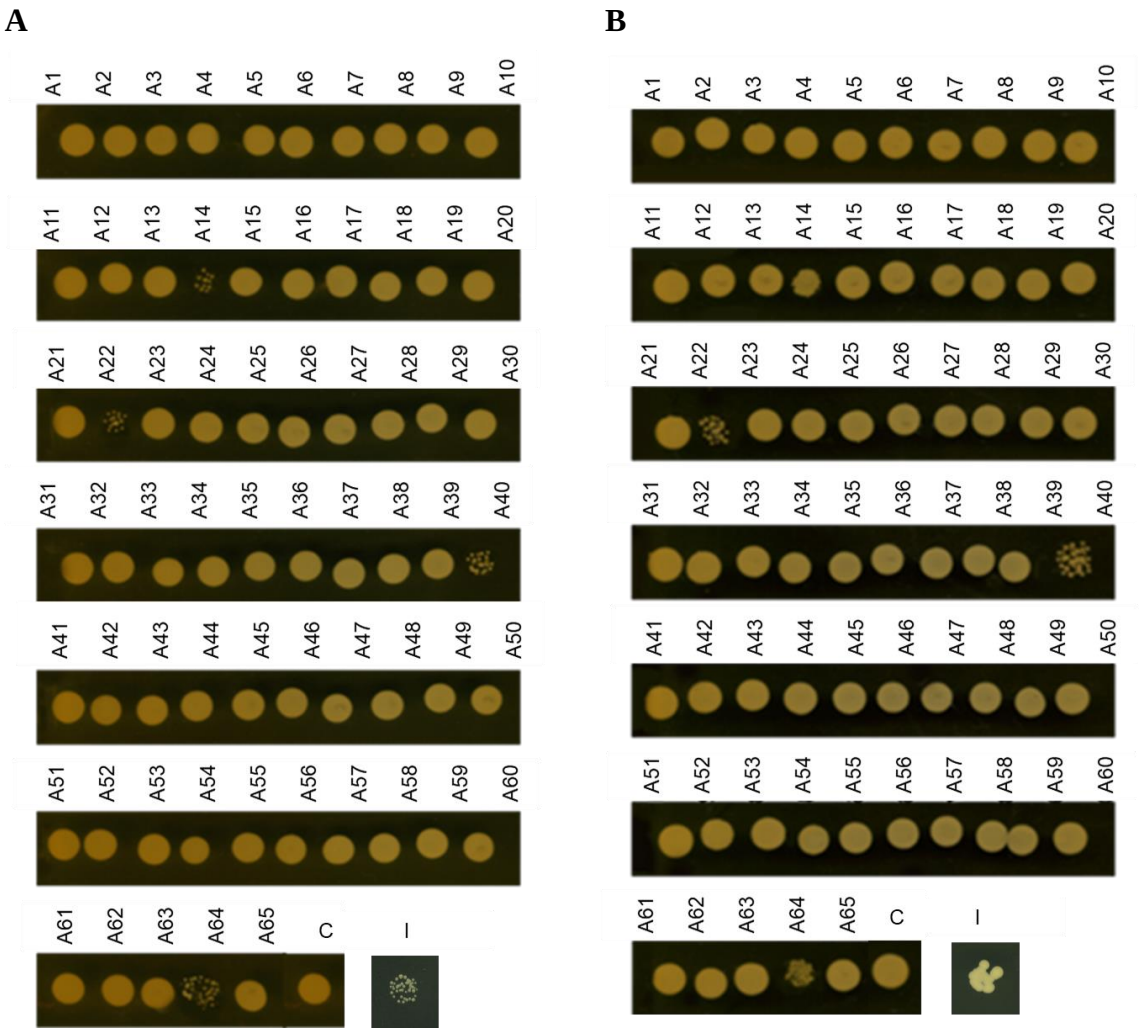

Figure 3.6. ***Growth of C. albicans on YPD plates after incubation with crude marine extracts from Library I.*** *Yeast cells were incubated with the indicated extracts for 24 h* ***(A)*** *or 48 h* ***(B)*** *and a volume of 5 µL was spotted onto YPD agar plates. Images were digitalized after 24 h of incubation at 30 ºC. I, Inoculum: growth prior extract addition. C: DMSO-treated cells. The concentrations tested are listed in Table S.2.*

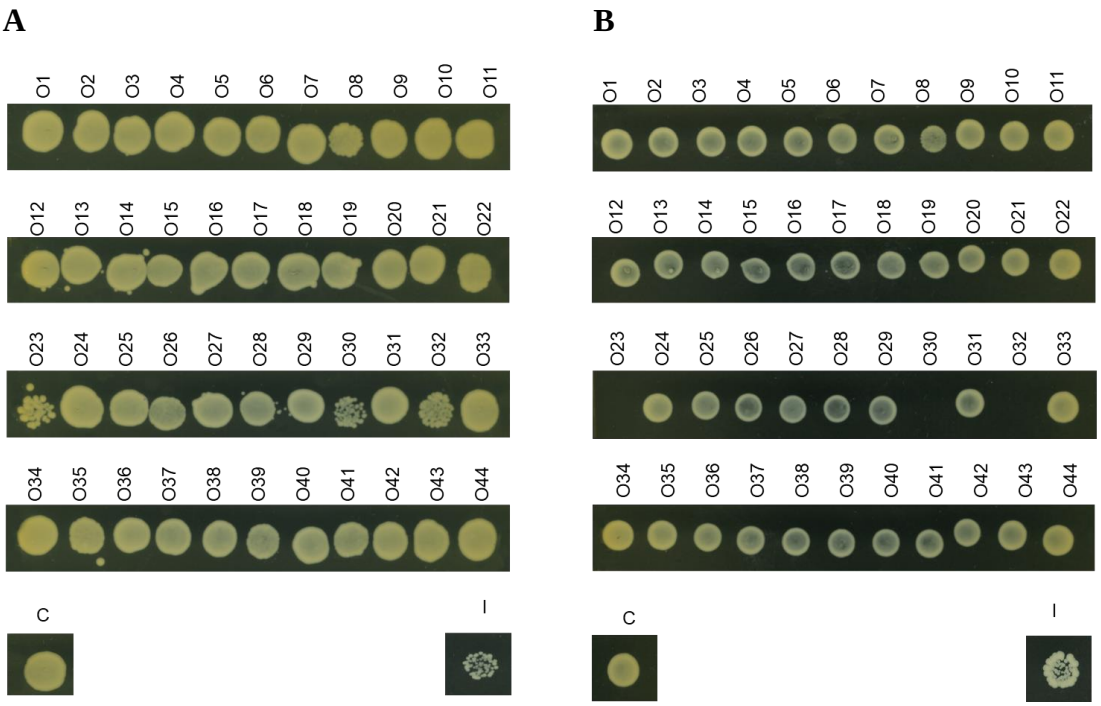

Figure 3.7. ***Growth of C. glabrata on YPD plates after incubation with crude marine extracts from Library II.*** *Yeast cells were incubated with the indicated extracts for 24 h* ***(A)*** *or 48 h* ***(B)*** *and a volume of 5 µL was spotted onto YPD agar plates. Images were digitalized after 24 h of incubation at 37 ºC. I, Inoculum: growth prior extract addition. C: DMSO-treated cells control. Cells were incubated with 250 µg/mL of each crude extract.*

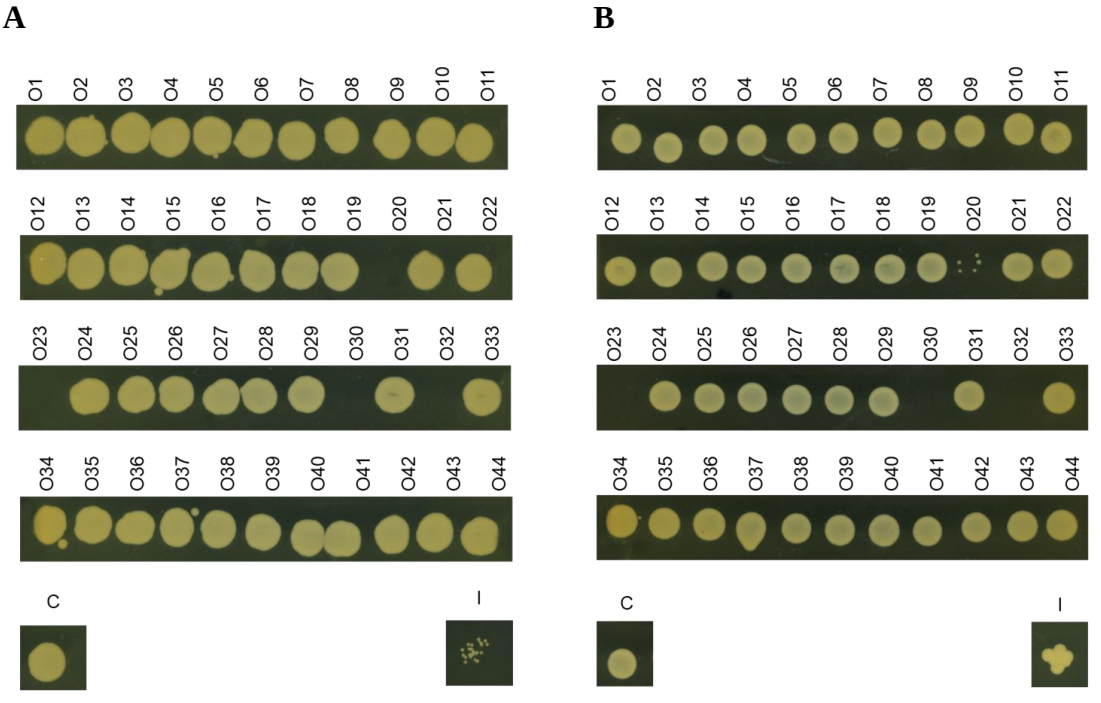

Figure 3.8. ***Growth of C. albicans on YPD plates after incubation with crude marine extracts from Library II.*** *Yeast cells were incubated with the indicated extracts for 24 h* ***(A)*** *or 48 h* ***(B)*** *and a volume of 5 µL was spotted onto YPD agar plates. Images were digitalized after 24 h of incubation at 30 ºC. I, Inoculum: growth prior extract addition. C: DMSO-treated cells control. Cells were incubated with 250 µg/mL of each crude extract.*

Several crude extracts from Library I, particularly A14, A22, A40, and A64, significantly decrease the visible growth of *C. glabrata* and *C. albicans* after 24 and 48 hours (**Figures 3.5** and **3.6**), pointing to a fungicidal effect of these extracts.

Three of the 44 extracts from Library II, O23, O30, and O32, showed a clear fungicidal activity against *C. glabrata* and *C. albicans* (**Figures 3.7** and **3.8**).

3.3. Antifungal activity of promising crude extracts

The minimum inhibitory concentration (MIC) against *Candida* spp. of the most active extracts (**Figures 3.1** to **3.4)** with fungicidal activity (**Figures 3.5** to **3.8**) was determined using the CLSI guidelines [78] for yeasts (**Tables 3.1** and **3.2**).

Table 3.1. ***MIC of the most active crude extracts (Library I) against C. glabrata and C. albicans.***

Extract	**MIC** (µg/ml)			
	C. glabrata		***C. albicans***	
	24 h	**48 h**	**24 h**	**48 h**
A14	1.30 - 2.59	1.30 - 2.59	2.59 - 5.19	2.59 - 5.19
A22	1.95 - 3.91	1.95 - 3.91	1.95 - 3.91	1.95 - 3.91
A40	3.91 - 7.81	3.91 - 7.81	1.95 - 3.91	1.95 - 3.91

Table 3.2. ***MIC of the most active crude extracts (Library II) against C. glabrata and C. albicans.***

Extract	**MIC** (µg/ml)			
	C. glabrata		***C. albicans***	
	24 h	**48 h**	**24 h**	**48 h**
O23	3.91 - 7.81	3.91 - 7.81	15.63 - 31.25	31.25 - 62.5
O30	1.95 - 3.91	3.91 - 7.81	3.91 - 7.81	7.81 - 15.63
O32	15.63 - 31.25	15.63 - 31.25	62.5 - 125	125 - 250

The tested extracts of Library I were generally more active than those of Library II. Interestingly, whereas the MICs of A14, A22, and A40 do not vary much between 24 and 48 hours, those of O23, O30, and O32 (Library II) always increase after 48 hours. Moreover, Library II extracts are clearly more active against *C. glabrata*, while this pattern is not consistent for Library I extracts.

The activity of extracts from Library I might be explained by several MNPs already described. The crude extract A14 from the marine sponge *Amphimedon compressa*

(**Table S.1**) may well be active due to the presence of the compound 8,8'-dienecyclostellettamine (**Figure 3.9**), which was isolated from this species and shown to be active against *Candida* species [83, 84].

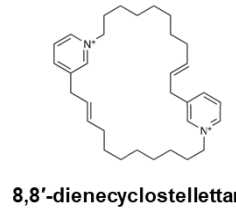

Figure 3.9. ***Chemical structure of 8,8'-dienecyclostellettamine present in A. compressa.***

Extract A22, from *Monanchora arbuscula* (**Table S.1**), has previously been reported to contain dehydrobatzelladine C and batzelladine L (**Figure 3.10**), two molecules active against *C. albicans*, *Aspergillus fumigatus* and *Aspergillus flavus* [85-87].

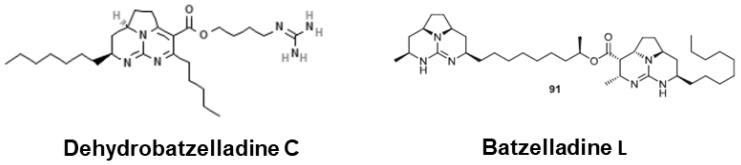

Figure 3.10. ***Chemical structures of dehydrobatzelladine C and batzelladine L present in M. arbuscula.***

Finally, the antifungal activity of A40, obtained from *Agelas citrina* (**Table S.1**) can be attributed to the presence of agelasidines (**Figure 3.11**), which have been shown to be active against *Candida* species [63, 70, 71, 88].

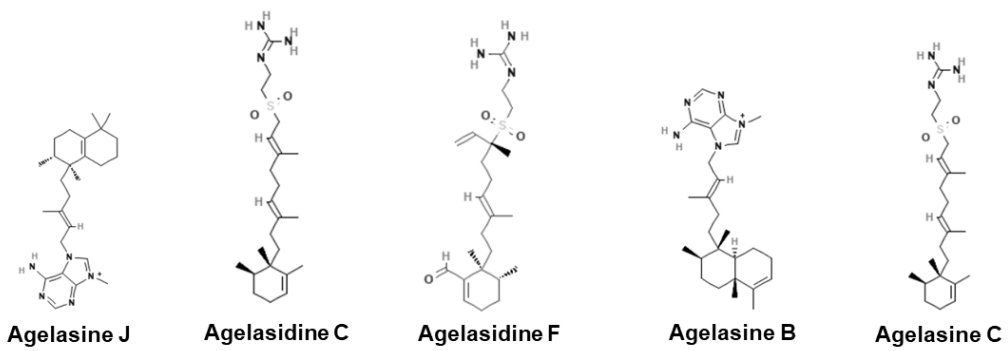

Figure 3.11. ***Chemical structures of agelasidines present in A. citrina.***

The taxonomic characterization of the extracts of Library II is still in progress and therefore this type of inference is very difficult to perform.

We then compared the fungicidal activity of the extracts of Library I and II by determining the minimum fungicidal concentration of each extract (**Figures 3.12** to **3.15** and **Table 3.3**).

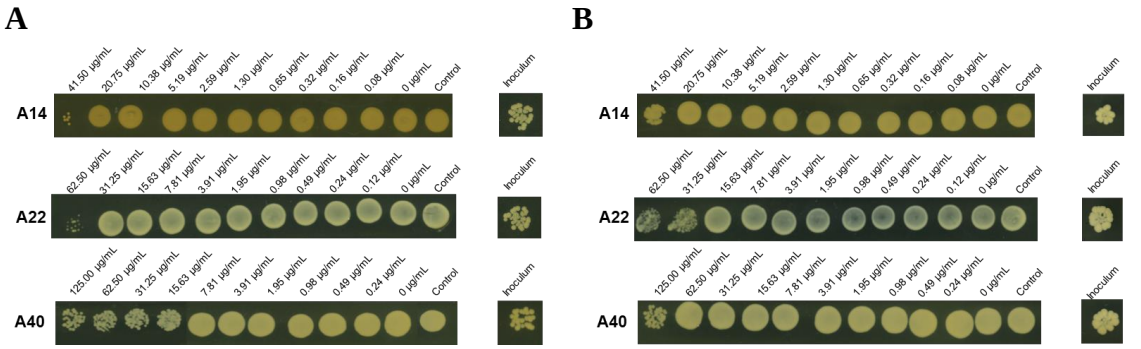

Figure 3.12. ***Growth of C. glabrata on YPD plates after incubation with A14, A22, and A40.*** *Yeast cells were incubated with the indicated extracts for 24 h* ***(A)*** *or 48 h* ***(B)*** *and a volume of 5 µL was spotted onto YPD agar plates. Images were digitalized after 24 h of incubation at 37 ºC. Inoculum: growth prior extract addition. Control: untreated cells.*

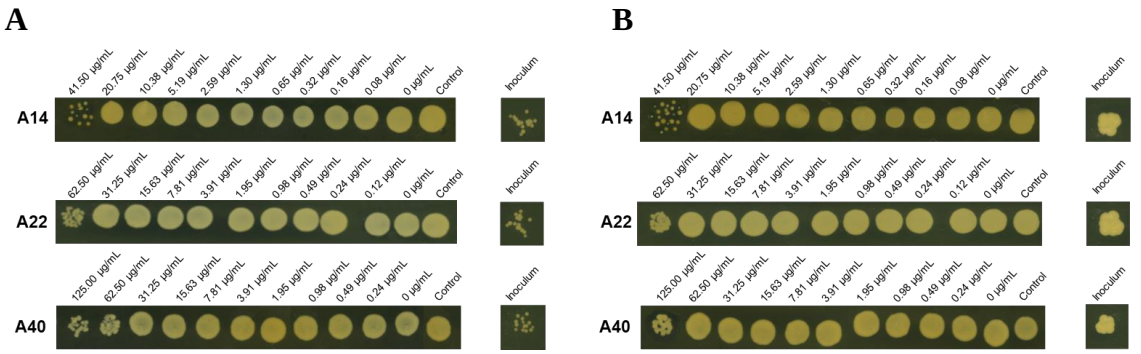

Figure 3.13. ***Growth of C. albicans on YPD plates after incubation with A14, A22, and A40.*** *Yeast cells were incubated with the indicated extracts for 24 h* ***(A)*** *or 48 h* ***(B)*** *and a volume of 5 µL was spotted onto YPD agar plates. Images were digitalized after 24 h of incubation at 30 ºC. Inoculum: growth prior extract addition. Control: untreated cells.*

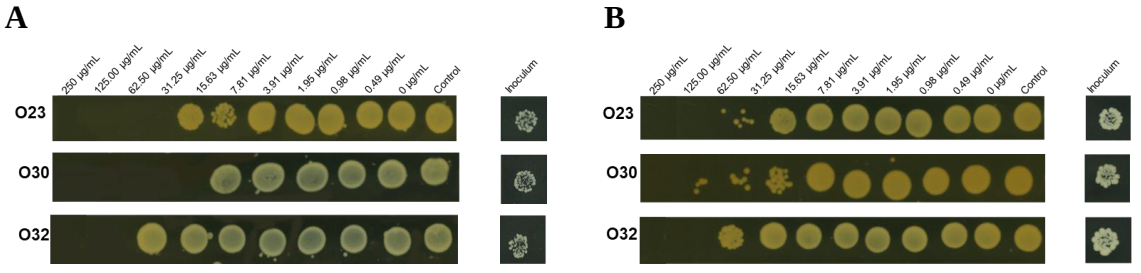

Figure 3.14. ***Growth of C. glabrata on YPD plates after incubation with O23, O30, and O32.*** *Yeast cells were incubated with the indicated extracts for 24 h* ***(A)*** *or 48 h* ***(B)*** *and a volume of 5 µL was spotted onto YPD agar plates. Images were digitalized after 24 h of incubation at 37 ºC. Inoculum: growth prior extract addition. Control: untreated cells.*

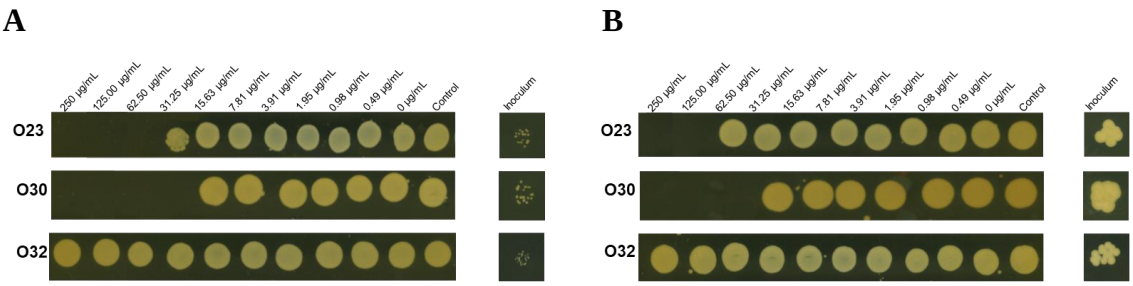

Figure 3.15. ***Growth of C. albicans on YPD plates after incubation with O23, O30, and O32.*** *Yeast cells were incubated with the indicated extracts for 24 h* ***(A)*** *or 48 h* ***(B)*** *and a volume of 5 µL was spotted onto YPD agar plates. Images were digitalized after 24 h of incubation at 30 ºC. Inoculum: growth prior extract addition. Control: untreated cells.*

The amount of crude extracts from Library I was very limited, and therefore the stock solutions prepared were not as concentrated as those for Library II and the range of concentrations tested to assess the MFC was lower. Nevertheless, the fungicidal activity of the extracts of Library II is higher than that of Library I (**Figures 3.12** to **3.15**). The highest concentration of A14, A22, and A40 tested appears to be slightly fungicidal against both *Candida* spp.. In Library II, O23 is fungicidal at concentrations four to eight-fold higher than the MIC upper-value for *C. glabrata*, and two-fold higher than the MIC upper-value for *C. albicans* (**Table 3.2** and **3.3**). O30 is fungicidal at concentrations greater than 3.91 µg/mL (24 hours) or 31.25 µg/mL (48 hours) in *C. glabrata* (two to eight-fold higher than the MIC upper-value) and in *C. albicans* it is fungicidal at concentrations higher than 7.81 µg/mL (two-fold higher than the MIC upper-value, **Table 3.2** and **3.3**).

O32 is as fungicidal as O23 against *C. glabrata*, but unlike the latter, it does not have fungicidal activity against *C. albicans* (**Table 3.3**).

Unexpectedly, we found discrepant results between the initial screening for fungicidal activity and the MFC values. For example, in the former, O32 was fungicidal on *C. albicans* (**Figure 3.8**), while this appears not to be the case, as discussed above (**Figure 3.15)**. Crude extracts are not homogeneous solutions and, therefore, this can explain this type of inconsistency.

Table 3.3. ***MFC of O23, O30, and O32 against C. glabrata and C. albicans.***

Extract	**MFC** (µg/mL)			
	C. glabrata		***C. albicans***	
	24 h	**48 h**	**24 h**	**48 h**
O23	31.25	62.5	62.5	62.5
O30	7.81	62.5	15.63	15.63
O32	31.25	62.5	*nf*	*nf*

nf – not fungicidal for concentrations ≤ 250 µg/mL

3.4. Crude extracts from Library II are not toxic to mammalian cells

One of the major challenges facing antifungal development is the potential toxicity to host cells. We thus decided to evaluate whether candidate extracts for further fractionation could be toxic to mammalian cells. We focused on Library II because we did not have enough biological material from Library I to perform this type of analysis. The human cervical cancer cell line (HeLa) was used to assess the toxicity of crude extracts O23, O30, and O32 to mammalian cells. Cells were treated with growing concentrations of the extracts and incubated for 24 hours at 37 ºC (**Figure 3.16).**

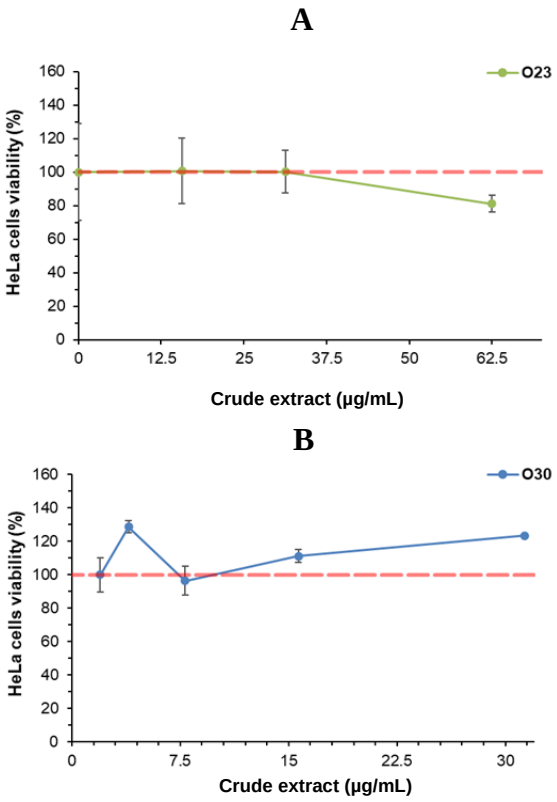

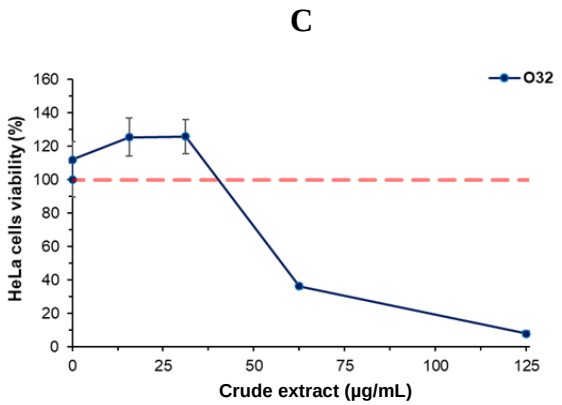

Figure 3.16. ***Cytotoxicity of O23 (A), O30 (B), and O32 (C) on HeLa cells.*** *The cellular viability was assessed using the MTT assay and the values are expressed as the percentage of viability relative to the untreated control.*

With the exception of the O32 extract, all other extracts have negligible toxicity to mammalian cells within the concentration range tested (**Figure 3.16).**

These results are indicative only and should be repeated once the active compound is isolated. It may be that the toxicity of the O32 extract results from compounds that do not contribute to its antifungal activity.

3.5. Bioassay-guided fractionation of the crude marine extract

Promising extracts from Library I (A22) and Library II (O23, O30, and O32) were next partitioned according to their polarity. The lack of a sufficient amount of A14 and A40 prevented us from proceeding with these extracts. The fractionation of A22 was performed in collaboration with the University of A Coruña. All other extracts were fractionated at ITQB NOVA under the scope of this work.

The partition was performed using liquid-liquid extraction with solvents with different polarities (hexane, dichloromethane, *n*-butanol, water-methanol, and water). After extraction, the fractions were concentrated under reduced pressure or vacuum to determine their mass: A22 WF: 217.00 mg, A22 DF: 106.30 mg, A22 HF 672.20 mg, A22 BF: 756.00 mg, A22 WMF: 755.80 mg. O23 WF: 217.73 mg, O23 DF: 17.44 mg, O23 HF 11.57 mg, O23 BF: 71.90 mg, O23 WMF: 24.70 mg. O30 WF: 3141.90 mg, O30 DF: 204.90 mg, O30 HF 77.70 mg, O30 BF: 920.80 mg, O30 WMF: 139.10 mg. O32 WF: 2111.50 mg, O32 DF: 222.10 mg, O32 HF 64.80 mg, O32 BF: 404.60 mg, O32 WMF: 126.60 mg.

The yield (%) of each fraction was calculated (**Table 3.4**) based on the equation below:

$$Yield\ of\ fraction\ (\%) = \frac{mass\ of\ dried\ fraction\ (mg)}{mass\ of\ crude\ extract\ (mg)} \times 100$$

Table 3.4. ***Yield of the fractions obtained after liquid-liquid extraction of crude extracts.***

	Yield (%)			
Fraction	**A22**	**O23**	**O30**	**O32**
Water (WF)	13.15	52.7	60.4	72.1
Dichloromethane (DF)	6.44	4.2	3.9	7.6
Hexane (HF)	40.74	2.8	1.5	2.2
***n*-butanol (BF)**	45.82	17.4	17.7	13.8
Water-methanol (WMF)	45.81	6.0	2.7	4.3
Loss (%)	51.96	16.8	13.8	18.1

For extract A22, the fractions *n*-butanol, water-methanol, and hexane had the highest yield, whereas for the Library II crudes (O23, O30, and O32) the fractions with the highest yield were invariably the water fraction followed by the *n*-butanol fraction (**Table 3.4**). This type of analysis is important because it allows us to predict how much crude we will need to collect if we need more material for further studies.

The dried fractions (hexane, dichloromethane, *n*-butanol, water-methanol, and water) were next re-dissolved in DMSO and tested against *C. glabrata* and *C. albicans.*

Yeast cells were incubated with 5 µL of each fraction and growth was recorded after 24 and 48 hours of incubation at 37 ºC (*C. glabrata*) or 30 ºC (*C. albicans*). The results are depicted in **Figures 3.17** to **3.20**.

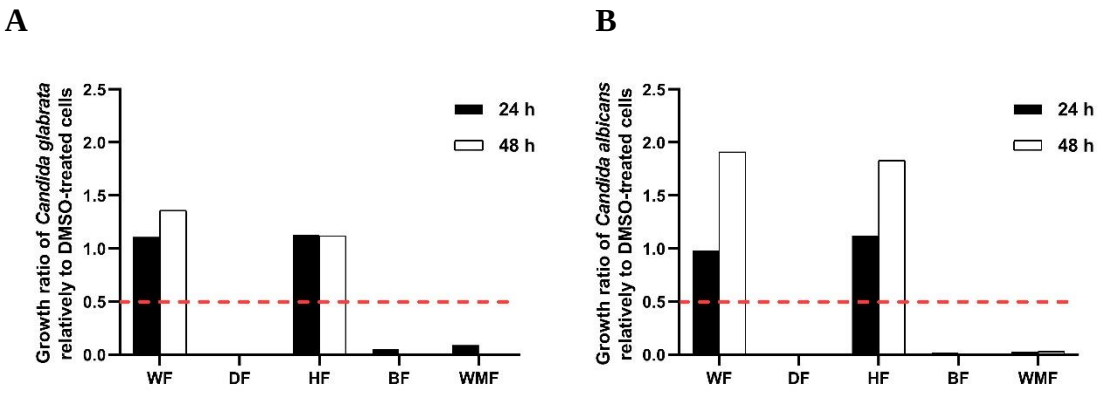

Figure 3.17. ***Susceptibility of Candida spp. to the fractions resulting from liquid-liquid extraction of A22.*** *Water (WF), dichloromethane (DF), hexane (HF), n-butanol (BF), and water-methanol (WMF) fraction (5 µL) were incubated with (**A**) C. glabrata and (**B**) C. albicans cells. Growth was monitored after 24 and 48 h of incubation at 37 ºC (C. glabrata) or 30 ºC (C. albicans) and growth ratios were determined relative to control (DMSO-treated cells). Ratios below 0.5 (red line) indicate active fractions.*

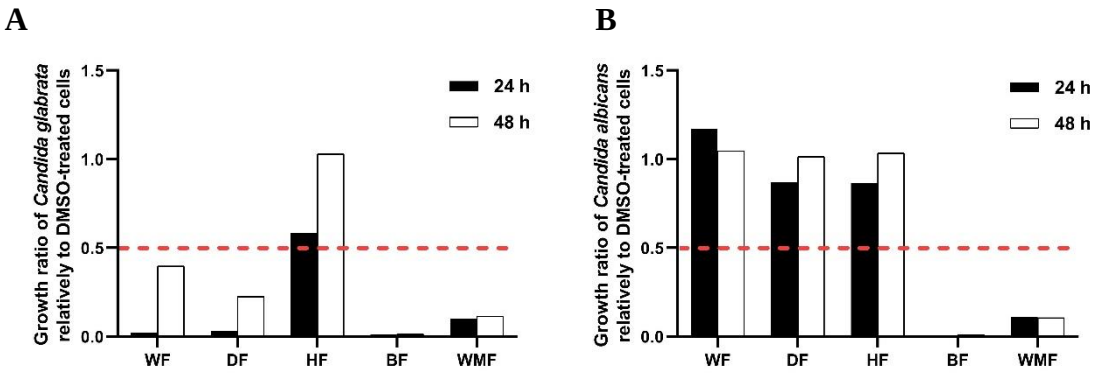

Figure 3.18. ***Susceptibility of Candida spp. to the fractions resulting from liquid-liquid extraction of O23 fraction.*** *Fractions: water (WF), dichloromethane (DF), hexane (HF), n-butanol (BF), and water-methanol (WMF) fraction (5 µL) were incubated with (**A**) C. glabrata and (**B**) C. albicans cells. Growth was monitored after 24 and 48 h of incubation at 37 ºC (C. glabrata) or 30 ºC (C. albicans) and growth ratios were determined relative to control (DMSO-treated cells). Ratios below 0.5 (red line) indicate active fractions.*

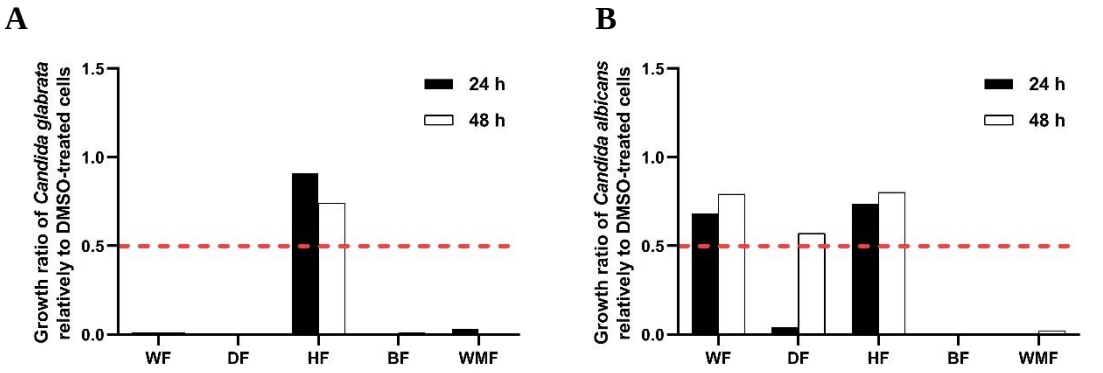

Figure 3.19. ***Susceptibility of Candida spp. to the fractions resulting from liquid-liquid extraction of O30 fraction.*** *Fractions: water (WF), dichloromethane (DF), hexane (HF), n-butanol (BF), and water-methanol (WMF) fraction (5 µL) were incubated with (**A**) C. glabrata and (**B**) C. albicans cells. Growth was monitored after 24 and 48 h of incubation at 37 ºC (C. glabrata) or 30 ºC (C. albicans) and growth ratios were determined relative to control (DMSO-treated cells). Ratios below 0.5 (red line) indicate active fractions.*

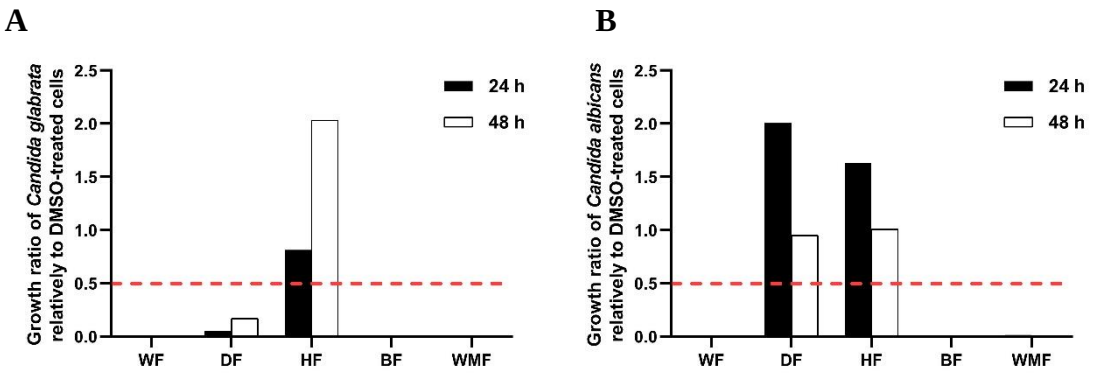

Figure 3.20. ***Susceptibility of Candida spp. to the fractions resulting from liquid-liquid extraction of O32 fraction.*** *Fractions: water (WF), dichloromethane (DF), hexane (HF), n-butanol (BF), and water-methanol (WMF) fraction (5 µL) were incubated with (**A**) C. glabrata and (**B**) C. albicans cells. Growth was monitored after 24 and 48 h of incubation at 37 ºC (C. glabrata) or 30 ºC (C. albicans) and growth ratios were determined relative to control (DMSO-treated cells). Ratios below 0.5 (red line) indicate active fractions.*

As shown in **Figure 3.17,** A22 fractions were slightly more active against *C. glabrata* with DF, BF, and WMF standing out as the most promising fractions for both species. With the exception of the HF, all other fractions resulting from O23, O30, and O32 were generally more active against *C. glabrata*, but BF and WMF were equally effective against both *C. glabrata* and *C. albicans*. These results reflect the presence of distinct compounds (MNPs) with antifungal activity in the same extract. The compounds also have different selectivity.

3.6. Evaluation of the fungicidal activity of the fractions

To understand if the fungicidal activity of the extracts was retained after fractionation, 5 µL of the cultures used to assess the susceptibility of *Candida* spp. to each fraction (**Figures 3.17** to **3.20**) were spotted onto YPD agar and the results are shown in **Figures 3.21** and **3.22**.

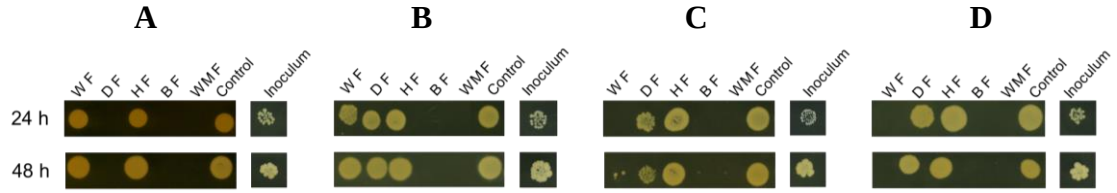

Figure 3.21. ***Growth of C. glabrata on YPD plates after incubation with the fractions resulting from extracts (A)*** *A22,* ***(B)*** *O23,* ***(C)*** *O30, and* ***(D)*** *O32. Yeast cells were incubated with the indicated extracts for 24 h or 48 h and a volume of 5 µL was spotted onto YPD agar plates. Images were digitalized after 24 h of incubation at 37 ºC. Water fraction (WF), dichloromethane fraction (DF), hexane fraction (HF), n-butanol fraction (BF), and water-methanol fraction (WMF). Inoculum: growth prior to fraction addition. Control: untreated cells. The A22 fractions concentrations tested were: 120 µg/mL (WF), 60 µg/mL (DF), 62.5 µg/mL (HF), 117.5 µg/mL (BF), 130 µg/mL (WMF); the concentration tested for the O fractions was 250 µg/mL.*

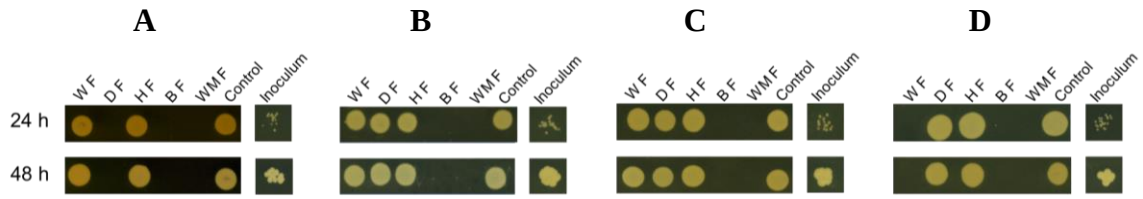

Figure 3.22. ***Growth of C. albicans on YPD plates after incubation with the fractions resulting from extracts (A)*** *A22,* ***(B)*** *O23,* ***(C)*** *O30, and* ***(D)*** *O32. Yeast cells were incubated with the indicated extracts for 24 h or 48 h and a volume of 5 µL was spotted onto YPD agar plates. Images were digitalized after 24 h of incubation at 30 ºC. Water fraction (WF), dichloromethane fraction (DF), hexane fraction (HF), n-butanol fraction (BF), and water-methanol fraction (WMF). Inoculum: growth prior to fraction addition. Control: untreated cells. A22 fractions concentrations tested: 120 µg/mL (WF), 60 µg/mL (DF), 62.5 µg/mL (HF), 117.5 µg/mL (BF), 130 µg/mL (WMF); the concentration tested for the O fractions was 250 µg/mL.*

All A22 derived fractions, that showed antifungal potential (**Figure 3.17**), DF, BF, and WMF, appear to be fungicidal on *C. glabrata* and *C. albicans* (**Figures 3.21** and **3.22**). The fact that this pattern is not so evident in the crude extract (**Figures 3.5** and **3.6**) indicates that the MNP responsible for such activity is being concentrated with the fractionation procedure.

As for A22, all BF and WMF fractions derived from Library II were fungicidal against both *Candida* species at the concentration tested (**Figures 3.21** and **3.22**). Interestingly, the most polar fractions are those that retain the greatest fungicidal activity.

3.7. Antifungal activity of promising fractions

Fractions with fungicidal activity against *Candida* spp. were further analyzed in terms of their antifungal potential. First, MICs were determined using CLSI guidelines [78], and then MFCs were assessed.

The dichloromethane (DF) and the water-methanol (WMF) fractions were the most active among those obtained from crude A22 (**Table 3.5**). As the MIC for all fractions is similar to or higher than that obtained with the crude extract (**Table 3.1**), we reason that A22 is composed of molecules with antifungal activity that can act synergistically.

Table 3.5. ***MIC of A22 most active fractions against C. glabrata and C. albicans.***

A22 Fraction	**MIC** (µg/mL)			
	C. glabrata		***C. albicans***	
	24 h	**48 h**	**24 h**	**48 h**
DF	1.88 - 3.75	1.88 - 3.75	3.75 - 7.5	7.5 - 15
BF	3.67 - 7.34	7.34 - 14.69	3.67 - 7.34	7.34 - 14.69
WMF	1.02 - 2.03	2.03 - 4.06	1.02 - 4.06	2.03 - 4.06

Dichloromethane fraction (DF), n-butanol fraction (BF), and water-methanol fraction (WMF).

The scenario is different for fractions resulting from extracts from Library II. In fact, for all of them, the MICs were lower than those of their cognate extracts, clearly indicating a successful purification/concentration step (**Tables 3.6, 3.7**, and **3.8**). For the O23-derived fractions, the MICs were two to eight-fold lower than the MICs before partition, for O30 the MICs of the most active fractions (BF and WMF) were two-fold lower than those before partition (in *C. albicans*) and for O32 promising fractions (WF, BF, and WMF) the MICs were four to thirty two-fold lower than the MIC before partitioning. Although this hypothesis is the most likely, at this point, we cannot confidently rule out the possibility that different compounds in the crude were acting antagonistically.

Table 3.6. ***MIC of O23 most active fractions against C. glabrata and C. albicans.***

O23 Fraction	**MIC** (µg/mL)			
	C. glabrata		***C. albicans***	
	24 h	**48 h**	**24 h**	**48 h**
BF	0.98 - 1.95	0.98 - 1.95	1.95 - 3.91	3.91 - 7.81
WMF	1.95 - 3.91	1.95 - 3.91	1.95 - 3.91	3.91 - 7.81

n-butanol fraction (BF) and water-methanol fraction (WMF).

Table 3.7. ***MIC of O30 most active fractions against C. glabrata and C. albicans.***

O30 Fraction	**MIC** (µg/mL)			
	C. glabrata		***C. albicans***	
	24 h	**48 h**	**24 h**	**48 h**
BF	1.95 - 3.91	3.91 - 7.81	3.91 - 7.81	3.91 - 7.81
WMF	1.95 - 3.91	3.91 - 7.81	3.91 - 7.81	3.91 - 7.81

n-butanol fraction (BF) and water-methanol fraction (WMF).

Table 3.8. ***MIC of O32 most active fractions against C. glabrata and C. albicans.***

O32 Fraction	MIC (μg/mL)			
	C. glabrata		*C. albicans*	
	24 h	**48 h**	**24 h**	**48 h**
WF	0.98 - 1.95	3.91 - 7.82	3.91 - 7.81	31.25 - 62.5
BF	0.49 - 0.98	0.98 - 1.95	1.95 - 3.91	3.91 - 7.81
WMF	1.95 - 3.91	3.91 - 7.81	3.91 - 7.81	7.81 - 15.63

Water fraction (WF), n-butanol fraction (BF), and water-methanol fraction (WMF).

We also calculated the MFC of each fraction and the results are presented in **Figures 3.23** to **3.30** and **Tables 3.9** to **3.12**.

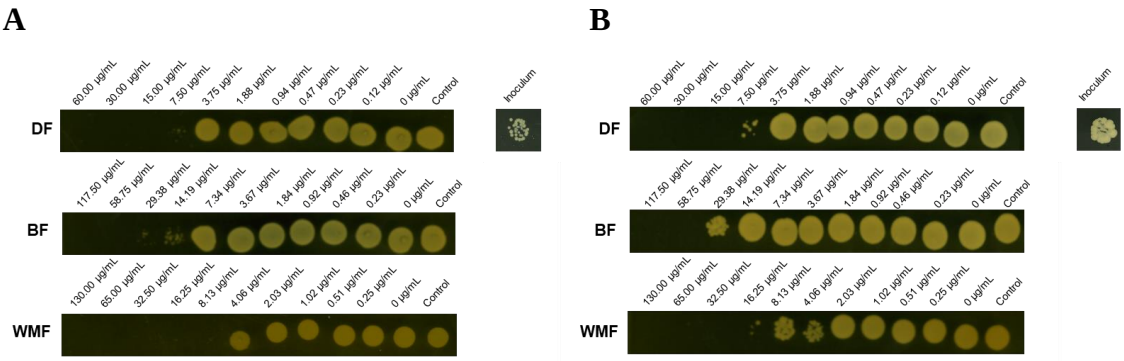

Figure 3.23. ***Growth of C. glabrata on YPD plates after incubation with A22 DF, BF, and WMF.*** *Yeast cells were incubated with the fractions for 24 h (**A**) or 48 h (**B**) and a volume of 5 μL was spotted onto YPD plates. Images were digitalized after 24 h of incubation at 37 ºC. Inoculum: growth prior to fraction addition. Control: untreated cells.*

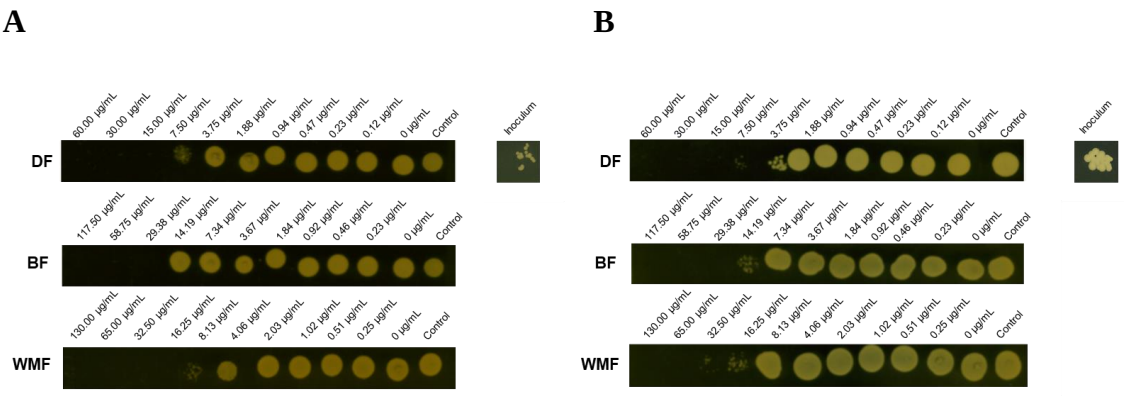

Figure 3.24. ***Growth of C. albicans on YPD plates after incubation with A22 DF, BF, and WMF.*** *Yeast cells were incubated with the fractions for 24 h (**A**) or 48 h (**B**) and a volume of 5 μL was spotted onto YPD plates. Images were digitalized after 24 h of incubation at 30 ºC. Inoculum: growth prior to fraction addition. Control: untreated cells.*

Table 3.9. ***MFC of A22 most active fractions against C. glabrata and C. albicans.***

	MFC (µg/mL)			
A22 Fraction	***C. glabrata***		***C. albicans***	
	24 h	**48 h**	**24 h**	**48 h**
DF	15	15	15	15
BF	58.75	58.75	29.38	29.38
WMF	8.13	16.25	16.25	65

Dichloromethane fraction (DF), n-butanol fraction (BF), and water-methanol fraction (WMF).

For both species, the dichloromethane (DF) fraction from A22 exhibits the highest fungicidal activity. We, therefore, decided to prioritize this fraction in the subsequent purification procedure.

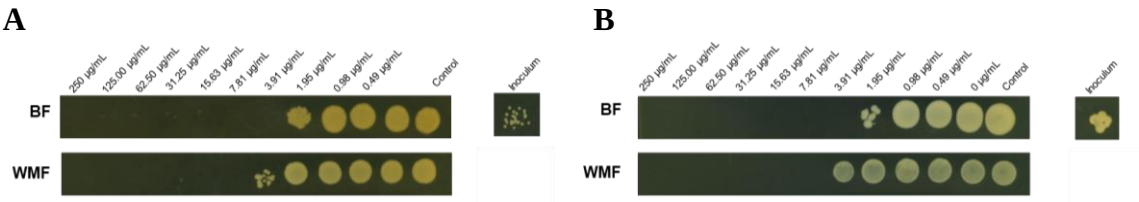

Figure 3.25. ***Growth of C. glabrata on YPD plates after incubation with O23 BF and WMF.*** *Yeast cells were incubated with the fractions for 24 h (**A**) or 48 h (**B**) and a volume of 5 µL was spotted onto YPD plates. Images were digitalized after 24 h of incubation at 37 ºC. Inoculum: growth prior to fraction addition. Control: untreated cells.*

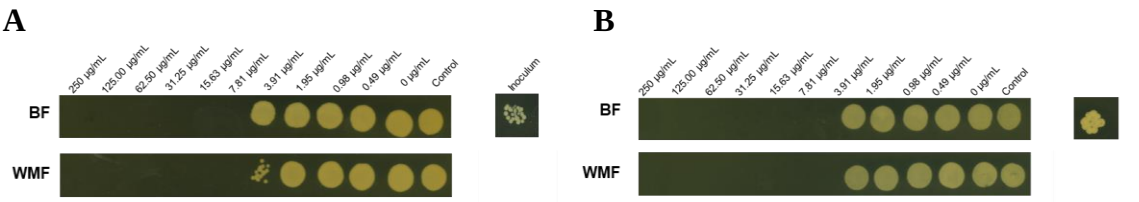

Figure 3.26. ***Growth of C. albicans on YPD plates after incubation with O23 BF and WMF.*** *Yeast cells were incubated with the fractions for 24 h (**A**) or 48 h (**B**) and a volume of 5 µL was spotted onto YPD plates. Images were digitalized after 24 h of incubation at 30 ºC. Inoculum: growth prior to fraction addition. Control: untreated cells.*

Table 3.10. ***MFC of O23 most active fractions against C. glabrata and C. albicans.***

	MFC (µg/mL)			
O23 Fraction	***C. glabrata***		***C. albicans***	
	24 h	**48 h**	**24 h**	**48 h**
BF	3.91	3.91	7.81	7.81
WMF	7.81	7.81	7.81	7.81

n-butanol fraction (BF) and water-methanol fraction (WMF).

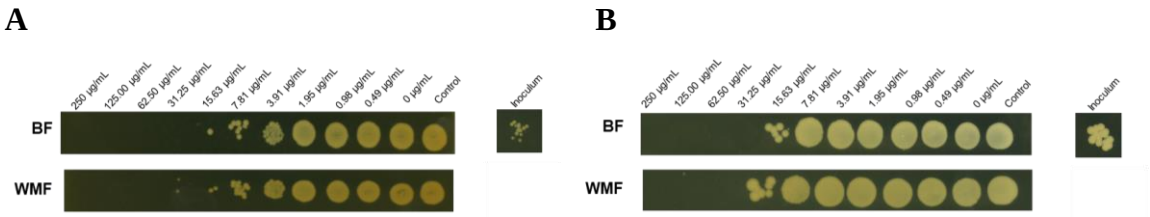

Figure 3.27. ***Growth of C. glabrata on YPD plates after incubation with O30 BF and WMF.*** *Yeast cells were incubated with the fractions for 24 h (**A**) or 48 h (**B**) and a volume of 5 µL was spotted onto YPD plates. Images were digitalized after 24 h of incubation at 37 ºC. Inoculum: growth prior to fraction addition. Control: untreated cells.*

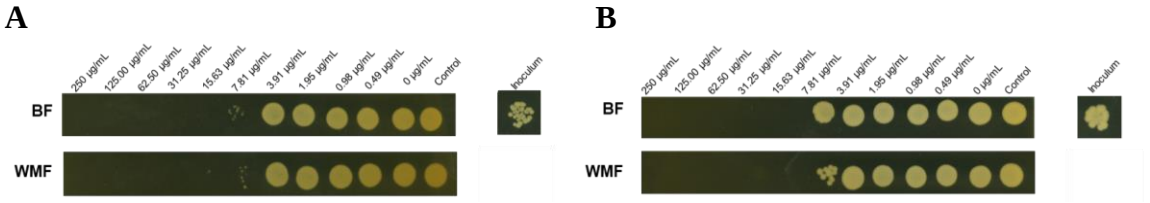

Figure 3.28. ***Growth of C. albicans on YPD plates after incubation with O30 BF and WMF.*** *Yeast cells were incubated with the fractions for 24 h (**A**) or 48 h (**B**) and a volume of 5 µL was spotted onto YPD plates. Images were digitalized after 24 h of incubation at 30 ºC. Inoculum: growth prior to fraction addition. Control: untreated cells.*

Table 3.11. ***MFC of O30 most active fractions against C. glabrata and C. albicans.***

O30 Fraction	MFC (µg/mL)			
	C. glabrata		*C. albicans*	
	24 h	**48 h**	**24 h**	**48 h**
BF	31.25	31.25	15.63	15.63
WMF	62.5	31.25	15.63	15.63

n-butanol fraction (BF) and water-methanol fraction (WMF).

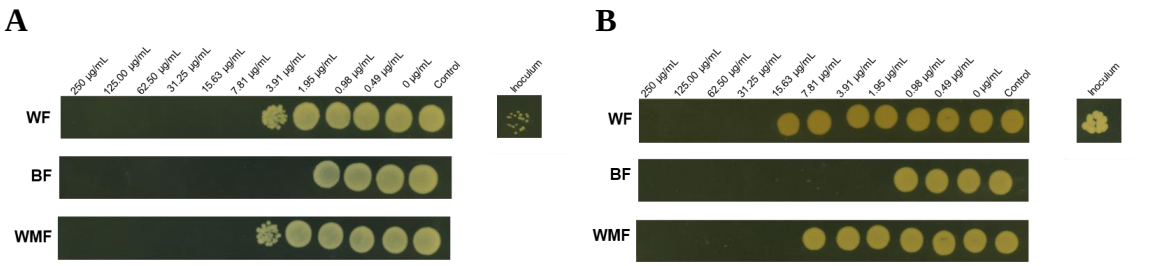

Figure 3.29. ***Growth of C. glabrata on YPD plates after incubation with O32 WF, BF, and WMF.*** *Yeast cells were incubated with the fractions for 24 h (**A**) or 48 h (**B**) and a volume of 5 µL was spotted onto YPD plates. Images were digitalized after 24 h of incubation at 37 ºC. Inoculum: growth prior to fraction addition. Control: untreated cells.*

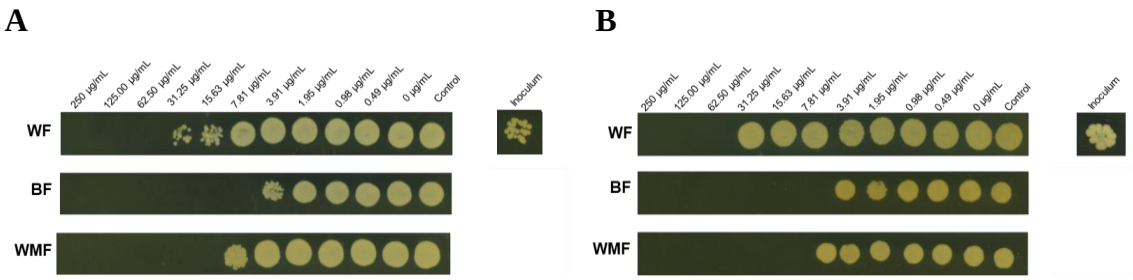

Figure 3.30. ***Growth of C. albicans on YPD plates after incubation with O32 WF, BF, and WMF.*** *Yeast cells were incubated with the fractions for 24 h* ***(A)*** *or 48 h* ***(B)*** *and a volume of 5 µL was spotted onto YPD plates. Images were digitalized after 24 h of incubation at 30 ºC. Inoculum: growth prior to fraction addition. Control: untreated cells.*

Table 3.12. ***MFC of O32 most active fractions against C. glabrata and C. albicans.***

	MFC (µg/mL)			
O32 Fraction	***C. glabrata***		***C. albicans***	
	24 h	**48 h**	**24 h**	**48 h**
WF	7.81	31.25	62.5	62.5
BF	1.95	1.95	7.81	7.81
WMF	7.81	15.63	15.63	15.63

Water fraction (WF), n-butanol fraction (BF), and water-methanol fraction (WMF).

For the extracts of Library II, the highest fungicidal activity was found in *n*-butanol fractions (BF).

In *C. glabrata*, O23 BF is fungicidal at 3.91 µg/mL (two-fold higher than the MIC upper-value) (**Table 3.10**). Similarly, in *C. albicans*, O23 BF is fungicidal at 7.81 µg/mL (concentration two-fold higher than the upper MIC value at 24 and 48 hours) (**Table 3.10**). O30 BF is fungicidal in *C. glabrata* at 31.25 µg/mL (four to eight-fold higher than the MIC upper-value) (**Table 3.11),** and in *C. albicans* at 15.63 µg/mL (two-fold higher than the MIC upper-value) (**Table 3.11**). O32 BF is fungicidal at concentrations of 1.95 µg/mL and 7.81 µg/mL in *C. glabrata* and *C. albicans*, respectively (two-fold higher than the MIC upper-value at 24 hours, and in the MIC upper-value concentration at 48 hours) (**Table 3.12**).

3.8. Fractionation of the O32 fractions (Library II)

The *n*-butanol and water-methanol fractions of extract O32 were next separated by HPLC.

3.8.1. Fractionation of the O32 BF

The *n*-butanol fraction originated three distinct peaks (A to C, **Figure 3.31**) with retention times of 10.051, 11.900, and 31.314 minutes (**Table 3.13**).

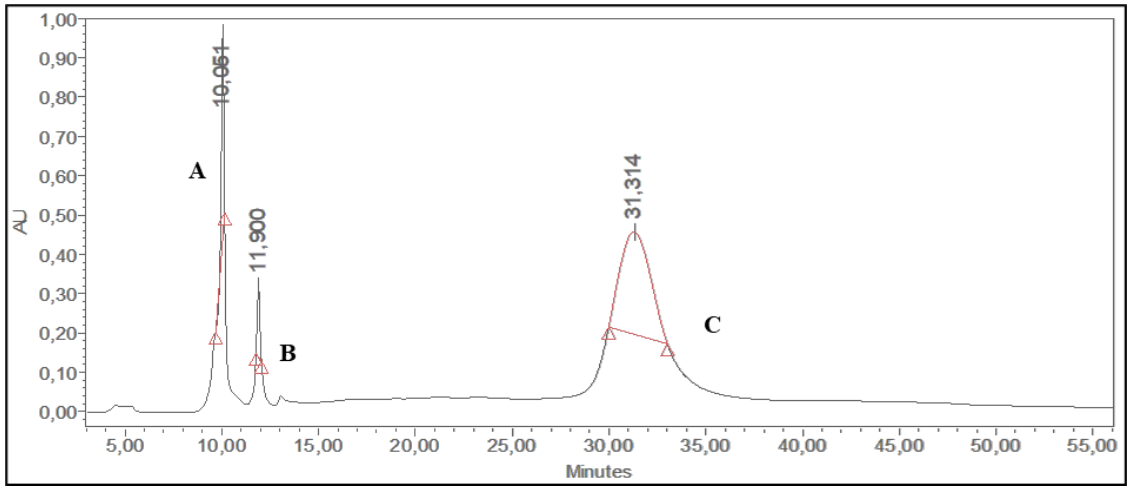

Figure 3.31. ***HPLC chromatogram of the O32 n-butanol fraction.***

Table 3.13. ***O32 n-butanol fraction retention times of A-C peaks.***

Peak	Retention Time (min)
A	10.051
B	11.900
C	31.314

3.8.2. Fractionation of the O32 WMF

As for the water-methanol fraction, six distinct peaks (A to F, **Figure 3.32**) with retention times of 9.888, 10.213, 10.617, 11.855, 13.004, and 31.266 minutes were obtained (**Table 3.14**).

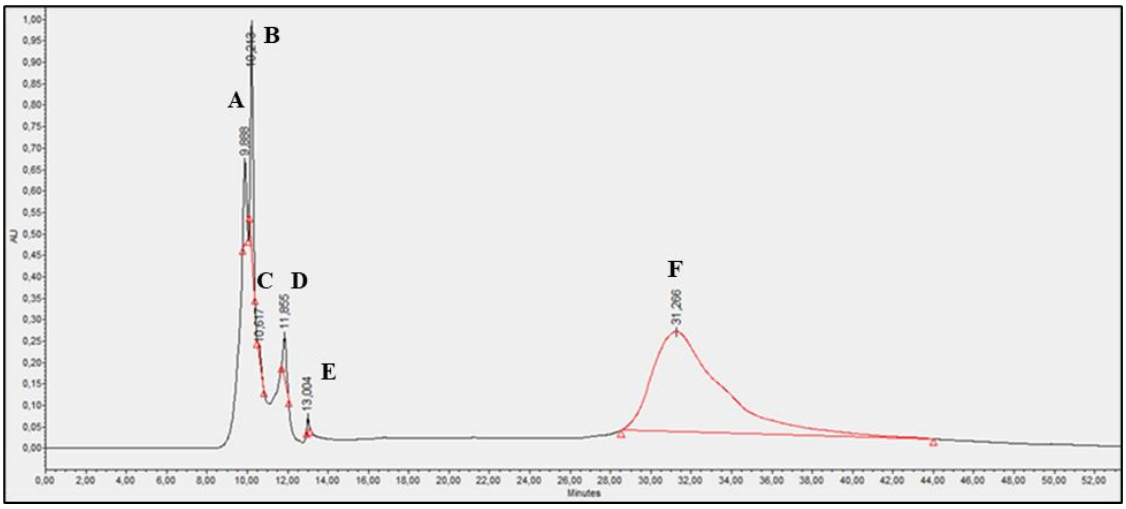

Figure 3.32. ***HPLC chromatogram of the O32 water-methanol fraction.***

Table 3.14. ***O32 water-methanol fraction retention times of A-F peaks.***

Peak	Retention Time (min)
A	9.888
B	10.213
C	10.617
D	11.855
E	13.004
F	31.266

All peaks will be isolated and subsequently analyzed by HRMS and NMR to identify the chemical structure of the compounds. Once the compounds have been identified, the antifungal activity will be analyzed. This process will be repeated with the other Library II subfractions. Simultaneously, we are adjusting a new method to separate a larger amount of the sub-fractions and speed up this process.

3.9. Solid Phase Extraction of the A22 DF (Library I) and evaluation of the antifungal potential of the resulting sub-fractions

The dichloromethane (DF) and the water-methanol (WMF) fractions were the most active among those obtained from crude A22 (**Table 3.5**).

The dichloromethane fraction (DF) was subjected to SPE, which originated seven new sub-fractions: R1 to R7. The antifungal activity of the fractions was next analyzed as described above (**Figures 3.33** and **3.34).** We found that all sub-fractions were active against *C. glabrata* and *C. albicans* with sub-fractions R2, R3, R4, and R5 excelling in terms of antifungal efficacy at the concentrations assayed (**Figure 3.33**). Accordingly, these fractions have fungicidal activity as indicated in **Figure 3.34**.

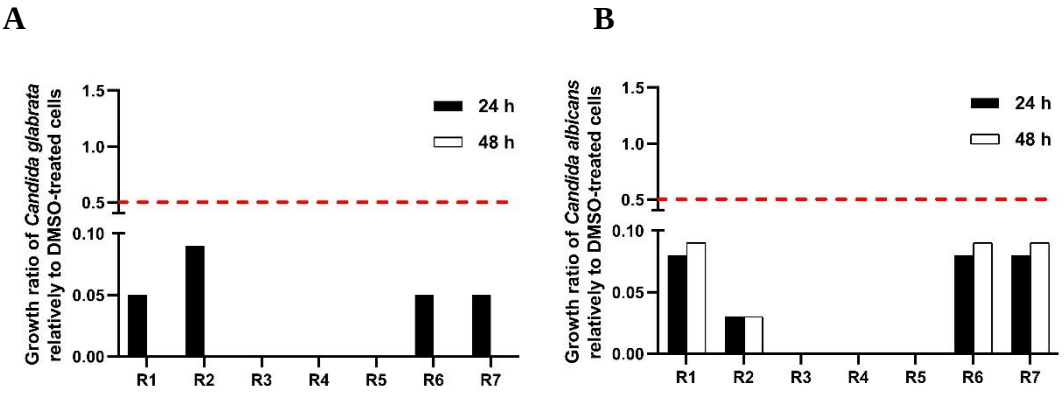

Figure 3.33. ***Susceptibility of Candida spp. to each A22 DF sub-fractions.*** *Sub-fractions: R1 to R7. Growth was monitored after 24 and 48 h of incubation at 37 ºC (C. glabrata (**A**)) and 30 ºC (C. albicans (**B**)). Growth ratios were determined relative to control (DMSO-treated cells). Ratios below 0.5 (red line) indicate active fractions The concentrations tested are listed in Table S.3.*

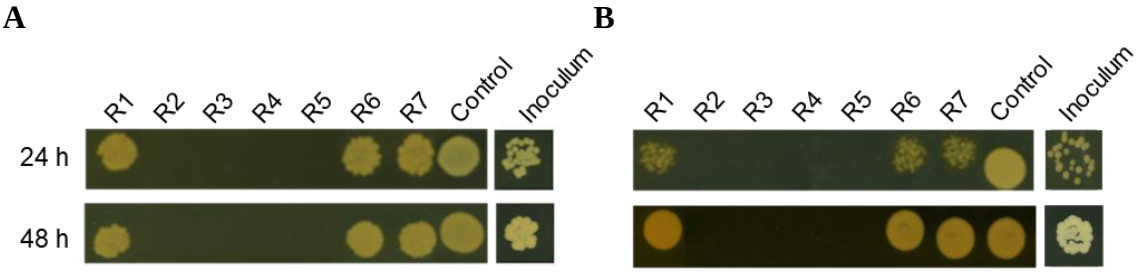

Figure 3.34. ***Growth of Candida spp. with different A22 DF sub-fractions: R1 to R7.*** *Yeast cells were incubated with the sub-fractions for 24 and 48 h and a volume of 5 µL was spotted onto YPD agar plates. Images were digitalized after 24 h of incubation at 37 ºC for C. glabrata (**A**) or 30 ºC for C. albicans (**B**). The concentrations tested are listed in Table S.4. Inoculum: cells prior to sub-fraction addition. Control: untreated cells.*

The MICs of the sub-fractions with fungicidal activity (R2 to R5) against *C. glabrata* and *C. albicans* were next determined.

All the sub-fractions appear to be very active against both *C. glabrata* and *C. albicans* with low MIC values (**Table 3.15**). With the exception of sub-fraction R4, all other sub-fractions had lower MICs than the originating DF fraction (**Table 3.5**), confirming the success of the fractionation step.

Table 3.15. ***MIC of A22 DF most active sub-fractions against C. glabrata and C. albicans.***

A22 Sub-fraction	**MIC** (µg/mL)			
	C. glabrata		***C. albicans***	
	24 h	**48 h**	**24 h**	**48 h**
R2	1.02 - 2.03	2.03 - 4.06	1.02 - 2.03	2.03 - 4.06
R3	1.41 - 2.81	2.81 - 5.63	1.41 - 2.81	2.81 - 5.63
R4	1.88 - 3.75	1.88 - 3.75	3.75 - 7.50	7.50 - 15.00
R5	0.90 - 1.80	1.80 - 3.59	0.90 - 1.80	1.8 - 3.59

In addition to *C. albicans* and *C. glabrata*, other *Candida* species are emerging as important pathogens. Among them are *C. krusei*, *C. tropicalis*, and *C. parapsilosis*, which together with *C. albicans* and *C. glabrata* are responsible for more than 90 percent of all yeast infections [4, 20, 21, 89]. Therefore, the most active fractions (R2-R5) were also tested against these species. All sub-fractions showed activity against *C. krusei*, *C. tropicalis*, and *C. parapsilosis*, with the sub-fractions R4 and R5 being generally the most actives (**Table 3.16**).

Table 3.16. ***MIC of A22 DF most active sub-fractions against C. krusei, C. tropicalis, and C. parapsilosis.***

A22 Sub-fraction	**MIC** (µg/mL)					
	C. krusei		***C. tropicalis***		***C. parapsilosis***	
	24 h	**48 h**	**24 h**	**48 h**	**24 h**	**48 h**
R2	7.34-14.69	14.69-29.38	7.34-14.69	7.34-14.69	7.34-14.69	14.69-29.38
R3	15.63-31.25	62.5-125	7.81-15.63	31.25-15.63	7.81-15.63	7.81-15.63
R4	5.63-11.25	5.63-11.25	2.81-5.63	5.63-11.25	2.81-5.63	2.81-5.63
R5	3.59-7.19	14.38-28.75	1.8-3.59	3.59-7.19	1.8-3.59	3.59-7.19

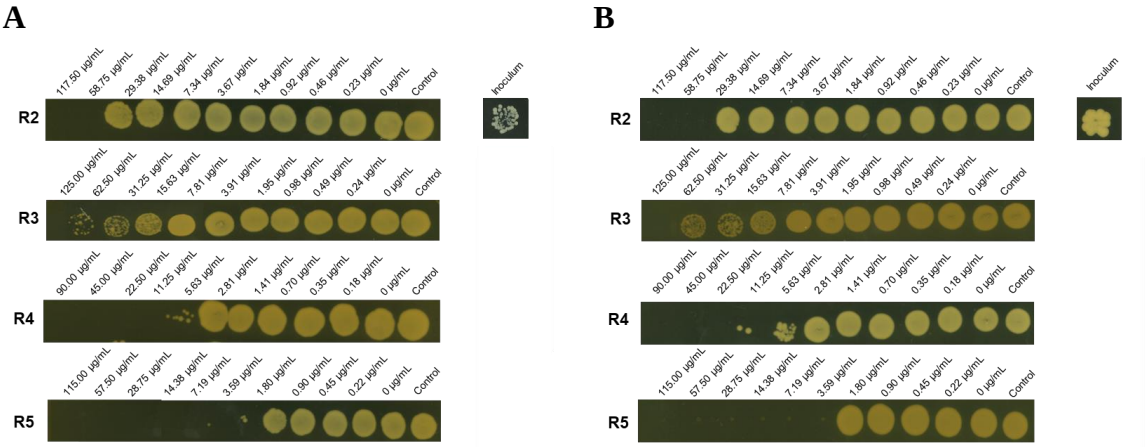

Figure 3.35. ***Fungicidal potential of sub-fractions R2 to R5 against C. glabrata.*** *Yeast cells were incubated with the indicated sub-fractions for 24 h (**A**) or 48 h (**B**) and a volume of 5 µL was spotted onto YPD plates. Images were digitalized after 24 h of incubation at 37 ºC. Inoculum: growth prior to sub-fraction addition. Control: untreated cells.*

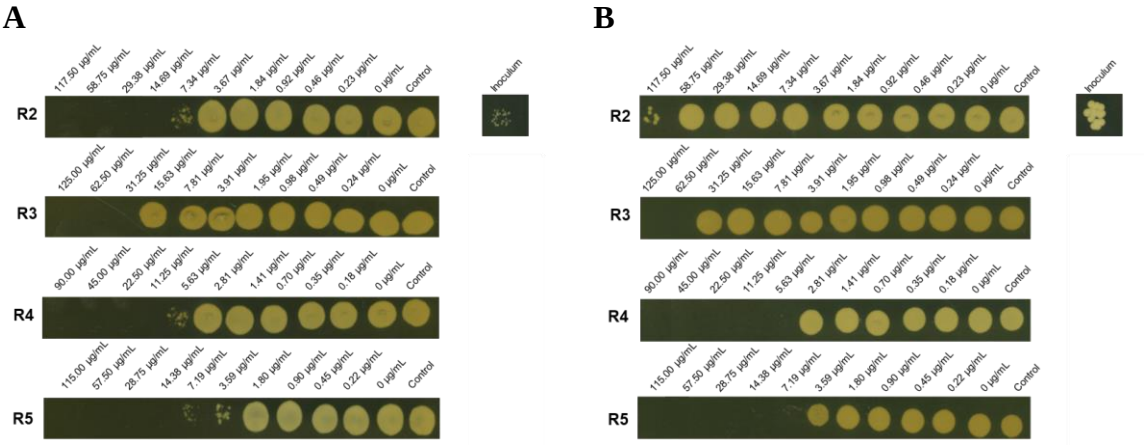

Figure 3.36. ***Fungicidal potential of sub-fractions R2 to R5 against C. albicans.*** *Yeast cells were incubated with the indicated sub-fractions for 24 h (**A**) or 48 h (**B**) and a volume of 5 µL was spotted onto YPD plates. Images were digitalized after 24 h of incubation at 30 ºC. Inoculum: growth prior to sub-fraction addition. Control: untreated cells.*

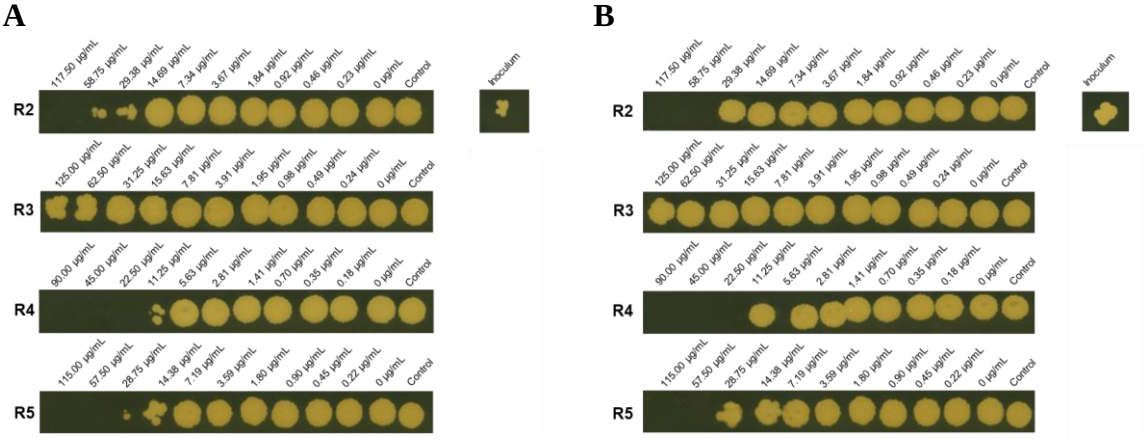

Figure 3.37. ***Fungicidal potential of sub-fractions R2 to R5 against C. krusei.*** *Yeast cells were incubated with the indicated sub-fractions for 24 h (**A**) or 48 h (**B**) and a volume of 5 µL was spotted onto YPD plates. Images were digitalized after 24 h of incubation at 30 ºC. Inoculum: growth prior to sub-fraction addition. Control: untreated cells.*

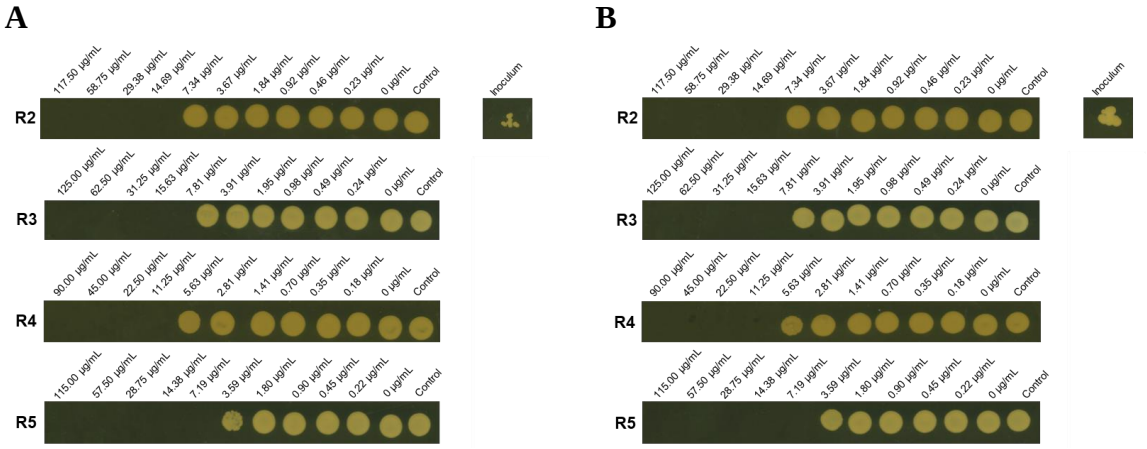

Figure 3.38. ***Fungicidal potential of sub-fractions R2 to R5 against C. tropicalis.*** *Yeast cells were incubated with the indicated sub-fractions for 24 h (**A**) or 48 h (**B**) and a volume of 5 µL was spotted onto YPD plates. Images were digitalized after 24 h of incubation at 30 ºC. Inoculum: growth prior to sub-fraction addition. Control: untreated cells.*

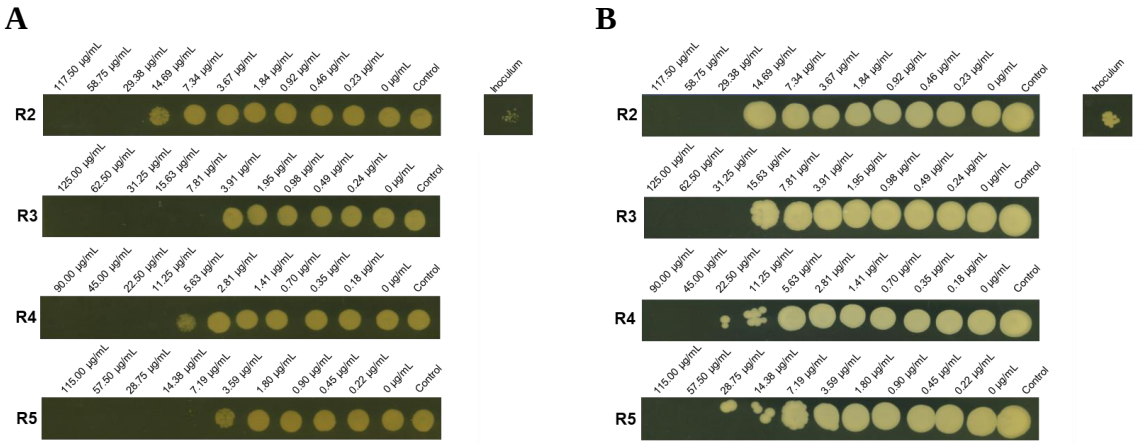

Figure 3.39. ***Fungicidal potential of sub-fractions R2 to R5 against C. parapsilosis.*** *Yeast cells were incubated with the indicated sub-fractions for 24 h (**A**) or 48 h (**B**) and a volume of 5 µL was spotted onto YPD plates. Images were digitalized after 24 h of incubation at 30 ºC. Inoculum: growth prior to sub-fraction addition. Control: untreated cells.*

Table 3.17. ***MFC of the most active A22 DF sub-fractions against C. glabrata, C. albicans, C. krusei, C. tropicalis, and C. parapsilosis.***

	MFC (µg/mL)							
	24 h				**48 h**			
	R2	**R3**	**R4**	**R5**	**R2**	**R3**	**R4**	**R5**
C. glabrata	58.75	125.00	11.25	3.59	58.75	125	22.50	3.59
C. albicans	14.69	31.25	11.25	14.38	*nf*	62.50	5.63	7.19
C. krusei	117.50	*nf*	22.50	57.50	58.75	*nf*	22.50	57.50
C. tropicalis	14.69	15.63	11.25	7.19	14.69	15.63	11.25	7.19
C. parapsilosis	29.38	7.81	11.25	7.19	29.38	31.25	45.00	57.50

nf - no fungicidal activity detected within the concentration range tested (Table S.4).

Analysis of the fungicidal potential of the sub-fractions revealed that both R4 and R5 sub-fractions have the strongest fungicidal activity (lower MFCs) against all species, with the R4 sub-fraction being slightly more active (**Figure 3.35** to **3.39** and **Table 3.17**). The exception was *C. parapsilosis*, for which sub-fractions R2 and R3 had the strongest activity at 48 hours (**Table 3.17**).

3.10. Dereplication analysis of the most promising sub-fractions

Dereplication is a useful tool for the pharmacological screening of NPs potentially containing multiple molecules. The process is based on the identification of previously known compounds and involves the determination of molecular masses and formulas, which are then cross-referenced with taxonomic information in the literature and/or NP structural databases. These processes maximize the discovery of new molecules while minimizing the re-isolation and structural characterization of compounds previously reported in the literature. Therefore, dereplication is a crucial step in the screening of crude extracts [74].

As a first attempt to identify the compounds responsible for the promising antifungal activity of sub-fractions R2, R3, R4, and R5, UHPLC-HRMS positive mode was used to perform dereplication analyses of these sub-fractions (**Figure 3.40**).

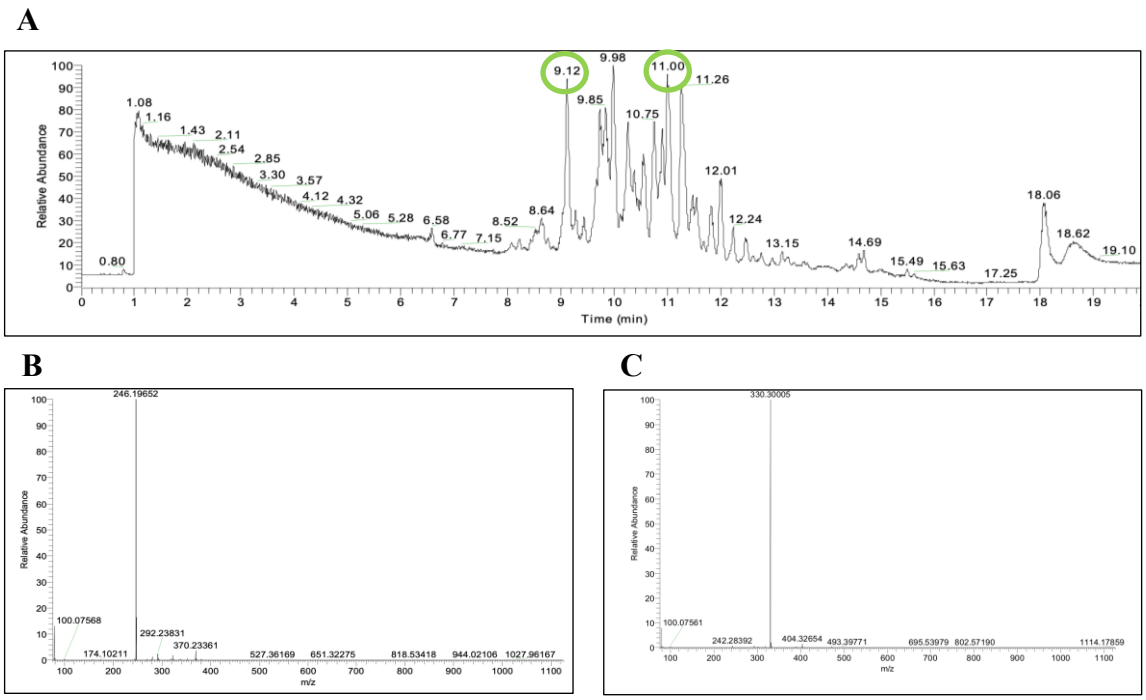

Figure 3.40. ***UHPLC-HRMS analysis of sub-fraction R4. (A)*** *UHPLC chromatogram.* ***(B)*** *HRMS of the chromatographic peak from the sub-fraction R4 eluted with a retention time of 9.12 minutes showing a* $[M+H]^+$ *ion adduct that matches with mirabilin B. (C) HRMS of the chromatographic peak from the sub-fraction R4 eluted with a retention time of 11.00 minutes showing a* $[M+H]^+$ *ion adduct that matches with Penaresidin B.*

Two compounds corresponding to the molecular ions found in the R4 sub-fraction were identified (**Figure 3.41**). The eluted compound with a retention time of 9.12 minutes (Compound **1**) showing a $[M+H]^+$ ion adduct at *m/z* 246.1965 matches with the previously described molecule mirabilin B [90] (**Figure 3.41.A**). Compound **2** also matches up with a reported molecule, penaresidin B [91], with a retention time of 11.00 minutes and an experimental value of $[M+H]^+$ *m/z* 330.3001 (**Figure 3.41.B**). A similar analysis was performed for R2, R3, and R5. A total of 19 molecular ions corresponding to 19 UHPLC signals were detected: three ions for R2, two for R3, and seven for R4 and R5. **Table 3.18** summarizes the results obtained. Thirteen of the 19 molecular ions were not identified and they might therefore be new compounds or molecules that have not yet been added to the AntiMarin [79] and CAS SciFinder [80].

Table 3.18. ***UHPLC-HRMS analysis of R2, R3, R4, and R5 sub-fractions.***

Sub-fractions	Retention Time (min)	Molecular Ion (*m/z*)	Compounds previously reported	References
R2	9.56	256.8662		
	10.49	259.2150		
	15.49	282.2792		
R3	12.00	330.3001	Penaresidin B (*m/z* 330.3002)	[91]
	12.21	404.3271		
R4	9.12	246.1965	Mirabilin B (*m/z* 246.1964)	[87, 90]
	9.98	248.2177		
	10.25	346.2488		
	10.75	348.2644		
	11.00	376.2960		
	11.26	318.3001		
	11.01	330.3001	Penaresidin B (*m/z* 330.3002)	[91]
R5	10.87	325.2749		
	11.22	318.3006		
	11.71	332.3156		
	11.90	330.3001	Penaresidin B (*m/z* 330.3002)	[91]
	12.14	404.3265		
	12.42	344.3158		
	15.49	282.2793		

Interestingly, dehydrobatzelladine C, one molecule isolated from *M. arbuscula* (from where A22 originated) with antifungal activity against *C. albicans* and *A. fumigatus* [85-87] was not identified in the R2 to R5 sub-fractions.

3.11. NMR analysis of R4 confirms the presence of Mirabilin B and Penaresidin B

^{13}C NMR spectra of the R4 sub-fraction indicate the presence of the main chemical shifts of compounds **1** and **2** (**Figure 3.41**) [94]. The chemical shift signals of ^{13}C in the experimental spectra were compared with the chemical shift values of ^{13}C reported in the literature for those compounds using Pearson's chi-squared goodness of fit test (χ^2) with Yates continuity correction (**Table 3.19**).

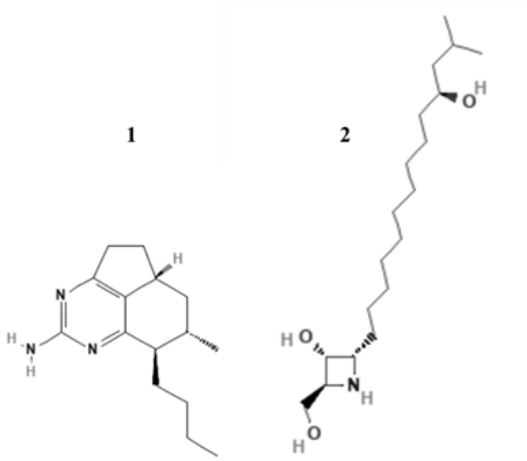

Figure 3.41. ***Chemical structure of the compounds present in R4 sub-fraction. 1:*** *Mirabilin B* and ***2:*** *Penaresidin B [94].*

Table 3.19. ***[a]Experimental and [b]reported [13]C NMR (125 MHz) data for Mirabilin B (Compound 1) and Penaresidin B (Compound 2).*** ** $CDCl_3$ **CD_3OD.*

Post.	Compound 1		Compound 2	
	$^a\delta_C$, Type*	$^b\delta_C$, Type**	$^a\delta_C$, Type*	$^b\delta_C$, Type**
1			61.3, CH_2	62.3, CH_2
2	176.3, C	176.2, C	66.3, CH	66.6, CH
3	126.9, C	126.8, C	66.9, CH	67.4, CH
4	167.3, C	167.3, C	65.4, CH	64.8, CH
5			27.2, CH_2	26.9, CH_2
6	164.6, C	164.6, C	27.2, CH_2	26.9, CH_2
7			27.2, CH_2	26.9, CH_2
8	39.2, CH	39.0, CH	27.2, CH_2	26.9, CH_2
9	40.4, CH_2	40.8, CH_2	27.2, CH_2	26.9, CH_2
10	35.1, CH	35.2, CH	27.2, CH_2	26.9, CH_2
11	48.8, CH	48.2, CH	27.2, CH_2	26.9, CH_2
12	34.4, CH_2	34.3, CH_2	27.2, CH_2	26.9, CH_2
13	34.2, CH_2	34.1, CH_2	27.2, CH_2	26.9, CH_2
14			72.6, CH	72.7, CH
15	21.6, CH_3	21.3, CH_3	34.9, CH_2	34.9, CH_2
16	31.6, CH_3	31.1, CH_3	24.8, CH	24.6, CH
17	28.6, CH_2	28.6, CH_2	25.6, CH_2	25.5, CH_2
18	24.2, CH_2	24.4, CH_2	11.5, CH_3	11.6, CH_3
19	14.4, CH_3	14.4, CH_3	22.3, CH_3	22.3, CH_3

The chi-squared goodness of fit test revealed that the experimental values for compound **1** did not differ significantly (99% confidence level) from those reported ($\chi_Y^2 = 0.0460$, *p*-value = 0.8302). The same was observed with compound **2** ($\chi_Y^2 = 0.0405$, *p*-value = 0.8405). Thus, our experimental data were not significantly different from those expected and confirm the presence of Mirabilin B and Penaresidin B in sub-fraction R4.

Chapter 4 – Conclusion

This work clearly indicates that MNPs produced by invertebrates of the Yucatan Peninsula had significant antifungal potential. Twenty-three of these species, collected in other regions of the globe, have already been shown to be active against medically important fungi and many compounds have been isolated (**Table S.5**). However, in our study not all of these species, gave rise to active extracts (*e.g*. extracts A2, A9, A13, A15, A17, A19, A24, A38, A53, A55, A59, A62, A65, **Figure 3.1** and **3.2)**. Insufficient tested material or the lack of synthesis of active MNPs in that environment (Yucatan Peninsula) or period could certainly explain these differences.

Our findings also highlight the still untapped potential of already explored species. This is the case of *Monanchora arbuscula*, in which the compounds dehydrobatzelladine C and batzelladine L, have been previously isolated and shown to have antifungal activity against *C. albicans*, *A. fumigatus* and, *A. flavus* [85-87]. This thesis brings to light novel compounds with antifungal activity that exist in *Monanchora arbuscula* (extract A22 in this work). Here, a bioguided fractionation combined with a dereplication approach indicates the absence of dehydrobatzelladine C and batzelladine L from one of the most active sub-fractions of extract A22, R4 (**Figure 3.41**). In R4, we found several compounds, of which we could only identify two, mirabilin B and penaresidin B [85-87]. Mirabilin B was reported to have antifungal activity against *Cryptococcus neoformans* [95] and also anti-leishmanial activity [96]. Penaresidin B has antibacterial and antifungal activity (including activity against *Cryptococcus neoformans, Aspergillus niger,* and *C. albicans*) [97] but it was shown to be cytotoxic [98]. Therefore it may well be that the antifungal activity observed in R4 results from these two compounds. In this sense, it would be interesting to test whether structural analogs of mirabilin B and penaresidin B also have antifungal activity. Our results also show that this type of approach can be useful to speed up the identification of new compounds, by allowing the prioritization of sub-fractions where compounds already described are not present.

One interesting aspect of the YP extracts is their fungicidal character **(Figures 3.5** to **3.8).** So far, there are only a few known MNPs, isolated from invertebrates, with fungicidal activity [49, 61, 67, 99, 100]. The fungicidal properties of antifungal molecules are particularly important in an infection setting where the host is not immunocompetent.

Immunosuppression is a well-known risk factor for the onset and progression of serious fungal infections [10, 15, 16], and few effective treatment options are available. In this context, it is extremely important to invest in the development of fungicidal drugs that can be used in these specific circumstances.

Another interesting feature of the extracts of Library II, in particular O23 and O30, is their marginal toxicity to mammalian cells. Fungal and mammalian cells share many cellular characteristics, and therefore, the development of selective drugs that target the former, but not the latter, is a challenging task. This has contributed greatly to discouraging investment by the pharmaceutical industry in the development of new drugs [61].

Finally, the fact that most of these extracts are more effective against *C. glabrata* than *C. albicans* is particularly promising, as this yeast is inherently more tolerant to current antifungals [29, 30]. In addition, IFIs caused by *C. glabrata* resistant to current drugs are on the rise, and treatment options are scarce [4, 20, 21].

We are currently separating the compounds present in the active sub-fractions of the extracts from Library II using LC-MS and HPLC. The isolated compounds will be then chemically characterized using NMR and HRMS. This workflow is extremely time consuming, as it requires protocol optimization for each compound. Once the compound is purified, further biological studies will be carried out. We will assess the spectrum of activity of the compounds against a panel of clinically relevant fungi (including filamentous and dermatophyte fungi). We will evaluate their antibiofilm activity and *in vivo* toxicity using animal models. Finally, it would also be interesting to determine the mechanisms of action of the compound by using, for example, a chemical genomics strategy.

Overall, this work highlights marine YP organisms as important reservoirs of new MNPs with promising fungicidal activity. In this sense, the purification and detailed chemical characterization of the active compounds is worth pursuing, as they may greatly advance the treatment of IFIs, especially those afflicting immunosuppressed patients.

Chapter 5 – References

1. WHO: The top 10 causes of death. Who.int. 2022. Available at: https://www.who.int/news-room/fact-sheets/detail/the-top-10-causes-of-death. Accessed date: 9 August 2022.

2. Hoenigl, M., Invasive Fungal Disease Complicating Coronavirus Disease 2019: When It Rains, It Spores. Clin Infect Dis, 2021. 73(7): p. e1645-e1648.

3. Segrelles-Calvo, G., et al., Candida sp. co-infection in COVID-19 patients with severe pneumonia: Prevalence study and associated risk factors. Respir Med, 2021. 188: p. 106619.

4. Kohler, J.R., A. Casadevall, and J. Perfect, The spectrum of fungi that infects humans. Cold Spring Harb Perspect Med, 2014. 5(1): p. a019273.

5. Shapiro, R.S., N. Robbins, and L.E. Cowen, Regulatory circuitry governing fungal development, drug resistance, and disease. Microbiol Mol Biol Rev, 2011. 75(2): p. 213-67.

6. Vandeputte, P., S. Ferrari, and A.T. Coste, Antifungal Resistance and New Strategies to Control Fungal Infections. International Journal of Microbiology, 2012. 2012: p. 1-26.

7. Bongomin, F., et al., Global and Multi-National Prevalence of Fungal Diseases-Estimate Precision. J Fungi (Basel), 2017. 3(4).

8. WHO: Global Tuberculosis Report. 2021. Who.int. 2022. Available at: https://www.who.int/publications/i/item/9789240037021. Accessed date: 9 August 2022.

9. WHO: World Malaria Report. 2021. Who.int. 2022. Available at: https://www.who.int/teams/global-malaria-programme/reports/world-malaria-report-2021. Accessed date: 9 August 2022.

10. Pappas, P.G., et al., Clinical Practice Guideline for the Management of Candidiasis: 2016, Update by the Infectious Diseases Society of America. Clin Infect Dis, 2016. 62(4): p. e1-50.

11. Sousa, F., et al., Current Insights on Antifungal Therapy: Novel Nanotechnology Approaches for Drug Delivery Systems and New Drugs from Natural Sources. Pharmaceuticals (Basel), 2020. 13(9).

12. Souza, A.C. and A.C. Amaral, Antifungal Therapy for Systemic Mycosis and the Nanobiotechnology Era: Improving Efficacy, Biodistribution and Toxicity. Front Microbiol, 2017. 8: p. 336.

13. Firacative, C., Invasive fungal disease in humans: are we aware of the real impact? Mem Inst Oswaldo Cruz, 2020. 115: p. e200430.

14. Stop neglecting fungi. Nature microbiology, 2, 17120.

15. Enoch, D.A., et al., The Changing Epidemiology of Invasive Fungal Infections. Methods Mol Biol, 2017. 1508: p. 17-65.

16. Chang, Y.-L., et al., New facets of antifungal therapy. Virulence, 2017. 8(2): p. 222-236.

17. Ghannoum, M. A., & Rice, L. B. Antifungal agents: mode of action, mechanisms of resistance, and correlation of these mechanisms with bacterial resistance. Clinical microbiology reviews. 1999 12(4), 501–517.

18. Soulountsi, V., T. Schizodimos, and S.C. Kotoulas, Deciphering the epidemiology of invasive candidiasis in the intensive care unit: is it possible? Infection, 2021. 49(6): p. 1107-1131.

19. Alves, R., et al., Adapting to survive: How Candida overcomes host-imposed constraints during human colonization. PLoS Pathog, 2020. 16(5): p. e1008478.

20. Pfaller, M.A. and D.J. Diekema, Epidemiology of invasive candidiasis: a persistent public health problem. Clin Microbiol Rev, 2007. 20(1): p. 133-63.

21. Pappas, P. G., Lionakis, M. S., Arendrup, M. C., Ostrosky-Zeichner, L., & Kullberg, B. J. (2018). Invasive candidiasis. Nature reviews. Disease primers, 4, 18026

22. Denning DW, Bromley MJ. Infectious Disease. How to bolster the antifungal pipeline. Science. 2015 ;347(6229):1414-6.

23. Chang, A., D. Neofytos, and D. Horn, Candidemia in the 21st century. Future Microbiol, 2008. 3(4): p. 463-72.
24. Vincent, J.-L., International Study of the Prevalence and Outcomes of Infection in Intensive Care Units. JAMA, 2009. 302(21): p. 2323.
25. Kotey, F. C., Dayie, N. T., Tetteh-Uarcoo, P. B., & Donkor, E. S. (2021). Candida Bloodstream Infections: Changes in Epidemiology and Increase in Drug Resistance. Infectious diseases, 14, 11786337211026927
26. McCarty, T. P., & Pappas, P. G. (2016). Invasive Candidiasis. Infectious disease clinics of North America, 30(1), 103–124.
27. Kim, H., et al., 2-Alkyl-4-hydroxyquinolines from a Marine-Derived Streptomyces sp. Inhibit Hyphal Growth Induction in Candida albicans. Mar Drugs, 2019. 17(2).
28. Lu, Y., et al., Synergistic regulation of hyphal elongation by hypoxia, CO(2), and nutrient conditions controls the virulence of Candida albicans. Cell Host Microbe, 2013. 14(5): p. 499-509.
29. Hassan, Y., S.Y. Chew, and L.T.L. Than, Candida glabrata: Pathogenicity and Resistance Mechanisms for Adaptation and Survival. Journal of Fungi, 2021. 7(8): p. 667.
30. Healey, K.R., et al., Genetic Drivers of Multidrug Resistance in. Front Microbiol, 2016. 7: p. 1995.
31. De Groot, P.W.J., et al., The Cell Wall of the Human Pathogen. Candida glabrata: Differential Incorporation of Novel Adhesin-Like Wall Proteins. Eukaryotic Cell, 2008. 7(11): p. 1951-1964.
32. Kasper, L., et al., Identification of Candida glabrata Genes Involved in pH Modulation and Modification of the Phagosomal Environment in Macrophages. PLoS ONE, 2014. 9(5): p. e96015.
33. Kasper, L., K. Seider, and B. Hube, Intracellular survival of Candida glabrata in macrophages: immune evasion and persistence. FEMS Yeast Research, 2015. 15(5): p. fov042.
34. Atriwal T, Azeem K, Husain FM, Hussain A, Khan MN, Alajmi MF, Abid M. Mechanistic Understanding of Candida albicans Biofilm Formation and Approaches for Its Inhibition. Front Microbiol. 2021;12:638609.
35. Talapko, J., et al., Candida albicans-The Virulence Factors and Clinical Manifestations of Infection. J Fungi (Basel), 2021. 7(2).
36. Chen A, Sobel JD. Emerging azole antifungals. Expert Opin Emerg Drugs. 2005. 10(1):21-33
37. Robbins, N., Wright, G. D., & Cowen, L. E. (2016). Antifungal Drugs: The Current Armamentarium and Development of New Agents. Microbiology spectrum, 4(5), 10.1128/microbiolspec.FUNK-0002-2016.
38. Bellmann, R. and P. Smuszkiewicz, Pharmacokinetics of antifungal drugs: practical implications for optimized treatment of patients. Infection, 2017. 45(6): p. 737-779.
39. Lewis, R.E., Current concepts in antifungal pharmacology. Mayo Clinic Proceedings, 2011. 86(8): p. 805-17.
40. Anne and C.J.D. Sobel, Emerging Azole antifungals. Expert Opinion on Emerging Drugs, 2005. 10: p. 21-33.
41. Maertens JA. History of the development of azole derivatives. Clin Microbiol Infect. 2004;10 Suppl 1:1-10.
42. Gold, J.A.W., et al., Treatment Practices for Adults with Candidemia at 9 Active Surveillance Sites-United States, 2017-2018. Clin Infect Dis, 2021. 73(9): p. 1609-1616.
43. Di Mambro, T., et al., The Yin and Yang of Current Antifungal Therapeutic Strategies: How Can We Harness Our Natural Defenses? Front Pharmacol, 2019. 10: p. 80.
44. Lupetti A, Danesi R, Campa M, Del Tacca M, Kelly S. Molecular basis of resistance to azole antifungals. Trends Mol Med. 2002;8(2):76-81.
45. WHO: Global action plan on antimicrobial resistance. 2015. Available at: https://ahpsr.who.int/publications/i/item/global-action-plan-on-antimicrobial-resistance Accessed date: 9 August 2022.

46. Lamoth, F., et al., Changes in the epidemiological landscape of invasive candidiasis. J Antimicrob Chemother, 2018. 73(suppl_1): p. i4-i13.
47. Berman, J. and D.J. Krysan, Drug resistance and tolerance in fungi. Nat Rev Microbiol, 2020. 18(6): p. 319-331.
48. Perlin, D.S., R. Rautemaa-Richardson, and A. Alastruey-Izquierdo, The global problem of antifungal resistance: prevalence, mechanisms, and management. Lancet Infect Dis, 2017. 17(12): p. e383-e392.
49. Barbosa, F., et al., Targeting antimicrobial drug resistance with marine natural products. Int J Antimicrob Agents, 2020. 56(1): p. 106005.
50. Masiá Canuto, M. and F. Gutiérrez Rodero, Antifungal drug resistance to azoles and polyenes. Lancet Infect Dis, 2002. 2(9): p. 550-63.
51. Jampilek, J., How can we bolster the antifungal drug discovery pipeline? Future Med Chem, 2016. 8(12): p. 1393-7.
52. CDC 2019 AR Threats Report. 2019 CDC.gov Available at: https://www.cdc.gov/drugresistance/biggest-threats.html#candida Accessed date: 9 August 2022
53. Shen, B., A New Golden Age of Natural Products Drug Discovery. Cell, 2015. 163(6): p. 1297-300.
54. Martins, A., et al., Marketed marine natural products in the pharmaceutical and cosmeceutical industries: tips for success. Mar Drugs, 2014. 12(2): p. 1066-101.
55. Demain, A.L. and A. Fang, The natural functions of secondary metabolites. Adv Biochem Eng Biotechnol, 2000. 69: p. 1-39.
56. Choudhary, A., et al., Current Status and Future Prospects of Marine Natural Products (MNPs) as Antimicrobials. Mar Drugs, 2017. 15(9).
57. Blunt, J.W., et al., Marine natural products. Nat Prod Rep, 2016. 33(3): p. 382-431.
58. Blunt, J.W., et al., Marine natural products. Nat Prod Rep, 2017. 34(3): p. 235-294.
59. El Amraoui B, El Wahidi M, Fassouane A. In vitro screening of antifungal activity of marine sponge extracts against five phytopathogenic fungi. Springer plus. 2014; 3:629. 2014.
60. Altmann, K.H., Drugs from the Oceans: Marine Natural Products as Leads for Drug Discovery. Chimia (Aarau), 2017. 71(10): p. 646-652.
61. Cardoso, J., et al., Marine-Derived Compounds and Prospects for Their Antifungal Application. Molecules, 2020. 25(24).
62. Carroll, A.R., et al., Marine natural products. Nat Prod Rep, 2021. 38(2): p. 362-413.
63. El-Hossary, E.M., et al., Antifungal potential of marine natural products. Eur J Med Chem, 2017. 126: p. 631-651.
64. Maslin, M., et al., Marine sponge aquaculture towards drug development: An ongoing history of technical, ecological, chemical considerations and challenges. Aquaculture Reports, 2021. 21.
65. Wong Chin, J.M., et al., Antimicrobial properties of marine fungi from sponges and brown algae of Mauritius. Mycology, 2021. 12(4): p. 231-244.
66. Mayer, A.M., et al., The odyssey of marine pharmaceuticals: a current pipeline perspective. Trends Pharmacol Sci, 2010. 31(6): p. 255-65.
67. Khotimchenko, Y., Pharmacological Potential of Sea Cucumbers. Int J Mol Sci, 2018. 19(5).
68. Hu, G.P., et al., Statistical research on marine natural products based on data obtained between 1985 and 2008. Mar Drugs, 2011. 9(4): p. 514-25.
69. MarinLit (Marine Natural Products), R.S.o. Chemistry, Editor.: https://marinlit.rsc.org/.
70. Stout, E.P., L.C. Yu, and T.F. Molinski, Antifungal Diterpene Alkaloids from the Caribbean Sponge Agelas citrina: Unified Configurational Assignments of Agelasidines and Agelasines. European Journal of Organic Chemistry, 2012. 2012(27): p. 5131-5135.
71. Pech-Puch, D., et al., Marine Organisms from the Yucatan Peninsula (Mexico) as a Potential Natural Source of Antibacterial Compounds. Mar Drugs, 2020. 18(7).
72. Pech-Puch, D., et al., Marine Natural Products from the Yucatan Peninsula. Mar Drugs, 2020. 18(1).

73. Li, X.-C., et al., Capisterones A and B, which Enhance Fluconazole Activity in Saccharomyces cerevisiae, from the Marine Green Alga Penicillus capitatus. Journal of Natural Products, 2006. 69(4): p. 542-546.
74. Atanasov, A.G., et al., Natural products in drug discovery: advances and opportunities. Nat Rev Drug Discov, 2021. 20(3): p. 200-216.
75. Krause, J. and G. Tobi, Discovery, Development, and Regulation of Natural Products, in Using Old Solutions to New Problems - Natural Drug Discovery in the 21st Century. 2013.
76. Morales, J.L., et al., Screening of Antibacterial and Antifungal Activities of Six Marine Macroalgae from Coasts of Yucatan Peninsula. Pharmaceutical Biology, 2008. 44(8): p. 632-635.
77. Pech-Puch, D., et al., Antiviral and Antiproliferative Potential of Marine Organisms from the Yucatan Peninsula, Mexico. Frontiers in Marine Science, 2020. 7.
78. CLSI, Reference Method for Broth Dilution Antifungal Susceptibility Testing of Yeasts., P. Wayne, Editor. 2016, Clinical and Laboratory Standards Institute.
79. Blunt, J.W., M.H.G. Munro, and H. Laatsch, AntiMarin Database, N.Z. University of Canterbury: Christchurch and G. University of Göttingen: Göttingen, Editors.
80. CAS SciFinder. Available from: https://www.cas.org/solutions/cas-scifinder-discovery-platform/cas-scifinder.
81. Animal Cell Culture Guide. Available from: https://www.atcc.org/resources/culture-guides/animal-cell-culture-guide. Accessed date: 9 August 2022;
82. Ghasemi, M., et al., The MTT Assay: Utility, Limitations, Pitfalls, and Interpretation in Bulk and Single-Cell Analysis. International Journal of Molecular Sciences, 2021. 22(23): p. 12827.
83. Xu, N.J., X. Sun, and X.J. Yan. A new cyclostellettamine from sponge Amphimedon compressa. Chinese Che. Letters, 2007, 18, 947-950.
84. Shady, N.H., Fouad, M.A., Kamel, M. S. Schirmeister, T., Abelmohsen, U.R., Natural Product Repertoire of the Genus Amphimedon.Mar. Drugs, 2018, 17.
85. Dalisay, D.S., J.P. Saludes, and T.F. Molinski, Ptilomycalin A inhibits laccase and melanization in Cryptococcus neoformans. Bioorg Med Chem, 2011. 19(22): p. 6654-7.
86. Arevabini, C., et al., Antifungal activity of metabolites from the marine sponges Amphimedon sp. and Monanchora arbuscula against Aspergillus flavus strains isolated from peanuts (Arachis hypogaea). Nat Prod Commun, 2014. 9(1): p. 33-6.
87. Hua, H.-M., et al., Crystallographic and NMR studies of antiinfective tricyclic guanidine alkaloids from the sponge Monanchora unguifera. Bioorganic & Medicinal Chemistry, 2004. 12(24): p. 6461-6464.
88. Aldholmi, M., et al., A Decade of Antifungal Leads from Natural Products: 2010–2019. Pharmaceuticals, 2019. 12(4): p. 182.
89. Turner, S.A. and G. Butler, The Candida Pathogenic Species Complex. Cold Spring Harbor Perspectives in Medicine, 2014. 4(9): p. a019778-a019778.
90. Patil, A.D.; Freyer, A.J.; Offen, P.; Bean, M.F.; Johnson, R.K. Three new tricyclic guanidine alkaloids from the sponge Batzella sp. J. Nat. Prod. 1997, 60, 704–707.
91. Fujiwara, T.; Hashimoto, K.; Umeda, M.; Murayama, S.; Ohno, Y.; Liu, B.; Nambu, H.; Yakura, T. Divergent total synthesis of penaresidin B and its straight side chain analogue. Tetrahedron 2018, 74, 4578–4591
92. Schellhaas, K.; Schmalz, H.; Bats, J.W. Short Enantioselective Total Synthesis of (‡) - Ptilocaulin. 1998, 57–65.
93. Harbour, G.C.; Tymiak, A.A.; Rinehart, K.L.; Shaw, P.D.; Hughes, R.G.; Mizsak, S.A.; Coats, J.H.; Zurenko, G.E.; Li, L.H.; Kuentzel, S.L. Ptilocaulin and Isoptilocaulin, Antimicrobial and Cytotoxic Cyclic Guanidines from the Caribbean Sponge Ptilocaulis aff. P. spiculifer (Lamarck, 1814). J. Am. Chem. Soc. 1981, 103, 5604–5606, doi:10.1021/ja00408a071.
94. National Center for Biotechnology Information. PubChem Compound Summary 2022: https://pubchem.ncbi.nlm.nih.gov/.

95. Yu, M., S.S. Pochapsky, and B.B. Snider, Synthesis of 7-Epineoptilocaulin, Mirabilin B, and Isoptilocaulin. A Unified Biosynthetic Proposal for the Ptilocaulin and Batzelladine Alkaloids. Synthesis and Structure Revision of Netamines E and G. The Journal of Organic Chemistry, 2008. 73(22): p. 9065-9074.

96. Tempone, A.G., et al., Marine alkaloids as bioactive agents against protozoal neglected tropical diseases and malaria. Natural Product Reports, 2021. 38(12): p. 2214-2235.

97. Ohshita, K., et al., Synthesis of penaresidin derivatives and its biological activity. Bioorg Med Chem, 2007. 15(14): p. 4910-6.

98. Fujiwara, T., et al., Divergent total synthesis of penaresidin B and its straight side chain analogue. Tetrahedron, 2018. 74: p. 4578-4591.

99. Dong, J., et al., Marine-natural-products for biocides development: first discovery of meridianin alkaloids as antiviral and anti-phytopathogenic-fungus agents. Pest Manag Sci, 2020. 76(10): p. 3369-3376.

100. Cheung, R.C.F., et al., Antifungal and antiviral products of marine organisms. Applied Microbiology and Biotechnology, 2014. 98(8): p. 3475-3494.

101. Kossuga, M.H., et al., (2S,3R)-2-aminododecan-3-ol, a new antifungal agent from the ascidian Clavelina oblonga. J Nat Prod, 2004. 67(11): p. 1879-81.

102. Raub, M.F., J.H. Cardellina, and T.F. Spande. The piclavines, antimicrobial doi.org/10.1016/S0040-4039(00)74183-9.

103. Suzuki, K., et al., Synthesis and antimicrobial activity of β-carboline derivatives with N. Bioorg Med Chem Lett, 2018. 28(17): p. 2976-2978.

104. Shaala, L., et al., Didemnaketals F and G, New Bioactive Spiroketals from a Red Sea Ascidian Didemnum Species. Marine Drugs, 2014. 12(9): p. 5021-5034.

105. Schupp, P.; Poehner, T.; Edrada, R.A.; Ebel, R.; Berg, A.; Wray, V.; Proksch, P. Eudistomins W, and X, two new β-carbolines from the micronesian tunicate Eudistoma sp. J. Nat. Prod. 2003, 66, 272–275, doi:10.1021/np020315n.

106. Cafieri, F.; Fattorusso, E.; Mangoni, A.; Taglialatela-Scafati, O. Clathramides, unique bromopyrrole alkaloids from the Caribbean sponge Agelas clathrodes. Tetrahedron 1996, 52, 13713–13720, doi:10.1016/0040-4020(96)00824-1.

107. Walker, R.P.; John Faulkner, D.; Van Engen, D.; Clardy, J. Sceptrin, an Antimicrobial Agent from the Sponge Agelas sceptrum. J. Am. Chem. Soc. 1981, 103, 6772–6773.

108. Ciminiello, P.; Fattorusso, E.; Magno, S.; Mangoni, A. Clathridine and its zinc complex, novel metabolites from the marine sponge clathrina clathrus. Tetrahedron 1989, 45, 3873–3878.

109. Galeano, E.; Martínez, A. Antimicrobial activity of marine sponges from Urabá Gulf, Colombian Caribbean region. J. Mycol. Med. 2007, 17, 21–24.

110. Rodriguez, A.D.; Yoshida, W.Y.; Scheuer, P.J. Popolohuanone A and B. two new sesquiterpenoid aminoquinones from a pacific sponge dysidea sp. Tetrahedron 1990, 46, 8025–8030.

111. Hirsch, S.; Rudi, A.; Kashman, Y.; Loya, Y. New avarone and avarol derivatives from the marine sponge dysidea cinerea. J. Nat. Prod. 1991, 54, 92–97,

112. Jacob, M.R.; Hossain, C.F.; Mohammed, K.A.; Smillie, T.J.; Clark, A.M.; Walker, L.A.; Nagle, D.G. Reversal of Fluconazole Resistance in Multidrug Efflux-Resistant Fungi by the Dysidea arenaria Sponge Sterol 9α,11α-Epoxycholest-7-ene-3β ,5α,6α,19-tetrol 6-Acetate. J. Nat. Prod. 2003, 66, 1618–1622.

113. Sionov, E.; Roth, D.; Sandovsky-Losica, H.; Kashman, Y.; Rudi, A.; Chill, L.; Berdicevsky, I.; Segal, E. Antifungal effect and possible mode of activity of a compound from the marine sponge Dysidea herbacea. J. Infect. 2005, 50, 453–460.

114. Ciavatta, M.L.; Lopez Gresa, M.P.; Gavagnin, M.; Romero, V.; Melck, D.; Manzo, E.; Guo, Y.W.; van Soest, R.; Cimino, G. Studies on puupehenone-metabolites of a Dysidea sp.: structure and biological activity. Tetrahedron 2007, 63, 1380–1384.

115. Lee, D.; Shin, J.; Yoon, K.M.; Kim, T.I.; Lee, S.H.; Lee, H.S.; Oh, K.B. Inhibition of Candida albicans isocitrate lyase activity by sesterterpene sulfates from the tropical sponge Dysidea sp. Bioorganic Med. Chem. Lett. 2008, 18, 5377–5380.

116. Skepper, C.K., D.S. Dalisay, and T.F. Molinski, Synthesis and Antifungal Activity of (−)Z-Dysidazirine. Organic Letters, 2008. 10(22): p. 5269-5271.
117. Pejin, B.; Ciric, A.; Markovic, D.; Tommonaro, G.; Sokovic, M. In vitro avarol does affect the growth of Candida sp. Nat. Prod. Res. 2016, 30, 1956–1960,
118. Gharpure, S., A. Akash, and B. Ankamwar, A Review on Antimicrobial Properties of Metal Nanoparticles. J Nanosci Nanotechnol, 2020. 20(6): p. 3303-3339.
119. Ayyad, S.E., et al., Two new polyacetylene derivatives from the Red Sea sponge Xestospongia sp. Z Naturforsch C J Biosci, 2015. 70(11-12): p. 297-303.
120. Chen, Y., et al., New bioactive peroxides from marine sponges of the family plakiniidae. J Nat Prod, 2002. 65(10): p. 1509-12.
121. Chen, Y.; Killday, K.B.; McCarthy, P.J.; Schimoler, R.; Chilson, K.; Selitrennikoff, C.; Pomponi, S.A.; Wright, A.E. Three new peroxides from the sponge Plakinastrella species. J. Nat. Prod. 2001, 64, 262–264, doi:10.1021/np000368+.
122. Xu, T., et al., The marine sponge-derived polyketide endoperoxide plakortide F acid mediates its antifungal activity by interfering with calcium homeostasis. Antimicrob Agents Chemother, 2011. 55(4): p. 1611-21.
123. Dyshlovoy, S.A., et al., Aaptamines from the Marine Sponge Aaptos sp. Display Anticancer Activities in Human Cancer Cell Lines and Modulate AP-1-, NF-κB-, and p53-Dependent Transcriptional Activity in Mouse JB6 Cl41 Cells. BioMed Research International, 2014. 2014: p. 1-7.
124. Yu, H.-B., et al., Aaptamine Derivatives with Antifungal and Anti-HIV-1 Activities from the South China Sea Sponge Aaptos aaptos.
125. He, Q., et al., A Review of the Secondary Metabolites from the Marine Sponges of the Genus Aaptos. Natural Product Communications, 2020. 15(9): p. 1934578X2095143.
126. Kazanjian, A. and M. Fariñas, Actividades biológicas del extracto acuoso de la esponja Aplysina lacunosa (Porifera: Aplysinidae).
127. El-Bondkly, A.A.M., M.M.A.A. El-Gendy, and A.M.A. El-Bondkly, Construction of Efficient Recombinant Strain Through Genome Shuffling in Marine Endophytic Fusarium sp. ALAA-20 for Improvement Lovastatin Production Using Agro-Industrial Wastes. Arabian Journal for Science and Engineering, 2021. 46(1): p. 175-190.
128. Rogers, E.W.; Molinski, T.F. Highly polar spiroisoxazolines from the sponge Aplysina fulva. J. Nat. Prod. 2007, 70, 1191–1194

Chapter 6 - Supplementary Material

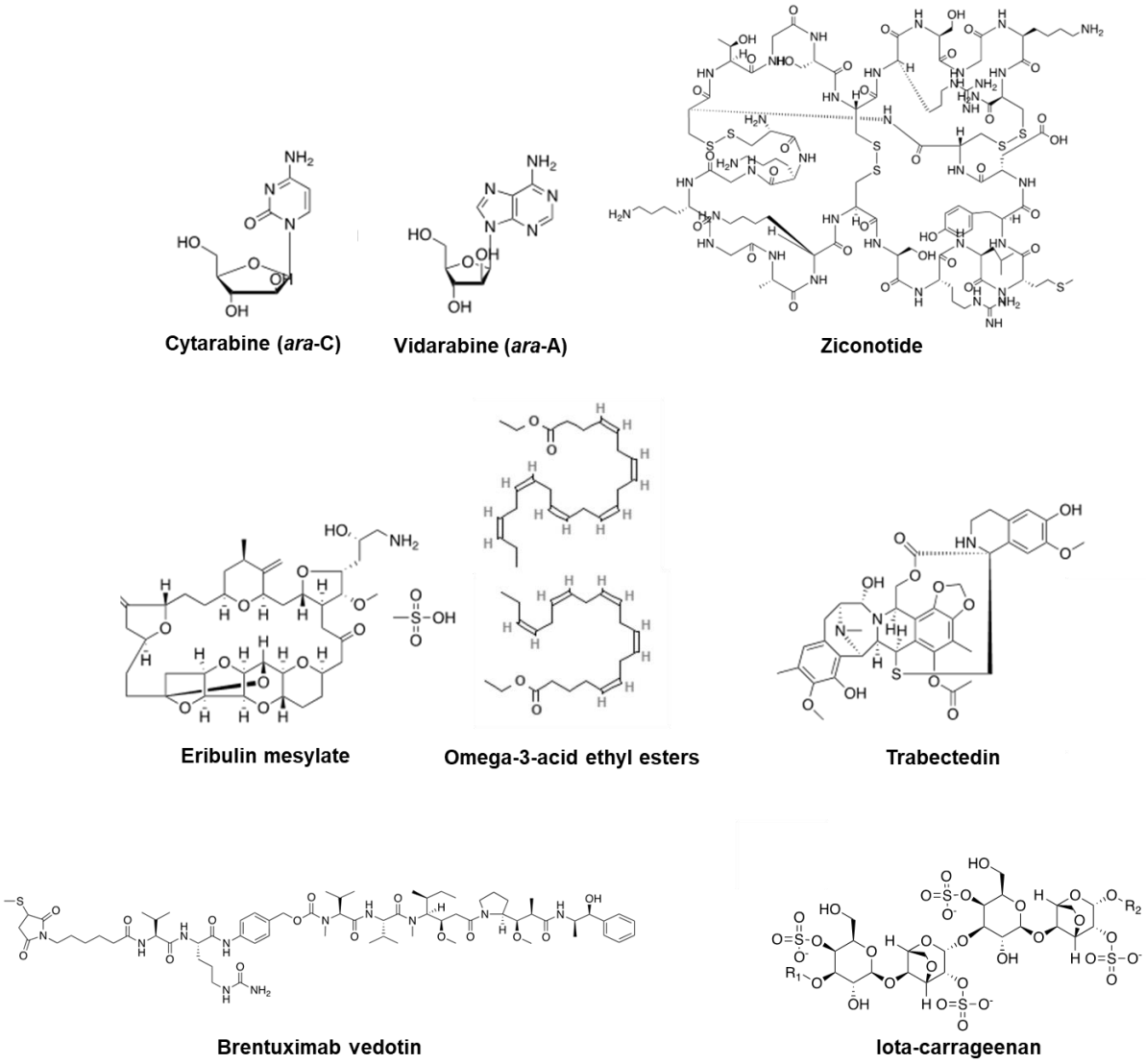

Figure S.1. ***Molecular structures of approved drugs based on MNPs.*** *Supports the information in Table 1.2.*

Table S.1. ***Taxonomic information of the species whose crude extracts are part of Library I.***

Code (extract)	Isolated Species	Code (extract)	Isolated Species
A1	*Molgula* sp.	**A31**	*Cliona varians*
A2	*Xestospongia muta*	**A32**	*Clathria virgultosa*
A3	*Aiolochroia crassa*	**A33**	*Ectyoplasia ferox*
A4	*Cinachyrella kuekenthali*	**A34**	*Scopalina ruetzleri*
A5	*Eudistoma amanitum*	**A35**	*Agelas sceptrum*
A6	*Ecteinascidia* sp.	**A36**	*Tridemnum solidum*
A7	*Briareum asbestinum*	**A37**	*Aplysina cauliformis*
A8	*Chondrilla caribensis f. hermatypica*	**A38**	*Didemnum* sp.
A9	*Eudistoma* sp.	**A39**	*Ectyoplasia* sp.
A10	*Mycale laevis*	**A40**	*Agelas citrina*
A11	*Didemnum perlucidum*	**A41**	*Niphates erecta*
A12	*Spongia tubulifera*	**A42**	*Chondrilla* sp.
A13	*Agelas clathrodes*	**A43**	*Polysyncraton* sp.
A14	*Amphimedon compressa*	**A44**	*Myrmekioderma gyroderma*
A15	*Plakinastrella onkodes*	**A45**	*Clathria gomezae*
A16	*Ircinia strobilina*	**A46**	*Niphates erecta*
A17	*Dysidea* sp.	**A47**	*Tethya* sp.
A18	*Polycarpa* sp.	**A48**	*Ircinia strobilina*
A19	*Scopalina ruetzleri*	**A49**	*Ircinia felix*
A20	*Cliona delitrix*	**A50**	*Phallusia nigra*
A21	*Aplysina fulva*	**A51**	*Callyspongia vaginalis*
A22	*Monanchora arbuscula*	**A52**	*Niphates digitalis*
A23	*Halichondria melanadocia*	**A53**	*Didemnum* sp.
A24	*Clavelina* sp.	**A54**	*Aiolochroia crassa*
A25	*Mycale laevis*	**A55**	*Scopalina ruetzleri*
A26	*Leucetta floridana*	**A56**	*Callyspongia plicifera*
A27	*Polyclinum* sp.	**A57**	*Melophlus hajdui*
A28	*Ircinia felix*	**A58**	*Aplysina fulva*
A29	*Niphates erecta*	**A59**	*Clathrina* sp.
A30	*Callyspongia longissima*	**A60**	*Aplysina muricyanna*

Code (extract)	Isolated Species
A61	*Agelas dilatata*
A62	*Aaptos* sp.
A63	*Aplysina fistularis*
A64	*Haliclona (Rhizoniera) curacaoensis*
A65	*Agelas clathrodes*

Table S.2. ***Library I crude extracts concentrations.*** *Extracts were dissolved in the smallest possible volume of DMSO with concentrations ranging from 0.5 to 5 mg/mL (extract stock concentration). The concentrations used in the bioguided assays varied between 12.5 and 125 µg/mL.*

Library I					
Code	**Extract stock concentration** (mg/mL)	**Maximum concentration tested** (µg/mL)	**Code**	**Extract stock concentration** (mg/mL)	**Maximum concentration tested** (µg/mL)
A1	5	125	**A28**	2.5	62.5
A2	1	25	**A29**	2.5	62.5
A3	1.43	35.75	**A30**	1.66	41.5
A4	0.5	12.5	**A31**	1.66	41.5
A5	2.5	62.5	**A32**	1	25
A6	2.5	62.5	**A33**	1.66	41.5
A7	5	125	**A34**	5	125
A8	2.5	62.5	**A35**	2.5	62.5
A9	5	125	**A36**	2.5	62.5
A10	5	125	**A37**	2.5	62.5
A11	2.5	62.5	**A38**	2.5	62.5
A12	2.5	62.5	**A39**	5	125
A13	1.66	41.5	**A40**	5	125
A14	1.66	41.5	**A41**	5	125
A15	5	125	**A42**	5	125
A16	2.5	62.5	**A43**	2.5	62.5
A17	5	125	**A44**	2.5	62.5
A18	2	50	**A45**	5	125
A19	1.25	31.25	**A46**	1	25
A20	2	50	**A47**	5	125
A21	5	125	**A48**	5	125
A22	2.5	62.5	**A49**	1.66	41.5
A23	1	25	**A50**	2.5	62.5
A24	1	25	**A51**	1.66	41.5
A25	1	25	**A52**	1	25
A26	1.25	31.25	**A53**	2.5	62.5
A27	5	125	**A54**	5	125

Library I					
Code	**Extract stock concentration** (mg/mL)	**Maximum concentration tested** (µg/mL)	**Code**	**Extract stock concentration** (mg/mL)	**Maximum concentration tested** (µg/mL)
A55	1.66	41.5	**A61**	1.66	41.5
A56	1	25	**A62**	1.66	41.5
A57	2.5	62.5	**A63**	2.5	62.5
A58	1	25	**A64**	5	125
A59	2	50	**A65**	2.5	62.5
A60	2.5	62.5			

Table S.3. ***A22 dichloromethane (A22 DF) sub-fractions concentrations.*** *Fractions were dissolved in the smallest possible volume of DMSO with concentrations ranging from 2.4 to 5.4 mg/mL (extract stock concentration). The concentrations used in the bioguided assays varied between 60 to 135 µg/mL.*

Library I		
A22 DF Sub-fractions	**Fraction stock concentration** (mg/mL)	**Maximum concentration tested** (µg/mL)
R1	5.4	135
R2	5.2	130
R3	3.6	90
R4	2.4	60
R5	4.6	115
R6	5.4	135
R7	5.4	135

Table S.4. ***A22 dichloromethane (A22 DF) sub-fractions concentrations used to assess fungicidal activity and MIC of C. krusei, C. tropicalis, and C. parapsilosis.*** *Fractions were dissolved in the smallest possible volume of DMSO with concentrations ranging from 3.6 to 5 mg/mL (extract stock concentration). The concentrations used in the fungicidal assays varied between 90 to 125 µg/mL.*

Library I		
A22 DF Sub-fractions	**Fraction stock concentration** (mg/mL)	**Maximum concentration tested** (µg/mL)
R1	5.4	135
R2	4.7	117.5
R3	5.0	125
R4	3.6	90
R5	4.6	115
R6	5.4	135
R7	5.4	135

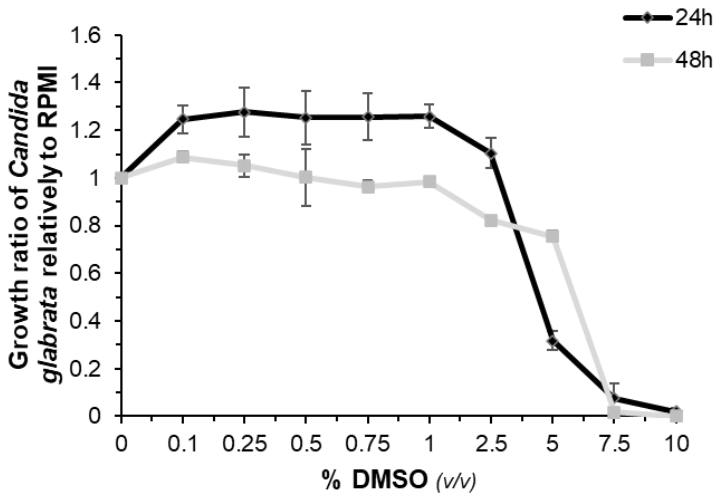

Figure S.2. ***DMSO effect on C. glabrata growth.*** *Cellular suspensions of Candida spp. (3x10^3 CFU/mL) were prepared from fresh cultures grown on YPD agar plates, and 100 µL were added to each well. The wells were incubated with 100 µL of RPMI medium supplemented with different DMSO concentrations (% v/v). Growth in the RPMI medium was recorded after 24 and 48 hours at 37 ºC by measuring OD_{600}. Growth ratios were determined relative to control (no DMSO-treated cells). The final DMSO concentrations range from 0.1 % (v/v) to 10 % (v/v).*

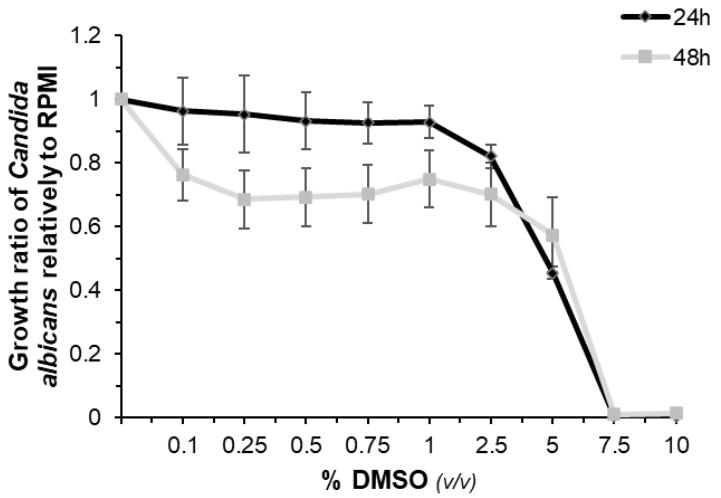

Figure S.3. ***DMSO effect on C. albicans growth.*** *Cellular suspensions of Candida spp. (3x10^3 CFU/mL) were prepared from fresh cultures grown on YPD agar plates, and 100 µL were added to each well. The wells were incubated with 100 µL of RPMI medium supplemented with different DMSO concentrations (% v/v). Growth in the RPMI medium was recorded after 24 and 48 hours at 30 ºC by measuring OD_{600}. Growth ratios were determined relative to control (no DMSO-treated cells). The final DMSO concentrations range from 0.1 % (v/v) to 10 % (v/v).*

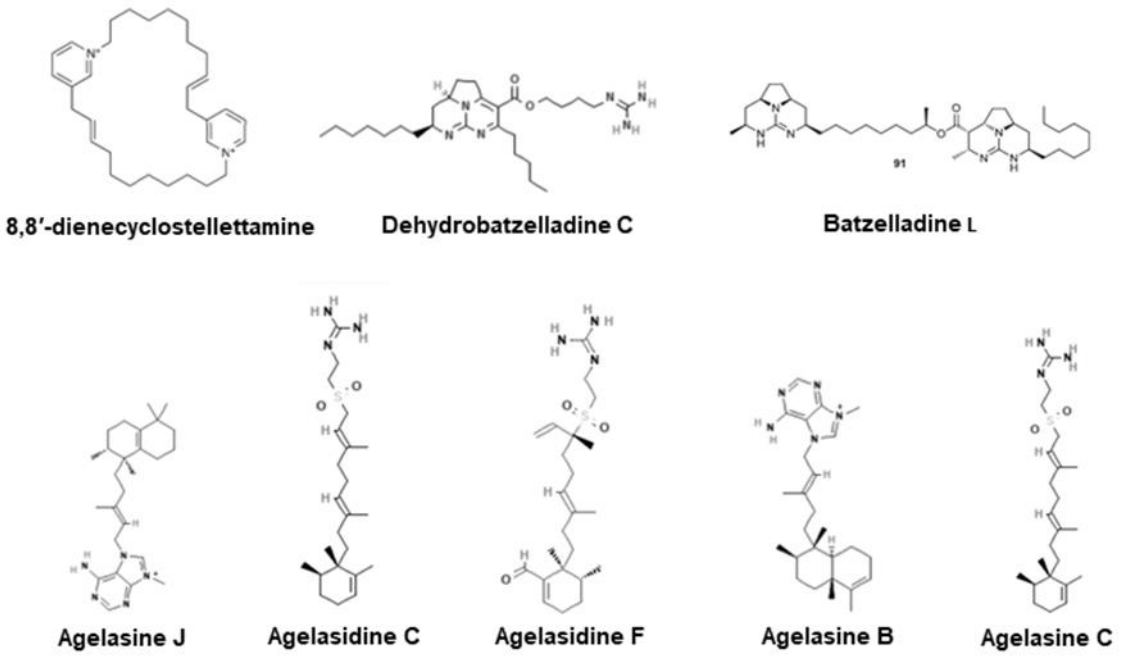

Figure S.4. ***Chemical structures of previously reported molecules active against Candida spp.*** *that may be responsible for A14, A22, and A40 antifungal activity.*

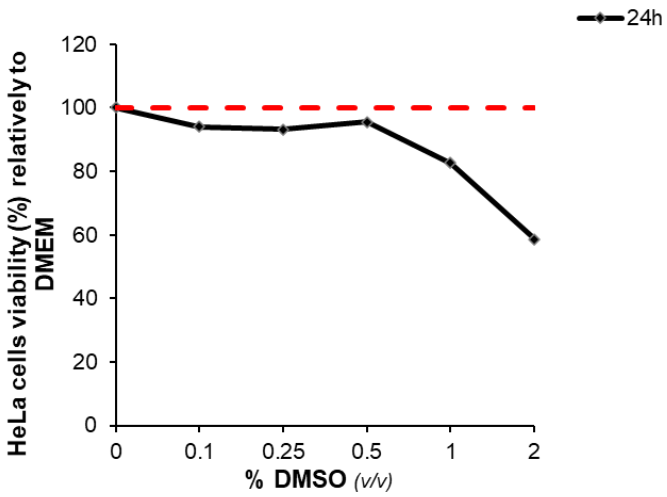

Figure S.5. ***DMSO effect on HeLa cells viability****. HeLa cells (5 x 10^3 cells/well) were seeded in 96-well plates. After 24 hours of growth, the wells were incubated with 100 µL of DMEM supplemented with different DMSO concentrations (% v/v), and plates were incubated for 24 hours. Cell viability was determined by MTT assay. The results of HeLa cell viability were expressed as the percentage of MTT reduction of treated cells relative to control (untreated cells: 0% DMSO). The final DMSO concentrations range from 0 % (v/v) to 2 % (v/v).*

Table S.5. ***Taxonomic information and previous antifungal activity reports of the species or genus studied of the 65 crude extracts from Library I.***

Order	Family	Genera/Species	Code	Antifungal activity reported	Reference
Aplousobranchia	Clavelinidae	*Clavelina* sp.	**A24**	(2S,3R)-2-aminododecan-3-ol isolated from *Clavelina oblonga:* active against *C. albicans* and *C. glabrata*. Inoldizines isolated from *Clavelina picta:* active against *C. albicans.*	[63, 101, 102]
	Didemnidae	*Didemnum* sp.	**A38** **A53**	Didemnoline B and C: active against *Saccharomyces cerevisiae*. Didemnaketal F and G: active against *C. albicans.* β-carboline: active against *C. albicans* and *C. krusei.*	[102-104]
	Polycitoridae	*Eudistoma* sp.	**A9**	Eudistomin W and X: active against *C. albicans.*	[105]
Agelasida	Agelisidae	*Agelas citrina*	**A40**	Agelasidine C, agelasidine E, and F: active against *C. albicans.*	[63, 70, 71, 88]
		Agelas clathrodes	**A13** **A65**	Clathramides A and B: active against *Aspergillus niger*.	[106]
		Agelas sceptrum	**A35**	Sceptrin: active against *C. albicans*, *Alternaria* sp., and *Cladosporium cucumerinum*.	[107]
Clathrinida	Clathrinidae	*Clathrina* sp.	**A59**	Clathridine: active against *C. albicans* and *Saccharomyces cerevisiae*.	[108]
	Leucittidae	*Leucetta floridana*	**A26**	Active against *C. albicans*.	[109]

Order	Family	Genera/Species	Code	Antifungal activity reported	Reference
Dictyoceratida	Dysideidae	*Dysidea* sp.	**A17**	3‘-hydroxyavarone, 3’,6‘di-hydroxyavarone, 6’-acetoxyavarol, 9α,11α-epoxycholest-7-ene-3β,5α,6α,19-tetrol 6-acetate: active against *C. albicans.* 3,5-dibromo-2-(3,5-dibromo-2-methoxyphenoxy) phenol: active against *C. albicans*, *C. glabrata*, *C. tropicalis*, *S. fumigatus*, *A. flavus*, and *A. niger.* Puupehenone: active against *C. albicans.* Sesterterpenes sulfates: active against *C. albicans*. Avarol: active in different *Candida* spp..	[110-117]
Haplosclerida	Niphatidae	*Amphimedon compressa*	**A14**	8,8’-dienecyclostellettamine: active against *C. albicans* and *A. fumigatus.*	[83, 84]
	Petrosiidae	*Xestospongia muta*	**A2**	Xestospongiamide: active against *A. niger* and *C. albicans*. Xestospongin C and D: active against fluconazole-resistance *Candida* spp.	[118, 119]
Homosclerophorida	Plakinidae	*Plakinastrella onkodes*	**A15**	Plakinic acid F, epiplakinic acid F, 1,2-dioxane ring peroxide acid: active against *C. albicans* and *A. fumigatus.* Plakortide F, 1,2-dioxolane peroxide acid: active against *C. albicans.*	[63, 120-122]
Poecilosclerida	Crambeidae	*Monanchora arbuscula*	**A22**	Dehydrobatzelladine C: active against *C. albicans* and *A. fumigatus.* Batzelladine L: active against *A. flavus.* Mirabilin B is active on *C. neoformans.*	[85-87]
Scopalinida	Scopalinidae	*Scopalina ruetzleri*	**A19** **A35** **A55**	Active against *C. albicans*.	[109]
Subertida	Subertidae	*Aaptos* sp.	**A62**	3-(phenethylamino)demethyl(oxy)aptamine: active against *C. albicans*, *C. parapsilosis*, *Trichophyton rubrum*, and *Microsporum gypseum.*	[123-125]

Order	Family	Genera/Species	Code	Antifungal activity reported	Reference
Tethyida	Tethyidae	*Tethya* sp.	**A47**	Active against *C. albicans*.	[126]
Vergogiida	Aplysinidae	*Aplysina fistularis*	**A63**	Lovastatin: active against *Candida*, *Aspergillus*, *Fusarium*, and *Trichophyton* species.	[127]
		Aplysina fulva	**A21** **A58**	Lectin: active against *C. albicans* and *C. tropicalis.*	[128]